Asymptotic Safety And High-Energy Scattering At The Large Hadron Collider

Rob Old

June 2, 2016

UNIVERSITY OF SUSSEX

ROBERT OLD DOCTOR OF PHILOSOPHY

ASYMPTOTIC SAFETY AND HIGH-ENERGY SCATTERING AT THE LARGE HADRON COLLIDER

SUMMARY

The fascinating idea that in higher-dimensional models the fundamental scale of gravity, the Planck scale, could be as low as the electroweak scale has stimulated a substantial body of work in the past decade. In addition to solving the hierarchy problem, a low quantum gravity scale also offers the exciting prospect that collider experiments become sensitive to the quantum nature of gravity. Quantum gravity signatures include missing energy due to graviton emission, enhancement of standard model reference processes via virtual graviton exchange, or the production and decay of mini black holes. Dedicated searches for all of these are presently under way at the Large Hadron Collider.

Previous predictions for colliders have been encumbered by the absence of a complete theory of quantum gravity. However, the recent years have also seen important progress in the understanding of gravity as an asymptotically safe quantum field theory, in which the high-energy behaviour is controlled by an interacting fixed point. The notorious divergences of perturbation theory are thus avoided, and the theory remains predictive at arbitrarily high energies.

In this thesis, we investigate the effects of asymptotic safety upon predictions for graviton-mediated processes in higher-dimensions at colliders. We consider single-graviton mediated effects in the Born approximation as well as the multi-graviton exchanges which dominate the forward scattering region at transplanckian energies, as described by the eikonal approximation. Cross sections are derived and a detailed comparison with findings from effective theory is made. Using the PYTHIA event generator we find that for some regions in parameter space quantum gravity effects are enhanced over the semiclassical predictions, as well as over standard model backgrounds. The use of our results to constrain our theory parameters is discussed.

Acknowledgements

This work has been carried out under the supervision of Daniel Litim. I am grateful for his tolerance of my often empty desk so that I could be with my family in Liverpool, and for his efforts in coercing me to the completion of this thesis. The staff at Sussex have proved helpful to a fault, and I have called on all of them for help and guidance at some point or another; special thanks in particular are due to Andrea Banfi, for his help with the HPC cluster; Francesco Hautmann, for his collaboration on the stationary phase and phenomenological work to be described; and to my second supervisor Stephan Huber, for his patient ear.

It is a source of great regret that I couldn't be around to share more beers than those I enjoyed with my fellow students, especially those with whom I have shared an office and a supervisor: Raul, Kostas, Edouard (and his knowledge of books, maths and Mathematica), Kevin (and long chats about black holes) and Jan (my linguistic mentor as well as collaborator).

I am grateful to Gudrun Hiller and Henning Sedello at the University of Dortmund for hospitality, and for making their code available to me, and to Eleni Vryonidou for correspondence and for kindly providing some of her data. I have been supported by an STFC studentship.

Finally, I must acknowledge the love and support of my family. Some who are no longer here to witness the completion of my PhD left me in no doubt that it would not have made the least difference to their opinion of me if they had, such was their unfailingly blind partiality. My parents made enormous sacrifices for my education, and better still brought me up in a house full of books- one of which, *A brief history of time*, led me directly along the path this thesis completes. My aunt "Tuts" Eileen has always been a well of support and humour. And last, but by no means least, to my most immediate family- Mary, James, Pascal and Merlin. For the last four years, and especially in the last few weeks, I have been negligent of my duties around the house/playing Xbox/going for walkies/ as a comfy knee undisturbed by a laptop (respectively). Words cannot express

how much I am looking forward to spending the rest of my life making good on the debt I've thus built up.

Contents

List of Figures

Chapter 1

Introduction

The investigation of scattering amplitudes describing the gravitational interactions of particles is a subject with a long history, stretching back at least as far as [3]. That it is such an area of active research more than fifty years later is testament to the fact that it is both difficult and interesting, a tangled thicket of seemingly impenetrable mysteries from which insights are hard-won, but amply rewarding.

As emphasised by Giddings [1], the scattering formulation provides a firm footing from which to begin exploring some of the deepest questions in physics. In quantum gravity, it is not even clear how to define *observables* with complete generality. Quantum field theory is usually couched in terms of n-point correlation functions of local fields,

$$G(x_1, \ldots, x_n) = \langle \phi(x_1) \ldots \phi(x_n) \rangle \tag{1.1}$$

but the classical theory of gravity, general relativity, has a gauge symmetry in the form of diffeomorphism invariance; a function like (1.1) will clearly not be a gauge-invariant quantity, as under a local transformation $x^\mu \to x^\mu + \epsilon^\mu(x)$ each field will vary by some amount $\delta\phi = \epsilon^\mu \partial_\mu \phi$. However, by working in an asymptotically flat spacetime, we can give meaning to the concept of momentum eigenstates defined at infinity which do not suffer from this problem, and hence formulate a gauge-invariant S-matrix. This formalism makes unitarity manifest, and has played an important role [4] in the emerging consensus that the decay of a black hole via Hawking radiation preserves information.

The scattering formulation also provides a convenient framework in which to check that the physical consequences of some theory are 'reasonable', in the sense that they do not conflict with already established physics. In particular, it is known that general relativity provides an excellent description of a wide range of physical phenomena. This strongly suggests that scattering amplitudes derived from the classical action for a symmetric tensor

$g_{\mu\nu}$ of rank two coupled to a matter described by a Lagrangian $\mathcal{L}_m$ (see e.g. [5]),

$$S = -\frac{1}{16\pi G_N}\int d^4x\sqrt{|\mathrm{Det}(g_{\mu\nu})|}\,(R+\mathcal{L}_m) \tag{1.2}$$

where R is the Ricci scalar corresponding to $g_{\mu\nu}$, should provide a useful description of physical processes in which the quantum mechanics of the colliding particles is important, but the gravitational field can be treated as classical. The most obvious example is that at low energies, we would usually expect to be able to apply leading order perturbation theory, and indeed the *Born amplitude* thus derived reproduces the result obtained by taking the Fourier transform of the Newtonian potential. However, it was first realised by t'Hooft [6] that due to the weakening of gravity with distance, we can consider the quantum mechanics of processes occurring at substantially higher energies even than the Planck scale, provided that we restrict our attention to large impact parameters. This picture was subsequently corroborated by the analysis of the Verlindes [7] and connected to the use of the eikonal approximation by Kabat and Ortiz [8]. In a similar vein it is natural to consider the relation of these ideas to the process of black hole formation via the Hoop conjecture [9]; a black hole is expected to form in a collision when the impact parameter of a collision becomes less than the Schwarzschild radius corresponding to the centre-of-mass energy.

Using the methods of effective field theory, one can go even further, and consider some radiative corrections to physical processes that arise when the quantum theory of the gravitational field is taken into account. Such a program has been initiated by Donoghue in particular [10, 11]. However, gravity is famously non-renormalizable [12, 13, 14], so that this procedure leaves us with expressions that depend explicitly on the method of regulating ultraviolet divergences.

This leads us naturally to wonder about the domain of validity of our effective field theory approach. Historically, this was always assumed to be comparable to the *Planck scale* M_{Pl}, defined by Newton's constant G_N via $G_N = M_{Pl}^{-2}$ in units such that $c = \hbar = 1$. This assumption was called into question by the famous proposal of Arkani-Hamed, Dimopoulos and Dvali (ADD) that spacetime might have more than four dimensions, but that only gravity can propagate in the extra dimensions [15, 16]. In this scenario the fundamental scale associated with gravity is lowered to ~ 1 TeV, with the apparent hugeness of the Planck scale being merely the emergent result of gravity spreading out over a relatively large compactified volume V_n associated with the extra dimensions. This idea was the stimulus for thousands of subsequent papers. As well as solving the hierarchy problem it offers the exciting possibility that that the riddles of quantum gravity can be

subjected to experimental probe at the Large Hadron Collider (LHC).

Of course, such a possibility creates an impetus to refine our theoretical understanding of quantum gravity to the point where concrete predictions about the corresponding phenomenology can be made. In recent years significant progress has been made in understanding gravity as an *asymptotically safe* field theory: one whose ultraviolet behaviour is governed by an interacting fixed point [17]. This offers an extremely conservative resolution to the problem of how gravity is fundamentally defined. An extremely broad body of computational evidence [18, 19, 20, 21, 22, 23, 24, 25, 26, 27] in support of this scenario has formed, and in consequence there is an increasing amount of discussion of the physical consequences of the theory. Previous investigations have looked into the effects of this modification of gravity upon black holes [28, 29, 30, 31, 32], cosmology [33, 34, 35, 36], and other processes relevant to the LHC [37, 38, 39, 40].

The purpose of this thesis is to consider the phenomenology of this theory of quantum gravity at the LHC, with specific reference to scattering at high energies. Chapter 2 develops the theoretical ideas of the ADD model, asymptotic safety, and transplanckian scattering necessary to understand the present work and place it in context. Chapter 3 derives the elastic scattering amplitudes of particles at transplanckian energies in our framework, and explores the relationship of our results to the semiclassical framework using the methods of the stationary phase approximation. Chapter 4 then explores the corresponding phenomenology of our amplitudes, investigating dijet production using the PYTHIA 8.1 event generator.

Chapter 2

Preliminaries

In this chapter we review the individual theoretical strands that inform our project. We begin by discussing some of the problems that have been encountered in trying to define a theory of quantum gravity, and the hierarchy problem of the Standard Model of particle physics. We review the framework of the renormalization group, and then discuss a putative solution to each of these problems in turn. We discuss Weinberg's *asymptotic safety* hypothesis for gravity, and review the computational evidence that supports it. We describe the higher-dimensional framework of Arkani-Hamed, Dimopoulos and Dvali, in which quantum gravity will become significant for LHC phenomenology. The chapter concludes with a discussion of semiclassical approaches to gravitational scattering, with particular reference to the *eikonal* amplitude, which will play a key role in the subsequent development of this thesis.

2.1 Scales and divergences in quantum gravity

Legend has it [41] that in the 1950s, when he first started to work on the subject, Feynman hoped that quantizing gravity might be "a piece of cake". After all, even today the principal approach used to investigate a quantum field theory is to compute, using Feynman's diagrams, correlation functions of the theory by perturbatively expanding around the free theory in powers of some weak coupling. In our experience, of course, the gravitational coupling is certainly suitably feeble; in the first lecture of [41], Feynman illustrates the point by computing the ratio of the Newtonian and Coulomb force between two charged protons:

$$\frac{F_{electric}}{F_{grav}} = 4.17 \times 10^{42} \tag{2.1}$$

Some results of the early investigations into quantum gravity were actually quite rewarding. For example, it is known from group theory that any attempt to treat the metric tensor $g_{\mu\nu}$ of general relativity as a field to be quantized will result in massless spin-2 particles. Fascinatingly, however, it also emerged [41, 42, 43, 44] that the quantum theory of a massless spin-2 particle is *inconsistent* unless it contains a gauge symmetry equivalent to the diffeomorphism invariance of the classical metric; which couples to all other fields universally through their energy-momentum tensor acting as a conserved source; and which must necessarily possess self-interactions such that the Einstein-Hilbert action is reproduced- provided that we restrict our attention to terms containing at most two derivatives of the "spin-2" field, a point to which we will return shortly. This theory also turns out to be infrared-safe [45].

Of course, quantum gravity is still the subject of intensive research today. The most infamous difficulty is that of interpreting the ultraviolet divergences that occur in perturbation theory, which cannot be renormalized into parameters present in the bare Lagrangaian. Such divergences occur at two-loop order in pure gravity [12, 13] and at one loop when gravity is coupled to scalar matter [14]. Such theories suffer from a lack of predictive power, and it is generally assumed that non-renormalizability is indicative of a need for new physics. The modern student is taught such behaviour can be anticipated from the fact that Newton's constant G_N has *negative mass dimension*. By dimensional analysis, a perturbative expansion of a dimensionless scattering amplitude $\mathcal{M}$ in any theory with a generic coupling G of mass dimension $[G] = -2$ must be of the form

$$\mathcal{M} = GE^2 + G^2E^4 + \dots \tag{2.2}$$

where E is some energy scale. If E is assumed to be a characteristic energy scale of the process under consideration, such as the centre of mass energy, then even our tree-level estimate would suggest that we might encounter difficulties with unitarity as E increases. However, if one regulates the divergences in Feynman diagrams with an ultraviolet cutoff Λ, then at higher orders in perturbation theory it naturally emerges that $E \sim \Lambda$. As we increase $\Lambda \to \infty$, as quantum mechanics tells us we must in order to sum over all intermediate states, then divergences appear at all orders in perturbation theory; to absorb them all into parameters of the model would require a model with infinitely many parameters to be determined by experiment, and hence lacking predictive power. It is assumed, then, that a new physical description of the process under consideration is needed before the energy scale E becomes comparable to the mass scale M defined by the constant G. This is borne out in practice by the Fermi theory of weak interactions. Beta

decay was originally described by a Lagrangian of the form

$$\mathcal{L}_I = G_F \bar{\psi}\psi\bar{\psi}\psi \tag{2.3}$$

where the Fermi constant G_F clearly has mass dimension $[G_F] = -2$. When the full Glashow-Weinberg-Salam (GWS) theory of weak interactions was developed, it turned out that $G_F \sim M_W^{-2}$; the negative mass dimension of the constant heralded the existence of the W-boson, which was too massive to have been detected in Fermi's day. A Lagrangian such as (2.3), which provides a good description of physics at energies below the masses of the weak bosons, but fails at the scale of electroweak physics of which it is ignorant, is called an *effective Lagrangian* , and can be obtained from the GWS theory by simple Feynman diagram analysis; one says that the weak bosons have been *integrated out* of the theory. By analogy, it is argued that at energies comparable to M_{Pl}, new physics (such as string theory) kicks in to restore order to the gravitational sector. The necessity of some new physics at short distance scales is also indicated by the infamous curvature singularities of classical general relativity, most notably those found at the centre of a black hole. Classically such spacetimes are *geodesically incomplete*, as a test particle that falls into the black hole will inevitably be drawn into the singularity where the metric field is no longer defined in a finite proper time.

It was the brilliant insight of Wilson [46, 47] to apply the logic of integrating out physically inaccessible degrees of freedom to high-momentum modes, relating early work on the renormalization group in particle physics to ideas from condensed matter such as Kadanoff's "block spin" scaling laws for a ferromagnet. This process generates terms not present in the bare Lagrangian- just as integrating out the W-boson induced a four-fermion interaction, when none is present in the GWS Lagrangian- and shifts the coefficients of those terms that are present. If we are interested in physics occurring at some momentum scale k, then it makes sense to formulate our description of that physics using the effective Lagrangian obtained by integrating out all momentum modes larger than k; the coefficients λ_i of the terms in this Lagrangian depend on k, $\lambda_i(k)$. From this point of view, we should regard the Einstein-Hilbert Lagrangian not as the fundamental definition of our theory of gravity, but as the leading order term in an effective Lagrangian which will contain all terms consistent with the gauge symmetry, which classically would be identified as scalars formed from the curvature tensor:

$$\mathcal{L} = \sqrt{g}(c_0 + c_1 R + c_2 R^2 + c_3 R^{\mu\nu}R_{\mu\nu} + \ldots\ldots) \tag{2.4}$$

where all the parameters $c_i(k)$ "run" with energy scale k, and at low energies c_0 =

$\Lambda_{CC}/(8\pi G_N)$ (where Λ_{CC} is the cosmological constant) and $c_1 = -(16\pi G_N)^{-1}$. It was suggested by Weinberg [17] that allowing Newton's constant to run with energy as $G(E)$ might solve the problems associated with the negative mass dimension of G_N. If at high energies $G(E) \sim E^{-2}$, then the corresponding dimensionless coupling $g = G(E)E^2$ will tend to a *fixed* value g_*. Together with an assumption that only finitely many measurements are necessary to specify the high-energy behaviour of the theory, this is referred to as the *asymptotic safety hypothesis*. Exciting theoretical developments made over the last two decades, to be reviewed in the next section, have led to a significant body of calculational evidence in support of this conjecture.

Whilst not as dramatic as the ultraviolet catastrophe of perturbative quantum gravity, the Wilsonian analysis of the Standard Model of particle physics reveals that it too possesses an unsatisfactory feature. When computing the k-dependence of running couplings, it is typically still necessary to regulate the divergences of perturbation theory. If one assumes that the theory will ultimately break down at some very high scale Λ, then scalar particles receive corrections to their bare (mass)^2 parameters on the order of Λ^2. The standard model, of course, contains just such a scalar: the celebrated Higgs boson, whose mass is measured [48, 49] to be $m_H \approx 125$ GeV. The most obvious candidate for physics beyond the standard model is gravity; but the Planck scale is vastly larger than that associated with any other physics known to man: $M_{Pl} \approx 10^{19}$GeV. (Indeed, the hugeness of the ratio $F_{electric}/F_{grav}$ given earlier is the result of the hugeness of the Planck scale relative to the proton mass.) From the Wilsonian point of view, the disparity between the measured Higgs mass and the "natural" value we would calculate requires the "initial" mass defined at the scale $k = \Lambda$ to be incredibly finely tuned such that the calculable quantum corrections reduce it to 10^{-17} of its initial value. This unnaturalness is the famous *hierarchy problem* of the standard model, and has led many theorists to believe that physics beyond the standard model must set in at much lower scales, on the order of $\Lambda = 1$ TeV, which might thus be experimentally accessible at the Large Hadron Collider.

One of the most exciting proposals as to what this new physics might be was made by Arkani-Hamed, Dimopoulous and Dvali [15]. They observed that the experimental constraints on the dimensionality of spacetime that come from gravity are far weaker than those that come from the Standard Model. In their scenario, the standard model is confined to a four-dimensional "brane" in a higher-dimensional spacetime, whilst gravity is capable of probing $d = 4 + n$ dimensions. The extra dimensions are still compactified, but the radius R of compactification can be far larger than in models in which the standard

model probes the extra dimensions; at the time of their proposal, $R \sim 1mm$ had not been ruled out by experiment! Correspondingly, in this model the truly fundamental scale M_D of the d-dimensional gravity theory is lowered significantly, being related to the Planck scale as $M_{Pl}^2 = 8\pi R^n M_D^{n+2}$. If realised in nature, this would mean that the LHC would become sensitive to the nature of quantum gravity, allowing us an unprecedented opportunity to develop our understanding.

Of course, it is in the nature of modern phenomenology that a precise prediction is necessary in order to discover anything, particularly in so messy an environment as in a hadron collider. This presents a problem to the experimentalist who wishes to discover quantum gravity without professing to understand it. One ingenious way around this problem is offered in the form of *semiclassical* approximations. After all, we are used to using gravity in its astrophysical setting, in which the masses involved are vastly higher than the paltry $M_{Pl} \sim 2 \times 10^{-8} kg$; the condition is that we do not probe *short distances*. In particular, in [50] the *eikonal* approximation was employed to compute a semi-classical approximation to the elastic scattering of partons at "transplanckian" ($E \gg M_D$) energies through small angles.

In this thesis, we consider that asymptotic safety offers us a well-defined, predictive theory of quantum gravity, and investigate its experimental consequences if large extra dimensions are to be found at the LHC. The remainder of this chapter is dedicated to a more detailed review of the different aspects of our theoretical framework: the asymptotic safety conjecture, the ADD scenario, and the physics of transplanckian scattering.

2.2 Asymptotically safe gravity

2.2.1 Asymptotic safety

In order to formulate the asymptotic safety hypothesis more precisely, we will begin by reviewing some of the concepts of the renormalisation group in more detail. Our treatment will follow that of Weinberg's original proposal [17]. As discussed in the preceding section, when defining a quantum field theory it is not sufficient merely to specify the Lagrangian; it is also necessary to specify the scale at which we are defining the theory. When one talks about e.g. "ϕ^4 theory", it is implicitly assumed the *bare* Lagrangian is being defined at the cutoff scale Λ which defines the domain of validity of the theory, which for a fundamental theory will be infinity. If we choose some functional basis (such as powers of the scalar field ϕ), then we can think of the couplings $\bar{g}_i$ as "co-ordinates" of this bare

Lagrangian in an infinite dimensional space, and specify the action as $S_{bare}[\{\bar{g}_i\}]$. The result of integrating out the modes above the scale μ is the effective action $S_{eff}[\{\bar{g}_i(\mu)\}]$; as $\mu \to 0$ we are performing the full path integral, and recover the so-called "quantum" or "average" action Γ. In the functional space parametrized by our couplings, this evolution is governed by an infinite set of coupled first-order differential equations:

$$\mu \frac{dg_j(\mu)}{d\mu} = \beta_j(\{g_i(\mu)\}) \tag{2.5}$$

In these equations the β-functions depend only on *dimensionless* variables; if a coupling $\bar{g}_i$ has mass dimension d_i, we define corresponding dimensionless couplings $g_i = \mu^{-d_i}\bar{g}_i$. Let us consider the couplings at a finite scale μ, and consider how this system evolves as $\mu \to \infty$. For the theory to make sense up to arbitrarily high energies, it is necessary that each coupling tends to a limiting value $g_{i,*}$. In order for this to happen, each of the β functions of the theory must vanish when evaluated at the limiting values:

$$\beta_j(\{g_{i,*}\}) = 0 \tag{2.6}$$

Such a set of values $g_{i,*}$ for the couplings is said to define a *fixed point* for the RG flow of the theory space.

In order for such a fixed point to have any relevance to the real world, it is necessary that it is connected by the RG flow to the point in theory space where we find ourselves to live, in the sense that if at very high energies the measured values of our couplings differ from their fixed point values by some small amount δg_i, then the solution to the equations (2.5) evolved to an RG scale μ must map these values of the couplings to the measured values $g_i(\mu)$. Of course, we cannot measure infinitely many couplings. For our theory to be predictive, we require that the *critical surface* of points which flow into the fixed point as $\mu \to \infty$ is *finite dimensional*.

It is interesting to consider the flow in the vicinity of the fixed point. When all the couplings are close to their fixed point values we can *linearise* the flow, defining a "displacement vector in coupling space" $\delta g_i = g_i - g_i^*$, and approximating the beta functions by the action of the so-called *stability matrix*

$$B_{ij} = \left.\frac{\partial \beta_i}{\partial g_j}\right|_{g_i = g_i^*} \tag{2.7}$$

In the vicinity of the fixed point, the flow thus becomes described by the simple system

$$\mu \frac{dg_j(\mu)}{d\mu} = B_{ij}\delta g_i \tag{2.8}$$

Once we recognise that powers of μ are eigenfunctions of the logarithmic derivative operator $\mu\partial_\mu$, it is clear that the solution to this system of equations is readily given in terms of the eigenvectors V^K and corresponding eigenvalues θ^K of the stability matrix:

$$g_i(\mu) = g_i^* + \sum_K c_K (V^K)_i \mu^{\theta^K} \tag{2.9}$$

This expression makes it clear that as $\mu \to \infty$, a point in theory space is drawn towards the fixed point by the RG flow if its displacement vector can be decomposed into eigenvectors whose eigenvalues θ^K are *negative*. These eigenvalues are called the *critical exponents* of the theory, and our requirement that the ultraviolet fixed point has a finite dimensional critical surface becomes the requirement that the corresponding stability matrix has finitely many negative critical exponents. This formulation leads us to the following heuristic argument. As $g_i = \mu^{-d_i}\bar{g}_i$, the RG equation for g_i has the form

$$\mu\frac{dg_i}{d\mu} = -d_i g_i + \mu^{-d_i}\frac{d\bar{g}_i(\mu)}{d\mu} \tag{2.10}$$

where the term $\sim \frac{d\bar{g}_i(\mu)}{d\mu}$ results from quantum corrections to the running of the coupling. Of course, the coupling $\bar{g}_i$ corresponding to any operator whose mass dimension exceeds that of our spacetime will have a negative mass dimension d_i, and so based on our expectations of classical scaling, we would expect only finitely many couplings (corresponding to perturbatively renormalizable and super-renormalizeable operators) to have negative critical exponents. In order for quantum corrections to change this picture, they would need to be so violent as to reverse the sign of *infinitely many* classical scaling exponents.

A brief comment on terminology is in order at this point. With the canonically normalized metric field $g_{\mu\nu}$ as in the Einstein-Hilbert Lagrangian, the factor $\frac{1}{16\pi G_N}$ appears in front of the *kinetic* term in the action, and it is therefore common to use the language of *field strength* or *wavefunction* renormalisation to describe the running of Newton's constant. Pre-empting the discussion of a higher-dimensional analog G_D of Newton's constant, in d spacetime dimensions the dimensionless running gravitational coupling is defined to be

$$g(\mu) = \mu^{d-2}G(\mu) \equiv \mu^{d-2}G_D Z^{-1}(\mu) \tag{2.11}$$

where $Z^{-1}(\mu)$ is the field strength renormalisation factor for the graviton. Eq. (2.10) then becomes [21, 51]

$$\mu\frac{d}{d\mu}g(\mu) = (d-2+\eta)g \tag{2.12}$$

where $\eta = \frac{dlnZ(\mu)}{dln\mu}$ is known as the *anomalous dimension* of the graviton. Gravity is unusual in that typically field strengths are *inessential* couplings- defined as couplings

which can be changed without affecting the Lagrangian when the fields are put on-shell [17]. (Our requirement for the finite dimensionality of the critical surface strictly speaking only refers to the number of essential couplings.) However, gravity is different because its universal coupling to all other fields effectively defines all length scales [52].

A theory whose high-energy behaviour is governed by a fixed point with a finite-dimensional critical surface is said to be *asymptotically safe*. Asymptotically free theories such as QCD are a special case of asymptotic safety, but this formulation allows for the more general possibility that a theory remains interacting at all scales.

When Weinberg proposed that asymptotic safety might offer a resolution to the problem of the high-energy behaviour of gravity, he was limited in his investigations by his ability to calculate the beta functions of the theory. He was able to show that gravity is asymptotically safe in $2 + \epsilon$ dimensions, where ϵ is assumed small, as gravity becomes renormalizable in two dimensions. The theory thus lay dormant until the advent of the *exact renormalisation group equation*, or ERGE, first derived by Wetterich [53].

2.2.2 The exact RG equation

Our treatment of this equation follows review articles such as [54]. In order to remove ambiguity in our conception of "large" and "small" momenta, we will assume that our theory has been analytically continued from Minkowski space (where one can have high-energy lightlike modes with $q^2 = 0$) to Euclidean 4-space. Then the vacuum-vacuum amplitude in the presence of a source, $Z[J]$, and its logarithm $W[J]$, are given by

$$Z[J] = e^{W[J]} = \int \mathcal{D}\varphi e^{-S_{bare}[\varphi]+J\cdot\varphi} \tag{2.13}$$

where we have adopted the shorthand $J \cdot \phi = \int d^d x J(x)\varphi(x)$, and the effective action $\Gamma[\phi]$ is defined as

$$\Gamma[\phi] = \sup_J \left(J \cdot \phi - W[J]\right) \tag{2.14}$$

This definition singles out a $J[\phi]$ which maximises $\Gamma[\phi]$.

The ERGE is formulated in terms of an action Γ_k that has only been averaged over those modes of momentum $p > k$, and satisfies

$$\Gamma_k \xrightarrow{k\to\Lambda} S_{bare} \tag{2.15}$$

$$\xrightarrow{k\to 0} \Gamma \tag{2.16}$$

The notational distinction between this quantity and the orignal Wilsonian effective action $S_{eff}[\{g_i(k)\}]$ at the scale k is essentially one of useage and emphasis. In a textbook

presentation such as [55], $S_{eff}[\{g_i(k)\}]$ is presented as somehow containing less information than S_{bare}, as we have "averaged over" the high-energy modes. However, in that context the path integral over modes of momentum $> k$ is performed in the absence of a source, and consequently we lose the ability to describe how the theory responds to being "driven" by a source whose Fourier transform contains high-frequency modes. In other words, the vertices of that action are not appropriate for computing Feynman diagrams in which momenta larger than k are flowing through the external legs. In contrast, the full effective action Γ contains *all* the information about the theory; it is the generating function of one-particle irreducible (1PI) diagrams.

Instead of attempting to perform the path integral over a restricted set of modes directly, the ERGE is formulated using an integral over *all* momentum modes, but by modifying the bare action with the addition of a "regulator" term $\Delta S_k[\phi]$ that suppresses the contribution of modes of momentum $p < k$. This term takes the form of a momentum-dependant mass term:

$$\Delta S_k[\varphi] = \frac{1}{2}\int \frac{d^d q}{(2\pi)^d}\varphi(-q)R_k(q)\varphi(q) \tag{2.17}$$

To suppress low-frequency modes, we require that for $p < k$, $R_k(p) > 0$, and typically $R_k(p) \sim k^2$ for small p. Condition (2.16) is satisfied if we remove the regulator as k becomes small, so that $R_k(p) \xrightarrow{k\to 0} 0$. To satisfy (2.15), we must have $R_k(p) \xrightarrow{k\to\Lambda} \infty$; a careful treatment [53] shows that the functional integral becomes dominated by a saddle point in this limit, so that effectively no integral is performed, and $e^{-\Gamma_k} \sim e^{-S}$ up to a physically irrelevant constant factor.

Any function $R_k(p)$ that satisfies these properties will produce an RG flow with physically acceptable properties, in the sense that it reproduces the correct limiting behaviour.

Once we have chosen a regulator function, we define a regulated path integral (and corresponding derived quantities) by

$$Z_k[J] = e^{W_k[J]} = \int \mathcal{D}\varphi e^{-S_{bare}[\varphi]-\Delta S_k[\varphi]+J\cdot\varphi} \tag{2.18}$$

The "physical" running effective action Γ_k is related to the Legendre transform $\tilde{\Gamma}_k$ of W_k

$$\tilde{\Gamma}_k = \sup_J \left(J\cdot\phi - W_k[J]\right) \tag{2.19}$$

by

$$\Gamma_k = \tilde{\Gamma}_k - \Delta S_k \tag{2.20}$$

We introduce the "RG time" $t = \ln k$, so that $k\partial_k = \partial_t$; then Γ_k can be shown (see e.g. [54]) to satisfy the ERGE:

$$\partial_t \Gamma_k[\phi] = \frac{1}{2}\mathrm{Tr}\left[(\partial_t R_k)(\Gamma^{(2)}[\phi] + R_k)^{-1}\right] \tag{2.21}$$

It is important to note that as the regulator $R_k(q^2)$ vanishes for $q \gg k$, its derivative $\partial_t R_k$ also vanishes at large q. This means that the contribution of ultraviolet modes to the trace in (2.21) is strongly suppressed.

In practice, it is difficult to solve the flow equation exactly. If we consider the expansion of $\Gamma[\phi]$ in some functional basis $P_i[\phi]$ (e.g. powers of ϕ and its derivatives)

$$\Gamma[\phi] = \sum_{i=1}^{\infty} \bar{g}_i P_i[\phi] \tag{2.22}$$

then we can identify the coefficient of P_i in the expansion of the trace on the right hand side of the flow equation as the beta function $\beta_i(\{\bar{g}_j\})$ for the coupling g_i, and we recover our previous infinite tower of coupled 1st-order partial differential equations (2.5). Thus, solving the flow equation analytically is equivalent to solving this infinite tower of equations.

This does, however, suggest a natural method for obtaining approximate solutions, which is to consider a restriction of the theory space to some finite set of N couplings, so that once the functions β_i have been calculated, the system of equations can be solved via elementary methods. The ERGE thus enters here as a tool for calculating the β_i functions provided that we can evaluate the trace in (2.21). This can be done using e.g. heat kernel methods.

This approach offers the exciting possibility of investigating the *strong coupling* regime where perturbation theory fails. It is particularly well-suited to investigate the asymptotic safety hypothesis, in which we are interested in the *fixed points* of the flow of what has become an N-dimensional vector field $\partial_t \bar{g}_i$ in some N-dimensional *theory space*. A realistic theory of asymptotically safe gravity requires us to find two fixed points connected to each other by the RG flow, one of which at the "infra-red" $k \to 0$ end of the flow must describe the observed world in which gravitational effects are typically extremely weak.

It is, however, natural to wonder to what extent throwing infinitely many terms away affects our answers in the absence of a small expansion parameter. A partial answer to this question can be given based on arguments of *consistency*. One check that can be made is to investigate the dependence of the flow, in particular the location of the fixed points and their corresponding critical exponents, on the specific choice of regulator R_k. Were it possible to include all terms in Γ, then as we have seen above these endpoints

should be independent of this choice; their dependence upon it therefore provides some clue as to how sensitive our picture of the flow is to those terms which we have neglected. Another check that can be performed is to vary the number of terms included; If the flow can be calculated with $N = 6$ and $N = 7$, and the projection of the 7-dimensional flow onto the 6-dimensional subspace formed by setting the seventh coupling to zero is close to that calculated in the 6-dimensional case, then we might be inclined to guess that the flow when $N = 8$ will not be too dissimilar to that we've already calculated, and so on. Some regulators are found to accelerate the convergence of the flow to such a stable picture; this is referred to as *optimising* the flow [56, 57].

In the asymptotic safety scenario, we require that the "ultra-violet" fixed point has a finite-dimensional critical surface. By restricting our attention to a finite dimensional theory space, we seemingly preclude any possibility of finding anything other than a finite-dimensional critical surface! Again, we must appeal to our earlier reasoning, and proceed inductively (in the philosophical rather than mathematical sense). If we find that for some large set of couplings that only the first two are relevant in the UV, then we might guess that they are the only two couplings that are; if we find that every even power of the field is relevant, then we are likely to assume that there are infinitely many UV-relevant terms in the full theory, which we would thus regard as fundamentally "sick" (Weinberg's heuristic argument given above notwithstanding).

Happily, all evidence presently suggests that there exists an ultraviolet fixed point with a three-dimensional critical surface. The most spectacular evidence for this picture came in [27], in which the theory space under consideration was that of polynomials in the Ricci scalar $\sqrt{g}R^n$ of order 35. It was reported there that the UV fixed point existed with a three-dimensional critical surface determined by the cosmological constant, R and R^2, and all higher curvature invariants exhibit their canonical scaling dimension. It has been shown that the fixed point persists in higher dimensions [18, 19, 20, 21] and when gravity is coupled to matter [22, 23, 24, 25, 26]. The reader is referred to review articles [58, 59] for a more detailed overview.

For comparison to our subsequent approximations, it will be helpful to have a relatively simple description of the beta functions for d-dimensional gravity obtained using the ERGE. It was shown in [20] that retaining only the Ricci scalar in the gravitational Lagrangian, the β-function for the dimensionless Newton's constant $g(\mu)$ defined by (2.11) is given by

$$\beta_g = c_d \frac{(1 - 4dg/c_d)(d-2)g/c_d}{1 + 2(2-d)g/c_d} \tag{2.23}$$

where $c_d = \Gamma(d/2+2)(4\pi)^{d/2-1}$. We see that β_g vanishes at the Gaussian fixed point $g = 0$, and at the non-Gaussian value $g_* = c_d/4d$. Associated to each fixed point is a critical exponent θ_{FP}, defined by $d\beta/dg(g_{FP}) = -\theta_{FP}$; these are found to be

$$\theta_G = 2 - d \tag{2.24}$$

$$\theta_{NG} = 2d\frac{d-2}{d+2} \tag{2.25}$$

These have opposite signs, which reflect the fact that the Gaussian fixed point is IR-relevant, whilst the non-Gaussian value fixed point g_* is UV attractive. This flow is readily integrated, so that imposing the boundary condition $g(\mu = \Lambda) \equiv g_\Lambda$, $g(\mu)$ is determined implicitly by

$$\frac{\mu}{\Lambda} = \left(\frac{g(\mu)}{g_\Lambda}\right)^{-1/\theta_G}\left(\frac{g_* - g(\mu)}{g_* - g_\Lambda}\right)^{-1/\theta_{NG}} \tag{2.26}$$

As the theoretical picture becomes increasingly compelling, and calculations of ever-increasing difficulty serve only to confirm this existing picture, investigations into asymptotic safety must now begin to consider whether or not it actually describes the real world. It is to this end that we consider the exciting prospect that quantum gravity may reveal its true nature to us at the LHC.

2.2.3 A practical implementation of asymptotic safety

As discussed in the previous section, the endpoint of an RG flow is described by a functional Γ whose functional derivatives $\delta^{(n)}\Gamma/\delta\phi(p_1)\dots\delta\phi(p_n)$ describe 1PI n-point vertices; using these functions as vertices in tree-level Feynman diagrams is equivalent to the use of bare vertices and summing over Feynman diagrams with different topologies. The computational strategy adopted here, following [40], is to use in this spirit information derived from the RG studies of gravity described in the previous section. We implement the "RG improvement" for the gravitational coupling G_D

$$G_D \to G(\mu) \tag{2.27}$$

using the framework first introduced in [40], via the use of functional ansätze for the field strength renormalization $Z^{-1}(\mu)$ for the graviton. As discussed above in equation (2.11), this renormalization induces a running gravitational constant defined by

$$G(\mu) = G_D Z^{-1}(\mu) \tag{2.28}$$

Diagramatically, this can be viewed as using the exact *propagator* for the graviton between classical vertices encoding the coupling to matter. We assume that the principal effects of

the RG running of gravity can be encoded using a running G_D in this way. A more exact treatment would allow for a separate contribution from the coupling to matter.

We know that at low energies $Z(\mu) \sim 1$, and at high energies we must have $Z^{-1}(\mu) \sim \mu^{-(n+2)}$ (in $d = 4 + n$ dimensions) for there to be a fixed point. The distinction between "low" and "high" energies is parametrised by an energy scale which we call Λ_T. This scale is analogous to the scale $\Lambda_{QCD} \sim 200$ MeV which emerges from the RG dynamics of QCD, and describes the onset of quantum corrections to the canonical scaling of Newton's coupling with energy. In [60] it was shown that this transition between the scaling behaviours becomes narrower as the number of extra dimensions increases, so it is meaningful to say that the transition occurs *at* the scale Λ_T. Taking the limit in which this this transition is infinitely narrow motivates the so-called "quenched" approximation to the running of $Z^{-1}(\mu)$,

$$Z_Q^{-1}(\mu) = 1 + \theta\left(\frac{\mu}{\Lambda_T} - 1\right)\left(\left(\frac{\Lambda_T}{\mu}\right)^{n+2} - 1\right) \tag{2.29}$$

We also find it necessary to use a smoother interpolation between the scaling regimes, which we refer to as the "linear" matching.

$$Z_L(\mu) = 1 + \left(\frac{\mu}{\Lambda_T}\right)^{n+2} \tag{2.30}$$

This parametrisation is similar to that used by Hewett and Rizzo [39]. Those authors, however, treat the 4-dimensional momentum carried by the graviton differently from that in the n-extra dimensions, a point which we will clarify once we have discussed the ADD model in more detail. Both of these parametrisations were introduced in [40].

We compare these ansätze to the flow defined by (2.26) in fig. 2.1. For the sake of consistency we have imposed the boundary condition $g_\Lambda = g_*/2$, using units of Λ_T for the RG scale μ and rescaling the coupling in terms of g_*. We see that the linear running (2.30) in particular provides a good approximation to the full solution of the RG equations. This figure also makes it obvious how the quenched approximation (2.29) consists of an *instantaneous* transition between classical and fixed point scaling of the gravitational coupling.

2.3 Quantum gravity at the LHC

The starting point for the proposal of Arkani-Hamed, Dimopoulos and Dvali [15] is the conjecture that the electroweak scale m_{EW} is the only fundamental scale in nature that relates to all physics known experimentally thus far. In this scenario, the hugeness of M_{Pl} relative to m_{EW} is something that emerges naturally from the model as a consequence

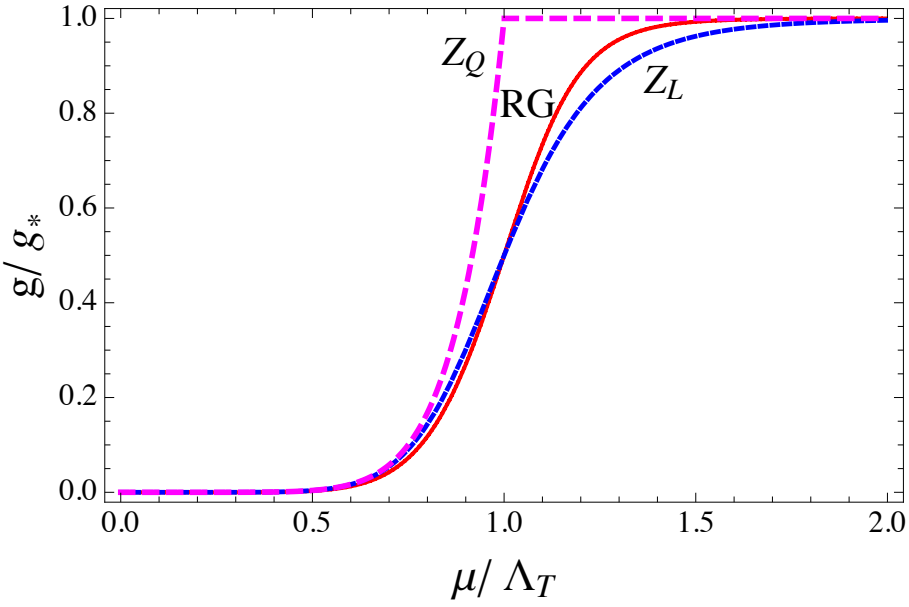

Figure 2.1: Comparison of the analytic solution (red) to the RG equations (2.26) in $n = 6$ to the parametrisations Z_Q (magenta) and Z_L (blue) for the field strength renormalisation factor for the graviton.

of the existence of n extra dimensions, which are compactified with characteristic scale R which can be far larger than previously considered. The novel feature of their proposal is that the Standard Model particles are confined to a four-dimensional hypersurface- the "brane"- in the higher-dimensional "bulk" spacetime, but gravity is not. An heuristic picture for this comes from string theory: one can imagine the standard model particles to be described by "open" strings which are "tied down" to the brane at both ends like the strings on a violin, whilst the gravitons are described by "closed strings"- loops of string like an elastic band which are free to propagate throughout the bulk. This string theory picture is however only heuristic; in their original paper [15] they present a field-theoretic construction in which the brane is a topological defect in a $SU(4) \times SU(2) \times SU(2)$ gauge theory in 6 dimensions. A key hypothesis of the present work is that one can construct a well-defined interacting quantum field theory of gravity that makes sense at all scales; our theory is perhaps most naturally regarded as distinct from string theory, and it is therefore important for our purposes that a purely field-theoretic realisation of the ADD brane is possible.

This means that all previous tests on the dimensionality of spacetime that come from electroweak and strong forces have only probed the dimensionality of the brane. Those tests that derive from gravitational physics- such as the r^{-2} law for gravitation- have only

probed spacetime on much larger scales; at the time of their proposal, it was consistent with existing measurements that the compactification scale R was as large as 1mm, and that sub-milimetre tests of the Newtonian force law would reveal a transition from r^{-2} to $r^{-(2+n)}$ behaviour! Neglecting numerical factors, based on Gauss' law the flux spreading into the compactified dimensions cannot exceed $\sim R^n$, and the corresponding force law becomes

$$\frac{1}{m_{EW}^{2+n}}\frac{m_1 m_2}{r^{n+2}} \xrightarrow{r \gg R} \frac{1}{m_{EW}^{2+n} R^n}\frac{m_1 m_2}{r^2} \tag{2.31}$$

which suggests that the Planck scale is related to m_{EW} and the length scale R as

$$M_{Pl}^2 \sim m_{EW}^{2+n} R^n \tag{2.32}$$

We can see how such a relationship emerges from the underlying field theory by considering a d-dimensional analog of the Einstein-Hilbert action (using the Myers-Perry convention for G_D [61])

$$S = \frac{1}{16\pi G_D}\int d^{4+n}x R \tag{2.33}$$

We now make two assumptions: that the 4-dimensional curvature of the brane is independent of the bulk co-ordinates, and that the extra dimensions are essentially flat. To justify this latter assumption, note that the characteristic energy scale associated with the physics that gives rise to the brane is likely to be $\sim m_{EW}$, so that at distances $r > 1/m_{EW}$ from the brane curvature will be negligible; but our relation (2.32) implies that the radius R of the extra dimensions $\sim (M_{Pl}/m_{EW})^{1/n} 1/m_{EW}$ -i.e. vastly larger than $1/m_{EW}$. Then the bulk volume integral in (2.33) factorises, so that

$$S = \frac{1}{16\pi G_D}\int d^4x R \int d^n y = \frac{V_n}{16\pi G_D}\int d^4x R \tag{2.34}$$

so that we have $G_N V_n = G_D$. We use the conventions of Giudice, Ratazzi and Wells [62], in which R is the radius of the compactified space (which is assumed to be a torus of volume $V_n = (2\pi R)^n$), and define the "fundamental" quantum gravity scale M_D to be such that

$$M_{Pl}^2 = 8\pi R^n M_D^{n+2} \tag{2.35}$$

At this stage in our argument, it is not clear that the lowered Planck mass is of direct experimental relevance from our vantage point on the brane: even if the "fundamental" gravity scale is $M_D \sim 1$ TeV, the four-dimensional theory appears to couple to gravity $\sim 1/M_{Pl}$. However, the four-dimensional observer sees a tower of *Kaluza-Klein* modes of the graviton; we have effectively gained an infinite number of species of graviton, with mass splittings $\Delta m_{KK} = 1/R$. From the d-dimensional point of view, the brane can exchange

momentum in the directions transverse to its orientation with the graviton; an observer who models the brane itself as an infinitely massive and inflexible "brick wall", such as one formulating a 4D effective field theory on the brane, will therefore lose d-dimensional momentum conservation, and bulk momenta will not be constrained at vertices in Feynman diagrams. A more formal way of seeing this is that the *position* of the brane in the bulk *spontaneously* breaks d-dimensional translational invariance; supplanting the bulk with a d-dimensional gravity theory gauges this translational invariance, and the KK modes of the graviton acquire a mass by eating the Goldstone bosons associated with the underlying broken symmetry [63].

The upshot of all of this is that associated to each graviton propagator is a sum over the bulk momenta carried by that graviton. The coupling of any individual KK-mode to the standard model is suppressed by M_{Pl}, and so the experimental signature of graviton emission at collider experiments is missing energy [62]. The energy carried off by gravitons into the bulk also implies astrophysical constraints due to the observed cooling rate of supernova 1987a [64, 65]. These latter constraints are extremely stringent for $n = 2$ (see Table 2.1) but hardly constrain higher dimensions; one finds from (2.35) that if $M_D \sim 1TeV$ the splitting is

$$\Delta m_{KK} \sim 10^{12-31/n}\text{eV} \tag{2.36}$$

so that for e.g. $n = 6$, $\Delta m_{KK} \sim 7$ MeV; the temperature of the supernova is estimated to be around T =30 MeV, and hence only a few modes can be excited. The uncertainty in the supernova temperature implies an uncertainty in the bound, but for $n = 2$ estimates on the bound vary between $10 - 100$ TeV [66]. By contrast, at colliders such splittings are negligible compared to the energy resolution; so unless n is very large, we can well approximate the sum over KK modes by an integral. As $m = n/R$, we have that

$$\sum_{\vec{n}} \frac{1}{p^2 + m_{\vec{n}}^2} \to \frac{1}{R^n} \int d^n m \frac{1}{p^2 + m^2} \tag{2.37}$$

For graviton emission processes, this sum is cut off by the conservation of energy. However, for internal graviton lines we must consider arbitrarily off-shell gravitons, and even a tree-level Feynman diagram featuring graviton exchange becomes associated with a "one-loop" structure. Of course, one finds that these integrals diverge, and we are confronted with the fact that gravity is not a renormalizable quantum field theory. In consequence, the method of regulating these UV divergences manifests itself in physical results. It is common practice, therefore, to introduce an ultraviolet cutoff which is taken to be at a somewhat arbitrary scale $\sim M_D$; this procedure is hoped to give us our "best estimate"

of the order of magnitude of the process' cross-section, together with the shape of the differential cross-section. This was the approach adopted in the papers [67, 62] in which the Feynman rules for the couplings of gravity to the standard model were laid down. In particular, bounds on processes mediated by virtual gravitons are often quoted in terms of the "string scale" M_S in the conventions of [67]; this is related to the scale M_D by [68]

$$M_S = 2\sqrt{\pi}\left[\Gamma\left(\frac{n}{2}\right)\right]^{1/(n+2)} M_D \tag{2.38}$$

It is important to emphasise the nature of this relationship. The authors [67] relate the string scale M_S to the d-dimensional analog of Newton's constant that we refer to as G_D; eq. ((2.38)) reflects the fact that refs. [67] and [62] adopt different definitions of a mass scale relating to G_D. We have used this rescaling to convert bounds quoted in terms of M_S to those on M_D. However, it must also be pointed out that the authors [67] choose M_S to be the scale at which they cut off their KK sum to give meaning to the amplitudes for processes mediated by virtual gravitons. This assumption is impossible to justify in any rigourous way; in the words of the authors of [62], these amplitudes are "not fully calculable", and hence there is a sense in which these bounds are little more than heuristic. It is also important to point out that often people informally refer to the cutoff scale of the KK tower as the 'string scale' being *lower* than M_D, in the expectation that the effective theory breaks down before the fundamental gravity scale; in this sense they are not describing the scale M_S as related to M_D by (2.38), as the numerical factors in that equation actually imply that $M_S > M_D$.

Process	n=2	n=3	n=4	n=5	n=6
$pp \to jj$	1.95	2.43	2.00	1.73	1.53
$pp \to e^+e^-$ or μ+μ^-	1.23	1.42	1.17	1.01	0.9
$pp \to j + \not{E}_T$	5.61	4.38	3.86	3.55	3.26

Table 2.1: Experimental constraints on the scale M_D from collider processes, taken from the CMS review [69]; bounds from ATLAS are comparable [70]. The data come from the $\sqrt{s} = 8$TeV LHC run, with at least L=19.6 fb^{-1} of integrated luminosity. Note that bounds on processes mediated by virtual gravitons are usually quoted in terms of the string scale M_S related to M_D by equation (2.38); we have converted them for consistent presentation here.

In light of this ambiguity, it clearly seems desirable to try and avoid guessing unknowns in our physical predictions. Furthermore, as the LHC is a hadron collider, we are inevitably

sensitive to a wide range of energy scales simultaneously. Whilst our effective field theory approach might be reliable in the "sub-Planckian" regime $\sqrt{s} \ll M_D$, we will encounter signals from the "Planckian $\sqrt{s} \sim M_D$ and even *transplanckian* region $\sqrt{s} \gg M_D$, and so it is clearly desirable to try and say something about these regimes as well. (Note that we are comparing our energy scales to the "fundamental" scale $M_D \ll M_{Pl}$, but the abuse of language in this terminology is conventional.)

In this latter regime it has been observed that general relativity provides an excellent description of gravity at extremely high (astrophysical) centre-of-mass energies [71], provided that we restrict our attention to objects which are well-separated in space. This therefore motivates the application of *semi-classical* approximations, in which we take the general relativistic description of the process under consideration as a starting point. We will discuss these in more detail in the next section. We should, however, conclude our discussion of the phenomenology of the ADD model by mentioning the most spectacular prediction of semiclassical gravity at the LHC: that of black hole production. The phenomenology of such a process typically assumes [72, 73, 74, 50] that for sufficiently large centre-of-mass energies black holes are produced with the geometric cross-section $\sigma \sim \pi R_S^2$, and decay thermally via Hawking radiation [75]; this would produce high multiplicity events with large transverse momentum, and a democratic production of species. This picture is, however, subject to corrections due to the d-dimensionality of the gravity theory [76] and departures from thermality [77]. Studies of asymptotically safe black holes have been carried out in [28, 29, 30, 31], and the corresponding phenomenology investigated in [32]. A further theoretical complication is that it is typically assumed that black holes have a minimum mass (on the order of the fundamental gravity scale), owing to the fact that their Compton wavelength cannot be less than their Schwarzschild radius [78]; for this reason experimental bounds on this signature are usually quoted in terms of a minimum black hole mass rather than constraining the gravity scale [69]. This minimum mass M_{BH} is a slowly decreasing function of M_D and n, and the precise details are model-dependant; however, typical values for values of M_{BH} are around 4.5-6 TeV for M_D in the 1.5-5 TeV region [69].

2.4 High-energy gravitational scattering

2.4.1 Semiclassical gravity

The astrophysical successes of general relativity make it clear that "high energies" and "short distances" are not, in general, the same thing. The combined centre of mass energy of a pair of stars interacting via gravity is incomparably huger than the energy scale of any fundamental physics dreamt up by theorists, and yet the large distances by which they are separated leaves them amenable to a description via well-understood physics. Clearly, our rule of thumb derived from Fourier analysis is inapplicable to such situations, because it is quite wrong to assume that the interaction between e.g. the Sun and the Earth is mediated by a *single* graviton. Rather, we should assume that *arbitrarily many* gravitons are being exchanged in this scenario, each of which carries only a minuscule fraction of the total momentum transferred between the two bodies. The fact that these gravitons are not probing the high-energy behaviour of the theory then leads to the possibility of describing the amplitudes using *semiclassical* approximations. By this, we mean that we will describe the gravitational field purely through the classical Lagrangian (2.33) for d-dimensional gravity, with the corresponding field equations and solutions, and neglecting any other operators that we would usually consider to arise from loop effects. We shall, however, consider loop *diagrams*, but a restricted class of loop diagrams which correspond to the higher orders in perturbation theory in the relativistic quantum mechanics of two particles interacting via a classical gravitational potential. (The meaning of this statement may become more transparent in light of the diagrammatic discussion of section 2.4.2.)

The interplay between the centre-of-mass energy E of a two-body system and the impact parameter b of their collision is nicely summarised in Fig. 2.2 by Giddings' "phase diagram" [1] for gravitational interactions. For any E there exists some sufficiently large b such that the gravitational interaction between two bodies is weak enough to be adequately described by the exchange of a single graviton- the *Born* amplitude. As we lower b, or increase E, it becomes necessary to consider the effects of many-graviton exchange- the *eikonal* regime. The central goal of the present work is to understand the theoretical description of this regime in the ADD framework, and to derive corresponding experimental signatures. The mathematical description of this regime is given by an elastic scattering amplitude $\mathcal{M}_{Eik}$; the "scattering" of the Earth and Moon is given by a pole in this scattering amplitude [1], as per the general framework of bound states in field theory (see e.g. [79]). We defer an explanation of the boundary between the Born and eikonal regimes in fig. 2.2 to the quantitative discussion of this amplitude in section 2.4.2.

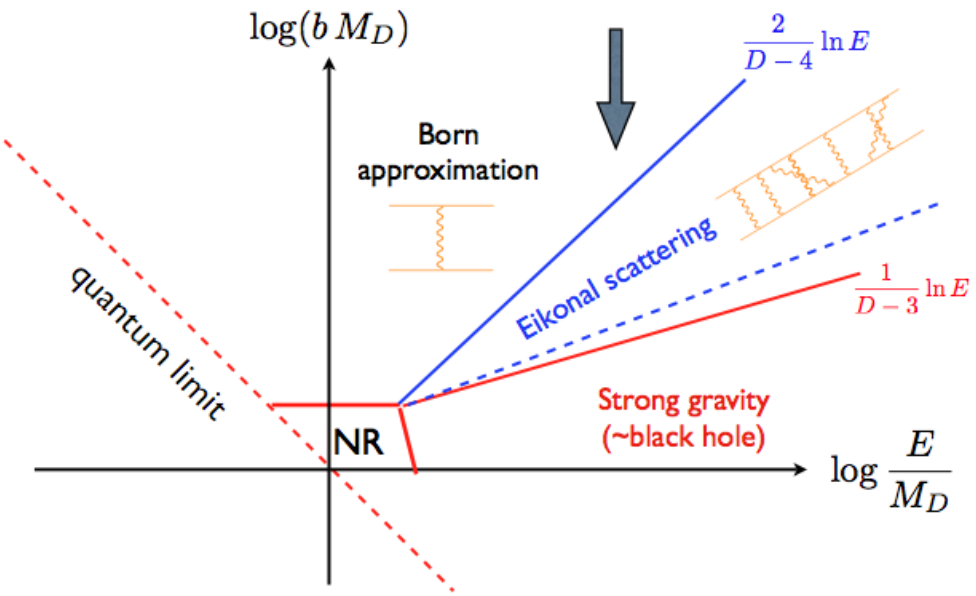

Figure 2.2: Giddings' proposed "Phase diagram" for gravitational scattering; reproduced from [1]. The "quantum limit" is imposed by the uncertainty prinicple $E > 1/b$ in natural units; the boundaries between the other regions are explained in the main text.

If either b is decreased further, or E increased, eventually b becomes equal to the *Schwarzschild radius* corresponding to E, which in D dimensions is given by [61]

$$R_S(E) = \frac{1}{\sqrt{\pi}}\left[\frac{8\Gamma(\frac{D-1}{2})}{D-2}\right]^{1/(D-3)} (G_D E)^{1/(D-3)} \tag{2.39}$$

In the region of the $E - b$ plane for which $b < R_S(E)$ (and b, E are not comparable to the Planck length or mass) we expect a black hole to form, which we might still hope to describe by semi-classical physics. The line $b = R_S(E)$ marks the division between the eikonal and black hole regimes in fig.2.2.

To the extent that the semi-classical approach is valid, the infamous problems of quantum gravity discussed above are thus relegated to the small region of the $E-b$ plane marked 'NR" (for "non-renormalizable") in fig. 2.2, in which both distance and energy scales are Planckian. Of course, anybody who thinks they have a theory of quantum gravity would do well to begin exploring its consequences in regions we believe we understand already. It is in this spirit that we turn our attention to the eikonal amplitude.

2.4.2 The eikonal amplitude

In this section we will derive the so-called *eikonal* amplitude which describes the elastic scattering of particles with asymptotically large centre-of-mass energies that are spatially well-separated. This derivation is quite general: we shall see that all of the physical input from one particular theory is encoded in the Born amplitude $\mathcal{A}_B$ of the theory, and our final form for the amplitude is the result of an argument based on combinatorics and kinematics, which holds as well for electrodynamics as it does for gravity. However, this expression turns out to be particularly useful for applications in gravity, for reasons that will be discussed subsequently. Important early references include [80, 81, 82, 83].

There exists a pretty argument based on unitarity that any 2-2 scattering amplitude for which the cross-section grows with energy must be peaked in the forward direction [79]. Recall the *optical theorem*: that if each particle in the initial state has momentum p and energy E in the centre-of-mass frame, then the total cross-section σ for the process is related to the forward scattering amplitude via

$$\mathrm{Im}\mathcal{M}(s, t = 0) = 2Ep\sigma \tag{2.40}$$

Here we have parametrised our amplitude for the 2-2 process with momenta $p_1, p_2 \to p_3, p_4$ as a function of the Mandelstam variables

$$\begin{aligned} s &= (p_1 + p_2)^2 \\ &= E_{CM}^2 \\ t &= (p_1 - p_3)^2 \\ &= -2p_{CM}^2(1 - \cos\theta_{CM}) \end{aligned}$$

where $E_{CM}, p_{CM}, \theta_{CM}$ are respectively the total energy, the momentum of either particle, and the scattering angle in the centre-of-mass frame. If the differential cross-section $\frac{d\sigma}{d\Omega}$ varies smoothly as a function of the scattering angle, then within some solid angle $\Delta\Omega$ about the variation in $\frac{d\sigma}{d\Omega}$ is bounded; let us agree to choose $\Delta\Omega$ so that $\frac{d\sigma}{d\Omega}$ does not change from its forward value by more than a factor of two. Then

$$\sigma = \int d\Omega \frac{d\sigma}{d\Omega} \geq \frac{1}{64\pi^2 E^2}\frac{1}{2}|\mathcal{M}(s, t = 0)|^2\Delta\Omega \geq \frac{1}{64\pi^2 E^2}\frac{1}{2}|\mathrm{Im}\mathcal{M}(s, t = 0)|^2\Delta\Omega \tag{2.41}$$

Here we have used the simplified form of the relationship between the differential cross-section and the scattering amplitude

$$\frac{d\sigma}{d\Omega} = \frac{|\mathcal{M}|^2}{64\pi^2 E^2} \tag{2.42}$$

for the case where all the particles have the same mass, but this does not affect the final outcome. Using (2.40) this then implies that

$$\Delta\Omega \leq \frac{32\pi^2}{p^2\sigma} \tag{2.43}$$

So we see that unless σ *decreases* with energy faster than $\sim E^{-2}$, the range of solid angle $\Delta\Omega$ into which the final state particles are scattered becomes increasingly narrow as the centre-of-mass energy E increases. As the graviton couples to the energy-momentum tensor of matter, we clearly expect gravitational cross-sections to grow with energy, and hence that scattering is strongly peaked in the forward direction. This suggests that as perturbation theory fails in the transplanckian region $E \gg M_D$, we can instead make an approximation to leading order in the scattering angle, or equivalently in the ratio $-t/s$. This approximation will be used to sum an infinite set of Feynman diagrams corresponding to the exchange of arbitrarily many low-energy gravitons.

In this $s \to \infty$ limit, we should lose little accuracy by neglecting particle masses; our expectation is therefore that the helicity of the colliding particles should be conserved. If we assume that a small momentum transfer corresponds to a negligible change in the separation of the particles in the space transverse to the direction defined by the incoming beam, helicity conservation follows from the conservation of the total angular momentum of each particle. We therefore assume each vertex is diagonal in any spin indices carried by the external particles, and so we lose nothing by deriving our amplitude on the assumption that these particles are scalars. We consider only the three-point vertex in which a matter particle emits or absorbs a graviton, and model this vertex as a function $-iV(p_j)$ only of the momentum p_j of the external particle, neglecting any dependence on the momentum q carried by the exchanged graviton. These vertices may carry spacetime indices that relate to the momentum of the external particles, but such indices will always appear contracted against an index from the other external particle's worldline, and we will leave such sums implicit. It is also convenient in this massless limit to formulate our argument in terms of the lightcone variables, taking the particles to be incident along the x-axis:

$$q^+ = q^0 + q^1 \tag{2.44}$$

$$q^- = q^0 - q^1 \tag{2.45}$$

so that the metric becomes

$$ds^2 = dx^+dx^- - d\mathbf{x}_\perp^2 \tag{2.46}$$

where $-d\mathbf{x}_\perp^2 = dx_2^2 + dx_3^2$ is the squared distance element in the two-dimensional plane

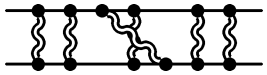

Figure 2.3: A typical ladder diagram, created by J. Schröder, that contributes to the eikonal amplitude. The straight lines represent the participating scattering particles. The wiggly lines represent virtual gravitons.

transverse to the axis defined by the incoming particles. Note that the Jacobian associated with this coordinate transformation has the value $|\mathcal{J}| = 2$.

Within this setup, we can write the Born amplitude (somewhat schematically) as

$$i\mathcal{A}_B(s, t = q^2 \approx -q_\perp^2) = (-i)V(p_1)iD(\mathbf{q}_\perp^2)(-i)V(p_2) \tag{2.47}$$

where $iD(\mathbf{q}_\perp^2)$ is the Feynman propagator for the exchanged gauge boson. We have approximated this as a function of the transverse momentum $\mathbf{q}_\perp$, as in the limit $p_1 \approx p_3$ we have the on-shell condition $p_3^2 \approx p_1 \cdot p_3 = p_1 \cdot (p_1 - q) = -p_1 \cdot q = 0$, and in the centre-of-mass frame $q^0 = 0$ as our scattering is elastic.

Having established the nature of the approximations we are making, we now consider n-gauge boson exchange processes, as described by "ladder" and "crossed ladder" Feynman diagrams of the form typified in figure 2.3. There are $n!$ such diagrams, corresponding to the permutations in which the n momenta q_i emitted in succession from the top worldline of the external particle (which we take to have 4-momentum p^+) can be absorbed by the worldline of the particle travelling in the q^- direction.

Corresponding to this figure is the amplitude

$$\begin{aligned} i\mathcal{M}_{n-boson} &= \sum_{\text{perms } \sigma} (-1)^n V(p^+)^n V(p^-)^n \int \frac{d^4q_1}{(2\pi)^4} \cdots \frac{d^4q_n}{(2\pi)^4} iD(q_1) \ldots iD(q_n) \\ &\times (2\pi)^4 \delta^{(4)}(q_1 + \ldots q_n - q) \\ &\times \frac{i}{(p^+ - q_1)^2} \cdots \frac{i}{(p^+ - q_n)^2} \\ &\times \frac{i}{(p^- - q_{\sigma(1)})^2} \cdots \frac{i}{(p^+ - q_{\sigma(n)})^2} \end{aligned} \tag{2.48}$$

where $\sigma(i)$ represents the action of the permutation corresponding to the specific diagram under consideration; the full n-boson exchange amplitude is described by the sum over such permutations. In the external propagators, we use that the external momenta are on-shell, and neglect terms quadratic in the transferred momentum compared to those which are linear in the external momentum:

$$(p \pm q_i)^2 \approx \pm 2p \cdot q_i \tag{2.49}$$

Throwing away terms of order q_i^2 is permissible even inside an integral over q_i because the propagators $D(q) \sim q^{-2}$; furthermore, so long as we are considering that the overall momentum transfer q^2 is small, any large momentum carried by q_i must be compensated for by a large momentum carried in the opposite direction by q_j, so we expect that the contribution of such large momentum modes will be suppressed by both phase space factors and multiple propagators. By contrast, no such argument yet exists as to why we should throw away $p \cdot q_i$ at this stage in our analysis; the orthogonality of the momentum transfer to the external momenta will rather emerge shortly.

We now make use of the identity [55]

$$\sum_{\text{perms } \sigma} \frac{1}{p \cdot q_{\sigma(1)}} \dots \frac{1}{p \cdot (q_{\sigma(1)} + \ldots + q_{\sigma(n)})} = \frac{1}{p \cdot q_1} \dots \frac{1}{p \cdot q_n} \tag{2.50}$$

For the terms that appear dotted with p^-, this sum over permutations has already appeared as we sum over Feynman diagrams. As our integrand is now symmetric under permutations of the the q_i apart from the propagator factor $(p^+ \cdot q_1) \dots$, permuting the q_i becomes equivalent to relabelling our integration variables, and so we can *average* over permutations to use this identity if we introduce a factor $1/n!$.

Now using [79]

$$\frac{1}{x - i\epsilon} = i\pi\delta(x) + P\left(\frac{1}{x}\right) \tag{2.51}$$

inside an integral (which can be understood from the residue theorem with a pole on the real axis) we can write

$$\frac{i}{2p^{\pm} \cdot q_j} = \frac{i}{2Eq^{\pm}} = -\pi \frac{\delta(q_j^{\pm})}{2E} \tag{2.52}$$

where E is the energy of either particle in the centre-of-mass frame. Here we have thrown away the principal value term because the principal value of the integral

$$\int_{-\infty}^{\infty} dq_+ \frac{1}{q_+} \frac{1}{q_+ q_- - q_\perp^2} \tag{2.53}$$

vanishes. Note that this approach is essentially similar to the use of the Cutkosky rules to put the external particles on-shell directly, which is that taken in [50]; the approach adopted here, however, allows a far more transparent treatment of the gauge boson momenta and the ensuing combinatorics. Note that there are $2(n-1)$ such factors in total, and the overall delta function allows us to set the $q^{\pm}$ components of the final gauge boson momentum equal to those at which we evaluate our amplitude; these we neglect by our earlier argument. Gathering factors and integrating out delta functions, and remembering to include the Jacobian factor of 2 when we change to the $q^{\pm}$ co-ordinates in our

integration measure, we find

$$\begin{aligned}\mathcal{M}_{n-boson}(s,t) &= \frac{i^n}{n!}\frac{1}{(8E^2)^{n-1}}V(p_1)^n V(p_2)^n \int \frac{d^2q_{1,\perp}}{(2\pi)^2}\cdots\int\frac{d^2q_{n,\perp}}{(2\pi)^2}\frac{1}{(2\pi)^2} \\ &\times \quad D(\mathbf{q}_{1,\perp}^2)\ldots D(\mathbf{q}_{n,\perp}^2)(2\pi)^4\delta^{(2)}(\mathbf{q}_{1,\perp}+\ldots\mathbf{q}_{n,\perp}-\mathbf{q}_\perp) \end{aligned} \tag{2.54}$$

Using the integral representation of the delta function,

$$\delta^{(2)}(\mathbf{q}) = \int \frac{d^2b}{(2\pi)^2}e^{i\mathbf{q}\cdot b} \tag{2.55}$$

where $\mathbf{b}$ is the impact parameter vector in the transverse space, and writing $8E^2 = 2s$, we can write this as

$$i\mathcal{M}_{n-boson} = 2s\frac{1}{n!}\int d^2b\left(iV(p_1)\int\frac{d^2q_\perp}{(2\pi)^2}e^{i\mathbf{b}\cdot\mathbf{q}_\perp}D(\mathbf{q}^2)V(p_2)\right)^n e^{-i\mathbf{b}\cdot\mathbf{q}} \tag{2.56}$$

Defining the *eikonal phase* $\chi(b)$ as

$$\begin{aligned}\chi(b) &\equiv \frac{1}{2s}\int\frac{d^2\mathbf{q}_\perp}{(2\pi)^2}e^{i\mathbf{b}\cdot\mathbf{q}_\perp}\mathcal{A}_B(s,t=-q_\perp^2) \\ &= \frac{V(p_1)V(p_2)}{2s}\int\frac{d^2\mathbf{q}_\perp}{(2\pi)^2}e^{i\mathbf{b}\cdot\mathbf{q}_\perp}D(\mathbf{q}^2)\end{aligned} \tag{2.57}$$

we see that

$$\mathcal{M}_{n-boson}(s,t=-q_\perp^2) = 2s\frac{1}{n!}\int d^2b e^{i\mathbf{b}\cdot\mathbf{q}_\perp}(i\chi(b))^n \tag{2.58}$$

This beautifully simple result leads us to sum the infinite series of diagrams for arbitary n, giving the final answer

$$\mathcal{M}_{Eik}(s,t=-q_\perp^2) = -2is\int d^2b e^{i\mathbf{b}\cdot\mathbf{q}_\perp}\left(e^{i\chi(b)}-1\right) \tag{2.59}$$

This derivation makes it clear that the summation of diagrams that leads to the eikonal form is valid independently of the details of theory. At the computational level, we begin with the Born amplitude of the theory (2.47), work out the corresponding eikonal phase χ defined by (2.57), and plug it into the general formula (2.59). This generality will be of use in the next chapter to us when we consider the different approaches to dealing with the tree-level divergences of the Born amplitude in the ADD scenario.

In light of our earlier discussion about forward scattering and unitarity, it is interesting to note that the the eikonal amplitude satisfies the optical theorem (2.40) if the eikonal phase χ is real; (2.40) implies that

$$\sigma = \frac{\mathrm{Im}\mathcal{A}_{eik}(s,0)}{s} = 2\int d^2b(1-e^{-\mathrm{Im}\chi}\cos\mathrm{Re}\chi) \tag{2.60}$$

Whilst in the massless limit our kinematic assumptions imply the relation

$$\frac{d\sigma}{dt} = \frac{|\mathcal{M}_{Eik}|^2}{64\pi sp^2} = \frac{|\mathcal{M}_{Eik}|^2}{16\pi s^2} \tag{2.61}$$

and hence

$$\begin{aligned}\sigma &= \int dt \frac{d\sigma}{dt} \\ &= \frac{1}{16\pi s^2}\int dt|\mathcal{M}_{Eik}|^2 \\ &= \int d^2b(1+e^{-2\mathrm{Im}\chi}-2e^{\mathrm{Im}\chi}\cos\mathrm{Re}\chi)\end{aligned}$$

Thus we see that if χ is real, then the eikonal will satisfy the optical theorem [50]. This can be understood in the following way. It will frequently be convenient to make use of the identity

$$\int d^n y e^{i\mathbf{x}\cdot\mathbf{y}} f(y) = \frac{(2\pi)^{n/2}}{x^{n/2-1}}\int_0^\infty dy y^{n/2} J_{n/2-1}(xy) f(y) \tag{2.62}$$

so that we can write (2.59) as

$$\mathcal{A}_{eik} = -4\pi i s \int dbbJ_0(qb)(e^{i\chi}-1) \tag{2.63}$$

It is instructive [84, 85] to compare this to the partial wave expansion of the scattering amplitude of a particle with momentum k from a potential:

$$f(\theta) = \sum_{\ell=0}^{\infty}(2\ell+1)\frac{e^{2i\delta_\ell}}{2ik}P_\ell(\cos\theta) \tag{2.64}$$

In the limit of large k, b presently under discussion, $\ell = kb$ is large. Furthermore, this limit is "semiclassical" in the sense that the spacing $\sim \hbar$ between angular momentum eigenstates becomes negligible compared to the large angular momenta under consideration, so that the sum can be replaced by an integral. Using the asymptotic behaviour of the Legendre polynomial in ℓ, $P_\ell(\cos\theta) \sim J_0(\ell\theta) \sim J_0(bq)$ (where we have approximated $\theta = q/k$), so that we have

$$f(\theta = q/k) \to -ik\int dbbJ_0(bq)(e^{2i\delta(b)}-1) \tag{2.65}$$

We see that χ acquires the interpretation of a phase shift, and the eikonal amplitude a sum over *all* partial waves which happens to be dominated by large angular momentum modes; this explains its unitarity so long as the phase shifts are real. In [86] the boundary between the elastic and black hole regions of fig. 2.2 was investigated by allowing the phase shifts to become complex, as black hole production is expected to be a highly inelastic process due to Hawking radiation.

It is also instructive to compare (2.57) to the relationship between the Born amplitude and the classical potential $V(\mathbf{x})$ [55]:

$$\mathcal{A}_B = -i\int d^3x V(\mathbf{x})e^{-i\mathbf{x}\cdot\mathbf{p}} \tag{2.66}$$

So we see that χ, as well as having the interpretation of a phase shift, will be closely related to the classical potential experienced by each particle due to the interaction. The difference is that in(2.57) the Fourier transform is only taken over the transverse co-ordinates to the beam axis; this can be understood if it is recognised that the phase shift results from integrating the potential experienced by a particle along its worldline.

Having discussed the eikonal amplitude in some generality, it is now perhaps appropriate to specify its particular relevance for gravity. As we have already observed, we expect based on our unitarity argument that forward scattering will be particularly relevant for gravity, as the cross-sections are expected to grow with energy. This is visible, for example, in the Born amplitude derived from an Einstein-Hilbert Lagrangian minimally coupled to matter, which in spacetime of arbitrary dimension takes the form [1]

$$\mathcal{A}_B(s,t) = -\frac{8\pi G_D s^2}{t} \tag{2.67}$$

As expected, we see that this grows strongly with s, and decays with t. The eikonal phase corresponding to (2.67) according to (2.57) is given by [1]

$$\chi(b,s) = \frac{4\pi}{nS_{n+2}} \frac{G_D s}{b^n} \tag{2.68}$$

where the factor

$$S_n = \frac{2\pi^{n/2}}{\Gamma(n/2)} \tag{2.69}$$

is the area of the n-dimensional unit sphere. We see from this equation that the dividing line between Born and eikonal regions in fig. 2.2 corresponds to the requirement that the modulus of $|\chi| \gtrsim 1$; for $|\chi| < 1$ we can expand the exponential in (2.59) in a series, the leading order term of which merely reproduces the Born amplitude.

To assess the validity of the approximation, we can also compare the relative contributions of the Feynman diagrams that are and are not included in the eikonal amplitude, at any fixed order in perturbation theory. This does of course require that one has a way of making sense of the diagrams which would ordinarily contain divergences, but such a programme has been undertaken in supergravity [87] and string theory [88], where it was found that the ladder and crossed ladder diagrams do indeed dominate those which are neglected. The eikonal amplitude and its leading corrections have been extensively investigated in string theory, [89, 90, 91, 92].

Furthermore, the eikonal amplitude for gravity has been shown to have a semi-classical interpretation. One of the early works that pioneered the use of semi-classical approximations at high energies was that of t'Hooft [6], who derived the elastic scattering amplitude

of a particle in response to the shockwave in an Aichelburg-Sexl metric [93]:

$$U(s,t) = \frac{\Gamma(1 - iG_N s)}{4\pi\Gamma(iG_n s)} \left(\frac{4}{-t}\right)^{1-iGs} \tag{2.70}$$

Kabat and Ortiz showed [8] that the eikonal amplitude for gravity, using (2.67) in $d = 4$ for the Born amplitude, is equivalent to this result (up to a choice of scale for a "graviton mass" introduced to regulate infrared divergences). It is interesting to note [6] that the absolute value, and hence the cross-section, of this expression is exactly identical to that of (2.67).

This completes our survey of the concepts necessary to understand the present work in context. We now turn our attention to the study of the eikonal regime at the LHC, if asymptotically safe quantum gravity is allowed to reveal itself by through the existence of large extra dimensions.

Chapter 3

Quantum gravity in the eikonal

In this chapter, we investigate the scattering amplitudes which describe transplanckian scattering if gravity probes a higher-dimensional spacetime whilst the colliding particles are confined to a 3+1-dimensional brane. We begin in section 3.1 by assessing the claim made in the literature [1, 8, 50] that the eikonal approximation is independent of the UV completion of the theory. We will demonstrate that there is good reason to question this hypothesis in the ADD framework, and argue that we are therefore compelled to describe the process using a genuine theory of quantum gravity. We then seize this exciting opportunity to explore the physics of asymptotically safe gravity. In section 3.2 we use the computational framework first presented in [40] to provide a practical approach to calculating these amplitudes. We will explore how sensitive our results are to the different approximations to the RG evolution of the gravitational coupling $G(\mu)$. In section 3.3 we explore the underlying reasons for the failure of the arguments offered in support of the expectation that semiclassical physics could be applied, using the techniques of the stationary phase approximation.

3.1 Semiclassical gravity?

In this section we explore methods of computing the eikonal scattering amplitudes that seek merely to parametrise our ignorance of the underlying gravity theory. As discussed in the preceding chapter, the calculation of the eikonal amplitude proceeds in essentially three steps: compute the Born amplitude of the theory; work out the corresponding eikonal phase $\chi(b)$ via (2.57); and insert the result into (2.59) to compute the eikonal amplitude $\mathcal{M}_{eik}$ itself.

3.1.1 Born amplitude

As discussed in section 2.3, in the ADD scenario there are infinitely many KK modes of the graviton, and the Born amplitude for a "single graviton exchange" sums over the entire KK tower. The corresponding Feynman diagrams do however have an identical topology to those of more familiar frameworks, and we can still talk about processes occurring in the "x-channel", where $x = s$, t or $u = -s - t$ is one of the Mandelstam variables. The Born amplitude in the x-channel may be written in the form $\mathcal{A} = \mathcal{S}(x) \cdot \mathcal{T}$ [62], where

$$\mathcal{T} = T^{\mu\nu}T_{\mu\nu} - \frac{1}{n+2}T^{\mu}_{\mu}T^{\nu}_{\nu} \tag{3.1}$$

is a function of the energy-momentum tensor $T^{\mu\nu}$ of the theory, and n is the number of compactified extra dimensions; and

$$\begin{aligned} S(x) &= \frac{1}{M_D^{n+2}} \int \frac{d^n m}{x - m^2} \\ &= \frac{1}{M_D^{n+2}} \frac{2\pi^{n/2}}{\Gamma(n/2)} \int dm \frac{m^{n-1}}{x - m^2} \end{aligned} \tag{3.2}$$

in which we have assumed that the spacing between the Kaluza-Klein masses m is well below our experimental resolution, such that we may replace the sum by an integral for analytic convenience. We will restrict our attention to t-channel processes, such that the denominator of the integrand 3.2 never vanishes as $t < 0$. This form is convenient because the coupling of the graviton to matter is independent of the KK mode under consideration, so that we may perform the sum $\mathcal{S}(x)$ over KK masses without specifying any particular $2 \to 2$ process; the details of a particular field content for our theory are encoded in $\mathcal{T}$. At sufficiently high energies, we may neglect both non-gravitational interactions and the masses of our particles; then T^{μ}_{μ} vanishes, and the matrix element of $T^{\mu\nu}$ between momentum eigenstates is simply [50]

$$\langle p|T^{\mu\nu}|p\rangle = 2p^{\mu}p^{\nu} \tag{3.3}$$

$\mathcal{T}$ then contributes a factor $(2p_1^{\mu}p_1^{\nu})(2p_{2,\mu}p_{2,\nu}) = s^2$. For subsequent convenience we define

$$C = \frac{s^2}{M_D^{n+2}} S_n \tag{3.4}$$

The integral (3.2) exhibits a logarithmic divergence for $n = 0$, but setting $n = m = 0$ and not doing the integral reproduces the Born amplitude of the Einstein-Hilbert action. In 2 or more extra dimensions the integral is UV divergent, and therefore requires regularization. In existing literature this has been done via dimensional regularization [50], a sharp UV

cut-off in effective field theory [62, 67], and by modelling the brane as a dynamical object with a finite width [94].

In $n = 2$ the regularised integrals also diverge as $q \to 0$; as our principal interest is in the ultraviolet physics of gravity, we will generally restrict our attention here to $n > 2$.

Dimensional Regularisation

In [50] the authors exploit the convergence of (3.2) for $0 < n < 2$ to obtain a result which may be analytically continued to a wider range of n:

$$\begin{aligned} \mathcal{A}_{DR} = C \int dm \frac{m^{n-1}}{t - m^2} &= -C(-t)^{n/2-1} \frac{1}{2} \int dx \frac{x^{n/2-1}}{1+x} \\ &= -\frac{s^2}{M_D^{n+2}} \pi^{n/2} (-t)^{n/2-1} \Gamma(1 - n/2) \end{aligned} \tag{3.5}$$

We have corrected this result for a minus sign not present in [50]. This has poles for even integers $n > 2$ but is otherwise well-behaved. Note that for $n \geq 2$ this is an *increasing* function of momentum transfer $q = \sqrt{-t}$, wheras for $0 < n < 2$ where the integral converges it is a *decreasing* function, as would be required for forward scattering to dominate. The use of this amplitude as the starting point for an eikonal calculation has thus been criticised in [94]. This behaviour can be understood on dimensional grounds- in the absence of a cutoff scale Λ, the momentum transfer $\sqrt{-t}$ provides the necessary powers of energy to keep the amplitude dimensionless. The fact that the Born amplitude contains no such scale means that the eikonal amplitude should in principle allow one to make predictions that constrain M_D directly; however, this argument only holds on the assumption that the eikonal amplitude is insensitive to the details of how the Born amplitude is regulated. This will be discussed in much greater detail below.

Effective Field Theory

In order to better understand how dimensional regularisation works, it is instructive to compare it to the results obtained by imposing a sharp UV cutoff in the integral in (3.2):

$$\int_0^{\Lambda} dm \frac{m^{n-1}}{t - m^2} = \frac{\Lambda^n}{nt} F(1, n/2, 1 + n/2, \Lambda^2/t) \tag{3.6}$$

so that

$$\mathcal{A}_{EFT} = C \frac{\Lambda^n}{nt} F(1, n/2, 1 + n/2, \Lambda^2/t) \tag{3.7}$$

Here and throughout, F denotes the hypergeometric function ${}_2F_1$.

The hypergeometric function is defined by the series expansion (B.6). We may expand F in this series, and partially re-sum it for the cases where n is definitely odd or even, to

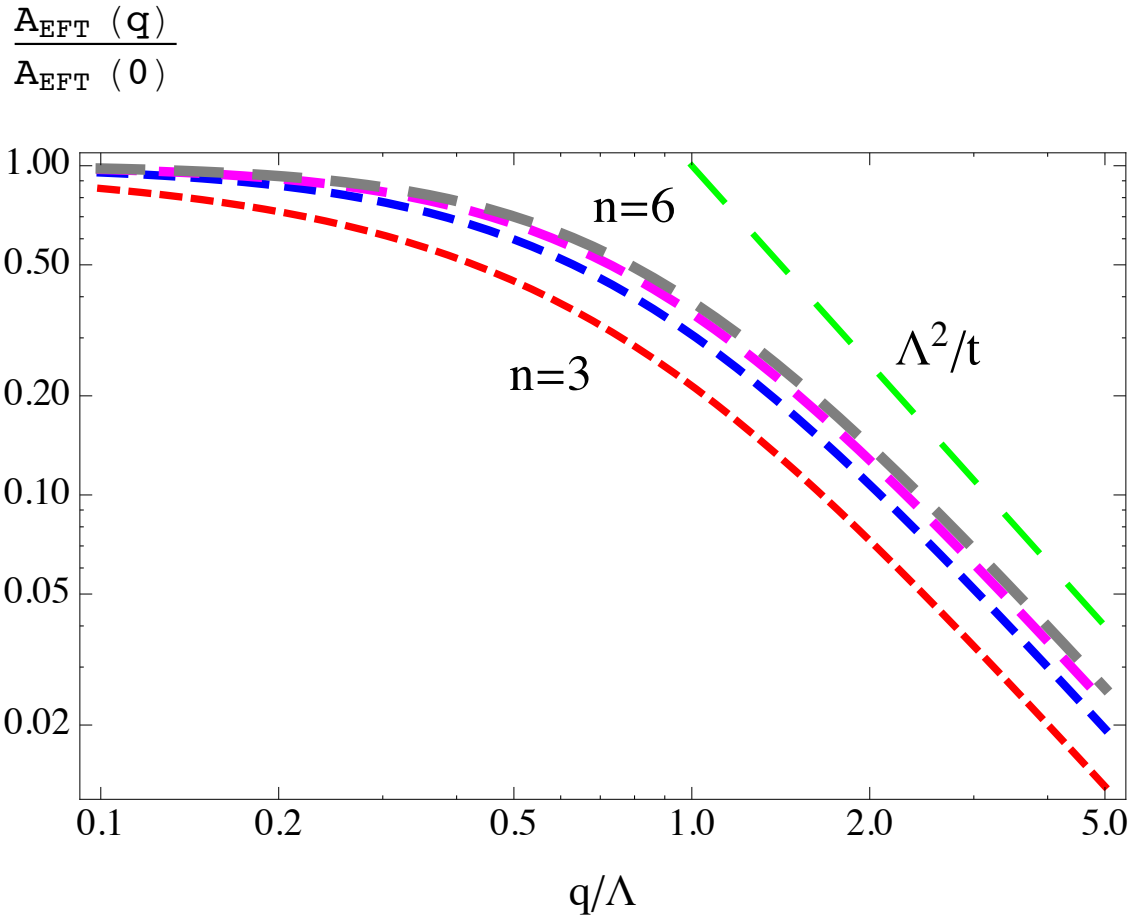

Figure 3.1: The Born Amplitude with a sharp UV cutoff for different numbers n of extra dimensions: n=3 (red), 4 (blue), 5 (magenta), 6 (grey). Each has been normalised to the value of each amplitude at $t = 0$; note that this procedure removes the dependence of the amplitudes on the values of the dimensionful parameters s,M,Λ except insofar as that Λ sets the scale on the horizontal axis. For comparison we also plot the asymptotic limit $\sim \Lambda^2/t$ (green).

recover the expansions presented for the cut-off amplitudes in [62, 67]:

$$F(1, n/2, 1 + n/2, \Lambda^2/t) = n \left(\frac{-t}{\Lambda^2}\right)^{n/2} \times \tag{3.8}$$
$$\begin{cases} -\frac{1}{2}\left[(-1)^{n/2} \ln\left(1 - \frac{\Lambda^2}{t}\right) + \sum_{j=1}^{n/2-1} \frac{1}{j}\left(\frac{\Lambda^2}{t}\right)^j\right] & \text{if } n \text{ is even} \\ (-1)^{(n-1)/2}\left[\tan^{-1}\left(\frac{\Lambda}{\sqrt{-t}}\right) - \sum_{j=0}^{(n-1)/2-1}(2j+1)^{-1}(-1)^j \sqrt{\left(\frac{\Lambda^2}{t}\right)}^{2j+1}\right] & \text{if } n \text{ is odd} \end{cases}$$

To understand how this is related to dimensional regularisation, we use the identity (B.9) so that *for odd* n we have

$$\mathcal{A}_{EFT} = \mathcal{A}_{DR} - C\frac{\Lambda^{n-2}}{n-2} F\left(1, 1 - \frac{n}{2}; 2 - \frac{n}{2}; \frac{-t}{\Lambda^2}\right) \tag{3.9}$$

The first term is the amplitude of dimensional regularisation, and is independent of Λ, whilst the second term diverges in the limit $\Lambda \to \infty$. We therefore see that dimensional regularisation corresponds to an infinite subtraction, as noted in [94], and that the t-dependence of the subtracted term totally changes the behaviour of the amplitude as a function of t.

As $F(\alpha, \beta; \gamma; 0) \equiv 1$, for large $-t \gg \Lambda^2$ we have that

$$\mathcal{A}_{EFT} \xrightarrow{-t/\Lambda^2 \to \infty} C\frac{\Lambda^n}{nt} \tag{3.10}$$

In the limit $-t/\Lambda^2 \to 0$, each term in the series expansions (3.8) vanishes; isolating the the terms of order $-t/\Lambda^2$, which have the same coefficient in even and odd n, we find:

$$C\frac{\Lambda^n}{nt}F(1, n/2, 1 + n/2, \Lambda^2/t) \xrightarrow{-t/\Lambda^2 \to 0} -C\frac{\Lambda^{n-2}}{n-2} \tag{3.11}$$

Note that as this limit is finite and independent of t, scattering at 4-momentum transfers that are small compared to Λ is *isotropic*; in terms of the Mandelstam variables, the channels s-, t- and u- all make comparable contributions to the amplitude [95]. It is often parametrised on dimensional grounds in terms of an effective mass M_{eff} as

$$S(x = 0) = -\frac{4\pi}{M_{\text{eff}}^4} \tag{3.12}$$

The limiting behaviour of $\mathcal{A}_{EFT}$ as $t \to 0, -t \to \infty$ is also easily observed from the defining integral 3.6.

3.1.2 Eikonal Phases

The defining relation (2.57) can be conveniently re-written using the expression (2.62), so that

$$\chi(b, s) = \frac{1}{4\pi s}\int_0^\infty dqqJ_0(qb)\mathcal{A}_B(s, t = -q^2) \tag{3.13}$$

Dimensional Regularisation

Corresponding to the Born amplitude (3.6) the authors [50] found that

$$\begin{aligned} \chi_{DR} &= -\frac{1}{4\pi s}\frac{s^2}{M^{n+2}}\pi^{n/2}\Gamma(1 - n/2)\int dqq^{n-1}J_0(qb) \\ &\equiv -\left(\frac{b_c}{b}\right)^n \end{aligned} \tag{3.14}$$

Passing from the first to the second line uses the result (B.1). (This result differs from that in [50] by the same minus sign as that in (3.6).) The parameter

$$b_c = \left(\frac{(4\pi)^{n/2-1}\Gamma(n/2)s}{4M^{n+2}}\right)^{1/n} \tag{3.15}$$

is the length scale at which χ_{DR} becomes of order one, and hence dictates when the eikonal is relevant. There are a number of important facts to appreciate about this result.

The first point to note is that $\chi_{DR}(b)$ is well-defined in all numbers of extra dimensions n, despite the fact that it has been derived via a Born amplitude that diverges for all even n. The second, particularly in light of (2.66), is the striking similarity between $\chi(b) \sim b^{-n}$ and a Newtonian potential $V(r) \sim r^{-(n+1)}$. In [96] it was shown that this result was equivalent to that obtained by exchanging the orders of integration in the Fourier transform in (2.57) and in the Born amplitude. Of course, this procedure is only strictly legitimate when both integrations are absolutely convergent. As discussed above, this will be the case when $0 < n < 2$. In fact, this is also the result obtained for χ in d flat dimensions [1].

There are two possible viewpoints that we might adopt regarding this result. The first is that although our regularisation process might appear to be mathematically suspect, it is physically reasonable that we have recovered the semiclassical result (3.15) in the context of a semiclassical calculation. However, we do not find this argument persuasive. It is easy to imagine that the effective potential that arises from integrating over all modes differs in some respect from the classical potential, and the KK tower certainly probes high-energy modes. We have seen in our discussion of the Born amplitude that dimensional regularisation amounts to an infinite subtraction. Looking at this result, it appears as if that subtraction amounts to the contribution of the entire KK tower! It therefore seems worthwhile to consider the eikonal phase with a cutoff imposed upon the KK tower, to see how this modifies our results.

Effective Field Theory

We calculate the eikonal phase for effective field theory by exchanging the order of integration of m and q. Note that in contrast to the dimensionally regularised case, all of our integrals are now absolutely convergent for finite Λ, and hence this procedure should not affect the final outcome. We thus find

$$\begin{aligned}
\chi_{EFT} &= -\frac{C}{4\pi s}\int_0^\Lambda dm m^{n-1}\int dq J_0(qb)\frac{q}{q^2+m^2} \\
&= -\frac{C}{4\pi s}\int_0^\Lambda dm m^{n-1}K_0(mb) \qquad (3.16) \\
&= -\frac{s\Lambda^n}{M_D^{n+2}}\frac{\pi^{n/2-1}}{2n^2}\left(\beta K_1(\beta){}_1F_2\left(1;1+\frac{n}{2},1+\frac{n}{2};\frac{\beta^2}{4}\right)\right. \\
&+ \left. nK_0(\beta){}_1F_2\left(1;1+\frac{n}{2},\frac{n}{2};\frac{\beta^2}{4}\right)\right) \qquad (3.17)
\end{aligned}$$

where we have defined $\beta = b\Lambda$.

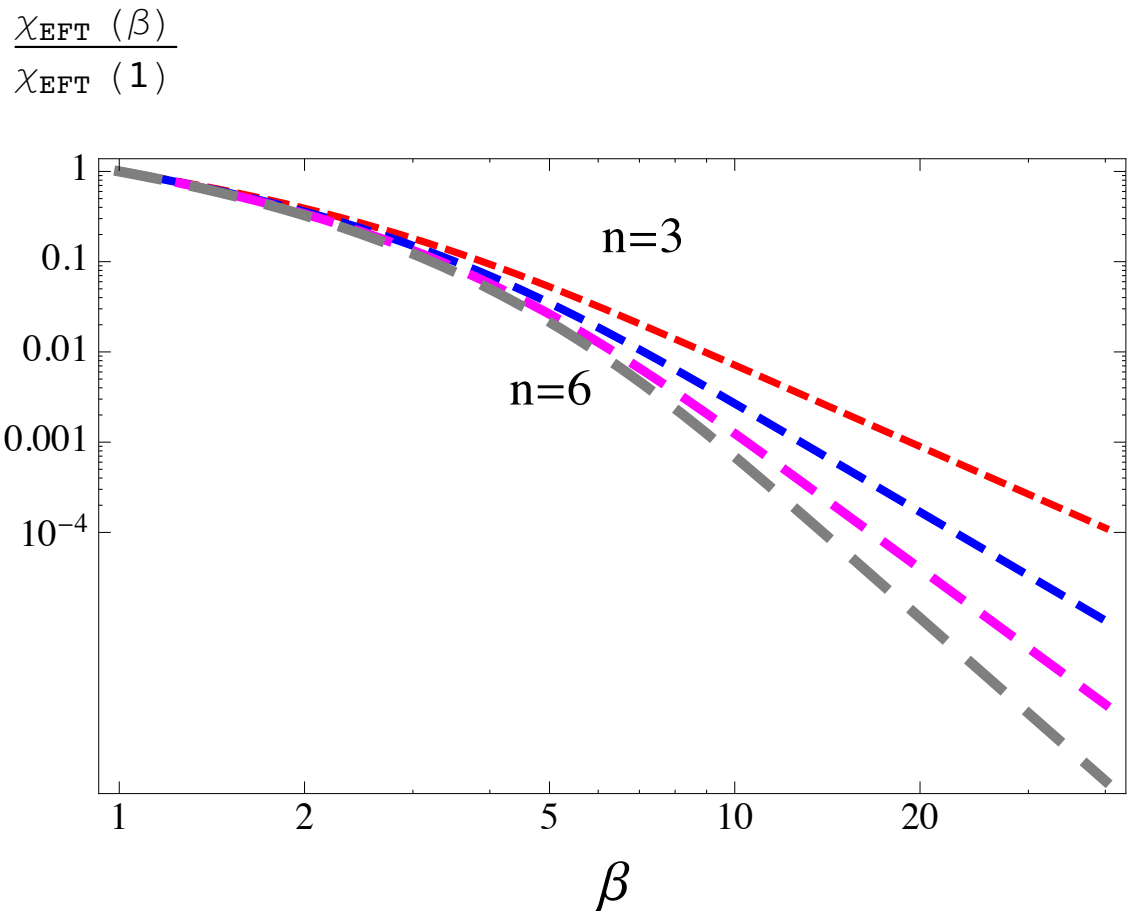

Figure 3.2: The eikonal phase in effective field theory for n varying from 3 to 6 (top to bottom), normalised to its value at $b = 1/\Lambda$. Note the variation of the scaling behaviour with n for large $\beta = b\Lambda$.

At $\beta = 0$, the hypergeometric series truncate to 1; the behaviour of χ_{EFT} at small impact parameters is therefore dominated by the modified Bessel functions $K_\nu(\beta)$. Using the series expansion (B.4) for K_ν at small arguments we see that

$$K \sim \log \beta \tag{3.18}$$

so we see that the short-distance behaviour of χ_{EFT} is dominated by a logarithmic divergence from the function $K_0(\beta)$.

For large impact parameters, we use the asymptotic expansions (B.5), (B.10) of the K_ν and ${}_1F_2$ functions to recover the expected behaviour

$$\chi_{EFT}(b) \sim -\left(\frac{b_c}{b}\right)^n \tag{3.19}$$

where b_c is defined as above, and we have neglected terms of order $e^{-\Lambda b}$. This limit was recovered in [97] by direct asymptotic expansion of eq. (3.16).

To what extent then is the eikonal phase χ independent of the regulator used in $\mathcal{A}_B$? This appears to depend on the relative contributions of the length scales greater or less than $\sim 1/\Lambda$. The authors [97] numerically integrated the eikonal amplitude using (3.16) with $\Lambda = M_D = 1\text{TeV}$ and for dimensional regularisation, and found little difference. However, that was in the context of the eikonal scattering of neutrinos from cosmic rays off neutrinos, with a centre-of-mass energy $\sqrt{s} \sim 10^{10}$ GeV rather higher than those accessible at the LHC. As the largeness of the centre of mass energy was crucial to the semi-classical rationale behind the eikonal, it seems worthwhile checking the regulator dependence of the eikonal amplitude at the LHC explicitly.

3.1.3 Eikonal amplitude

We now consider the eikonal amplitude corresponding to (3.15) and (3.17) in turn, to see to what extent the full eikonal amplitude is sensitive to the procedure used to define $\mathcal{A}_B$.

Dimensional Regularisation

Using the eikonal phase (3.15) we write

$$\begin{aligned}
\mathcal{M}_{DR} &= -4\pi i s \int dbbJ_0(qb)(e^{-i\left(\frac{b_c}{b}\right)^n} - 1) \\
&= -4\pi i s b_c^2 \int_0^\infty dx x J_0(xy)\left(e^{-ix^{-n}} - 1\right) \qquad (3.20) \\
&\equiv 4\pi s b_c^2 F_n(b_c q) \qquad (3.21)
\end{aligned}$$

It was shown in [98] that the functions F_n can be expressed in terms of Meijer-G functions. Correcting for various minus signs, we find that

$$\begin{aligned}
F_n(y) &= \frac{2^{-2/n-1}}{n}\left(R_n(y) + I_n(y)\right) \qquad (3.22) \\
R_n(y) &= G^{n+1,0}_{0,2(n+2)}\left(\frac{y^{2n}}{2^{2n+2}n^{2n}}\middle|_{0,\frac{n-2}{2n},\frac{1}{n},\ldots,\frac{n-1}{n},-\frac{1}{n},0,\frac{n-1}{n},\frac{n-2}{n},\ldots,\frac{1}{n}}\right) \qquad (3.23) \\
I_n(y) &= G^{n+1,0}_{0,2(n+2)}\left(\frac{y^{2n}}{2^{2n+2}n^{2n}}\middle|_{0,\frac{1}{n},\ldots,\frac{n-1}{n},\frac{n-1}{n},-\frac{1}{n},0,\frac{n-2}{2n},\frac{n-2}{n},\ldots,\frac{1}{n}}\right) \qquad (3.24)
\end{aligned}$$

We plot this in fig. 3.3 for different values of n. We note immediately that this regularisation scheme does not exhibit the same correspondence between the Born and Eikonal differential cross-sections that is found in ordinary four-dimensional gravity. The eikonal amplitudes shown here clearly demonstrate that forward scattering dominates, wheras the Born term (3.6) grows indefinitely as a function of q.

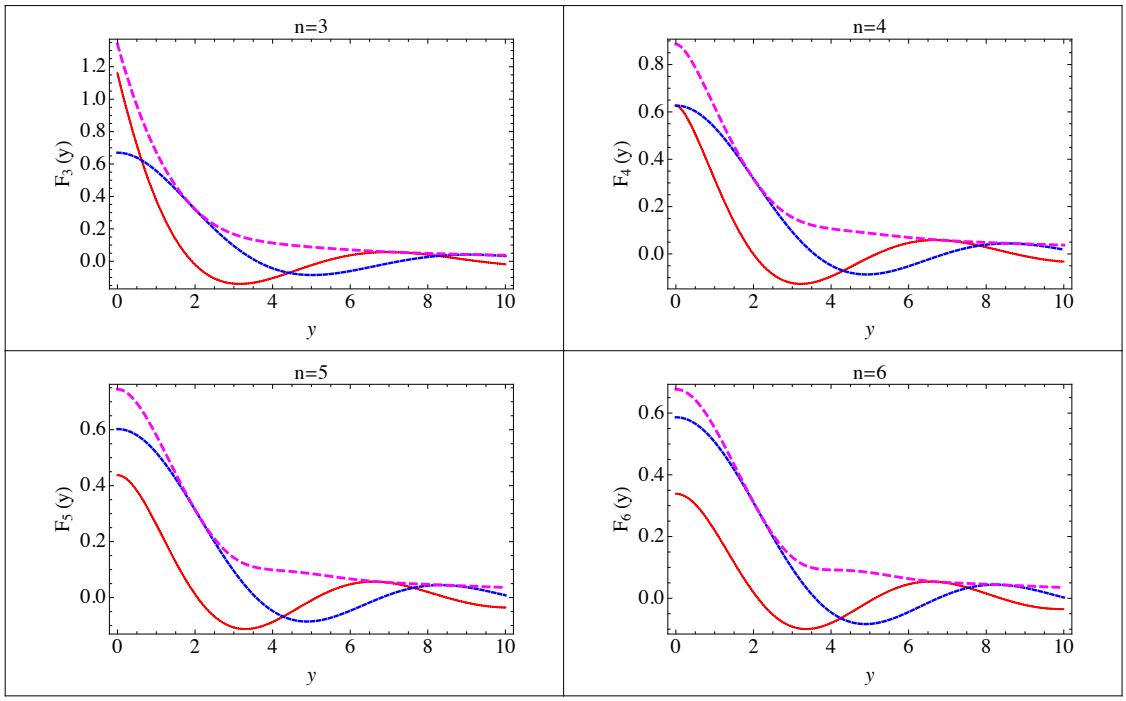

Figure 3.3: The functions $F_n(y)$ for the labelled values of n. The real parts are shown in red, the imaginary parts in blue, and the absolute values in magenta.

Effective Field Theory

For the more complicated eikonal phase corresponding to a sharp cutoff no corresponding closed form expression appears to exist. Figure 3.4 compares the dimensionally regularised result to the numerical integration of

$$\mathcal{M}_{EFT} = -4\pi i s \int dbbJ_0(qb)(e^{i\chi_{EFT}} - 1) \tag{3.25}$$

where χ_{EFT} is given in (3.17). We see that for $\Lambda \sim M_D$ at typical LHC energies there can be a factor of 2 difference between dimensional regularisation and effective field theory at small angles. This explicitly demonstrates that the eikonal amplitude is sensitive to our treatment of the Born amplitude. In [50] they allow for the possibility that quantum gravity effects might significantly alter their signal, but claim that the eikonal amplitude should nonetheless be insensitive to the regularisation procedure.

The fact that we cannot systematically and consistently eliminate the contribution of short-distance modes to physical results suggests that we are forced to confront the physics of the high energy scale directly. There are two candidates for the unknown physics: that which gives rise to the 3-brane, and that which solves the problems of quantum gravity. Phenomenological parametrisations of ascribing a thickness or tension to the brane yield an eikonal phase with a similar behaviour to that found in effective field theory [94]. Our

interest arises from the other possibility: that the LHC may offer us the opportunity to probe the physics of quantum gravity. Whilst the string corrections discussed in [50] are incalculable, in asymptotic safety a practical method for investigating the underlying theory of quantum gravity has already been outlined. The remainder of this work will be dedicated to understanding how asymptotic safety might reveal itself in this scenario.

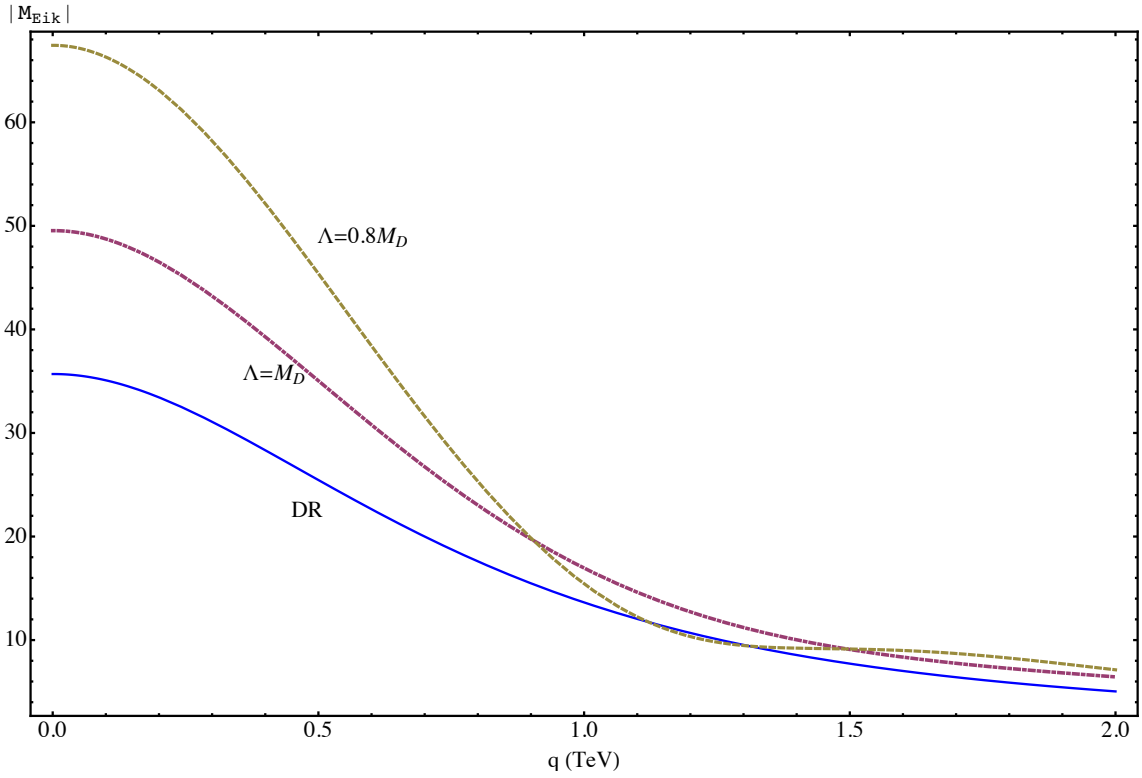

Figure 3.4: In this figure we compare the eikonal amplitude obtained via dimensional regularisation (blue) to that derived in effective field theory with $\Lambda = 0.8M_D$ (yellow) and $\Lambda = M_D$ (red). We have used the reference values of $\sqrt{s}$ =9 TeV; $M_D = 1.5$TeV in $n = 6$. Note that as the DR amplitude makes no reference to the scale Λ we have plotted our momentum transfer in units of TeV.

3.2 RG improvement

We now begin our investigation of asymptotically safe scattering amplitudes, using the parametrisations (2.29), (2.30) for the running gravitational constant. Implementing an RG improvement necessitates making a connection between the RG scale μ and some momentum scale in our physical problem. We will take μ to be the d-dimensional graviton momentum, so that

$$\mu^2 = -t + m^2 \tag{3.26}$$

As this matching depends on the KK mass m of the graviton, we must include the factor $Z^{-1}(\mu)$ inside our integrals over the bulk momenta of exchanged gravitons. Our approach therefore differs from that of Hewett and Rizzo [39], who use a parametrisation for $Z^{-1}(\mu)$ equivalent to (2.30), but only match the RG scale to the four-dimensional momentum transfer.

Further to the discussion in section (2.2.3), we also emphasise that we are treating the underlying gravity theory as that of d-dimensional spacetime, with no regard to the ADD construction. This is very much in keeping with the spirit of the model, but it is anticipated that there is at least one effect specific to this scenario that we neglect. Clearly, at very small $\mu < 1/R$ we must see *four*-dimensional gravity [60], which our parametrisations do not account for. The momentum transfers we will ultimately consider in our phenomenological study are sufficiently large that this approximation has no significant effect.

3.2.1 Born amplitude

Quenched approximation

The Born amplitude in the t-channel, retaining only the leading order in $-t/s$ is then given by

$$\mathcal{A}_Q = C \int dm \frac{m^{n-1}}{t - m^2} Z_Q^{-1}(\sqrt{-t + m^2}) \tag{3.27}$$

The subscript Q simply denotes that we are using the prescription (2.29). The functional form of the resulting integral depends on the value of $\sqrt{-t}/\Lambda_T \equiv \sqrt{-t'}$. For $\sqrt{-t'} > 1$ we are immediately in the fixed point regime, and the integral in (3.27) becomes comparatively simple. For $-t' < 1$ the resulting integral is more complicated, as we split the integration region up into intervals in which the integrand does and does not exhibit fixed point scaling.

The expressions for these different kinematic regions can be combined into the amplitude

$$\mathcal{A}_Q = C\Lambda_T^{n-2}\left[\frac{-2}{n(2+n)t'^2} + \theta(1+t')(1+t')^{n/2}\left(\frac{{}_2F_1\left(1, \frac{n}{2}, \frac{2+n}{2}, 1+\frac{1}{t'}\right)}{nt'} - \frac{(-2+nt')}{n(2+n)t'^2}\right)\right] \tag{3.28}$$

This result agrees with the high-energy limit $-t/s \to 0$ of the full Born amplitude (inclusive of $s-$, $t-$ and $u-$ channels) in asymptotic safety derived in [38, 37]. It is clear from this expression that for $-t' > 1$, the amplitude decays as $\sim 1/t'^2$, in constrast to the effective field theory result. This can be understood from the perspective of four-dimensional

physics: If $G_D(\mu) \sim \mu^{2-d}$, then in $d = 4$ the running Newton's constant must vary $\sim \mu^{-2}$; as we have integrated out all KK modes, from the matching (3.26) we must have $G_N(\mu) \sim 1/t$ at high energies. Using this running G_N in (2.67) reproduces $\sim t^{-2}$ behaviour, so that the four-dimensional G_N inherits the fixed point of the underlying d-dimensional gravity theory [40].

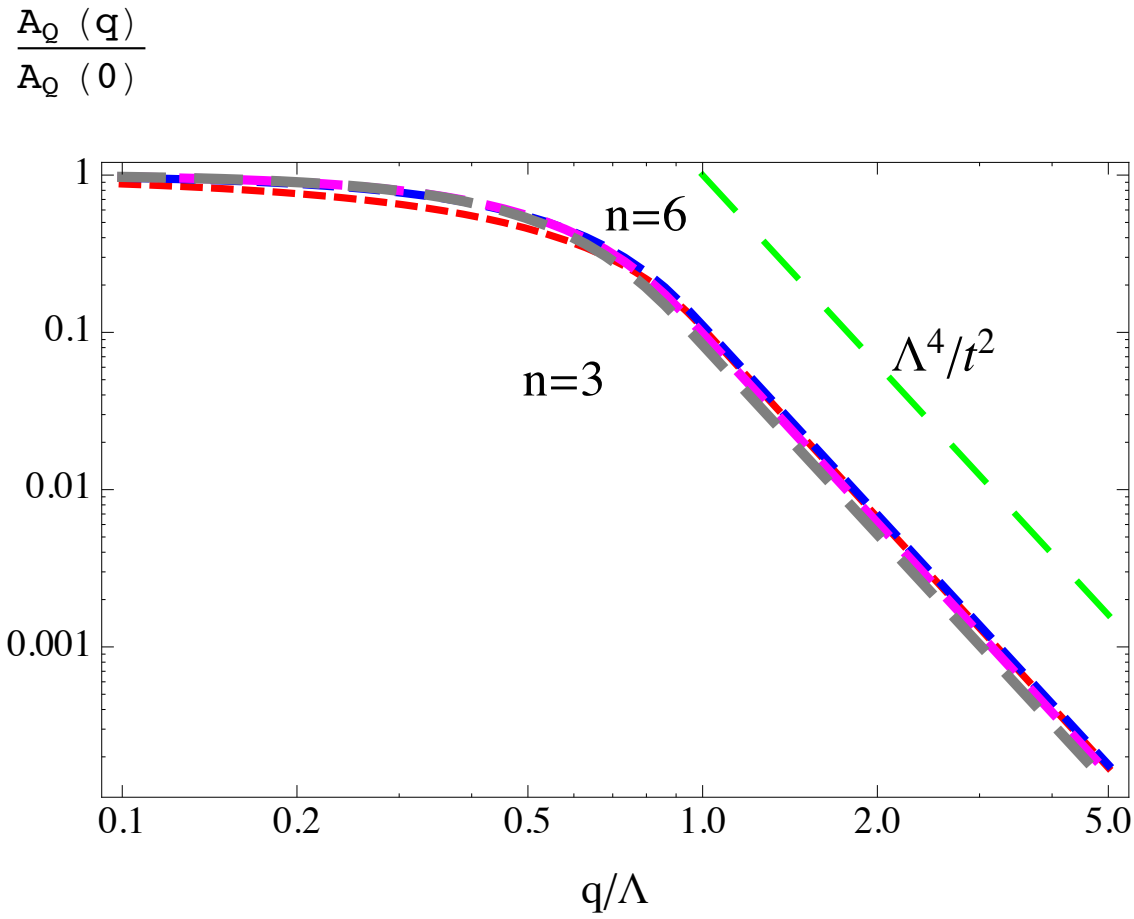

Figure 3.5: The quenched approximation to the RG-improved Born amplitude for different numbers n of extra dimensions, normalised to the value of each amplitude at $t = 0$ Note that this procedure removes the dependence of the amplitudes on the values of the dimensionful parameters s,M_D,Λ_T except insofar as that Λ_T sets the scale on the horizontal axis. Here we compare the amplitudes to their asymptotic limit $\sim 1/q^4$.

The hypergeometric function is related to the one that appeared in effective field theory by the substitution $1/t \to 1 + 1/t$, and we obtain expansions related to those of effective field theory by analytic continuation:

$$F(1,n/2,1+n/2,1+1/t') = n\left(1+\frac{1}{t'}\right)^{-n/2} \times \tag{3.29}$$
$$\begin{cases} \frac{1}{2}\left[\ln(-t') + \sum_{j=1}^{n/2-1}\frac{1}{j}\left(1+\frac{1}{t'}\right)^j\right] & \text{if } n \text{ is even} \\ \left[\tanh^{-1}\left(\sqrt{1+\frac{1}{t'}}\right) - \sum_{j=0}^{(n-1)/2-1}(2j+1)^{-1}(-1)^j\sqrt{\left(1+\frac{1}{t'}\right)}^{j+1/2}\right] & \text{if } n \text{ is odd} \end{cases}$$

We can use these to recover the $t' \to 0$ limit of $\mathcal{A}_Q$:

$$\mathcal{A}_Q = -C\Lambda_T^{n-2}\left(\frac{1}{n-2}+\frac{1}{4}\right) \tag{3.30}$$

The identity (B.9) gives us the relationship to dimensional regularisation:

$$\mathcal{A}_Q = \theta(1-t')\mathcal{A}_{DR} + C\Lambda_T^{n-2}D(t',n) \tag{3.31}$$

where

$$D(t',n) = \frac{-2}{n(2+n)t'^2} + \theta(1+t')\frac{(1+t')^{n/2-1}}{n-2}F\left(1,1-\frac{n}{2},2-\frac{n}{2},\frac{t'}{1+t'}\right) \tag{3.32}$$

Again, we see that dimensional regularisation differs from the large Λ_T limit of our amplitude by an infinite subtraction.

Linear Approximation

We defer our calculation of the Born amplitude using the prescription (2.30) to appendix A.1. We define

$$l = \begin{cases} 1 \text{ if } n \text{ is even} \\ 2 \text{ if } n \text{ is odd} \end{cases} \quad k = \begin{cases} \frac{n}{2}+1 \text{ if } n \text{ is even} \\ n+2 \text{ if } n \text{ is odd} \end{cases}$$

and find for the general result

$$\begin{aligned} \mathcal{A}_B(s,-q^2) &= -\frac{s^2\Lambda_T^{n-2}}{M_D^{n+2}}\frac{(2\pi)^{n/2+1-l}}{n+2}\frac{1}{(2k)^{n/2-1}}\frac{1}{q'^2} \\ &\quad \times G^{l,l+k}_{k+l,k+l}\left(\frac{1}{q'^{2k}}\middle| \begin{matrix} \frac{1}{l}\left(1-\frac{2}{2k}\right),\ldots,l-\frac{2}{2k},0,\frac{1}{k},\ldots,\frac{k-1}{k} \\ \frac{1}{l}\frac{n}{2k},\ldots,l-\frac{n}{2k},\frac{-n}{2k}\ldots,\frac{1}{k}\left(\frac{-n}{2}+k-1\right) \end{matrix}\right) \end{aligned} \tag{3.33}$$

A special case of this result for $n = 6$ was found in [40] in terms of elementary functions, and we have checked that our result agrees with that expression. Using (B.13) we again reproduce the universal q^{-4} behaviour.

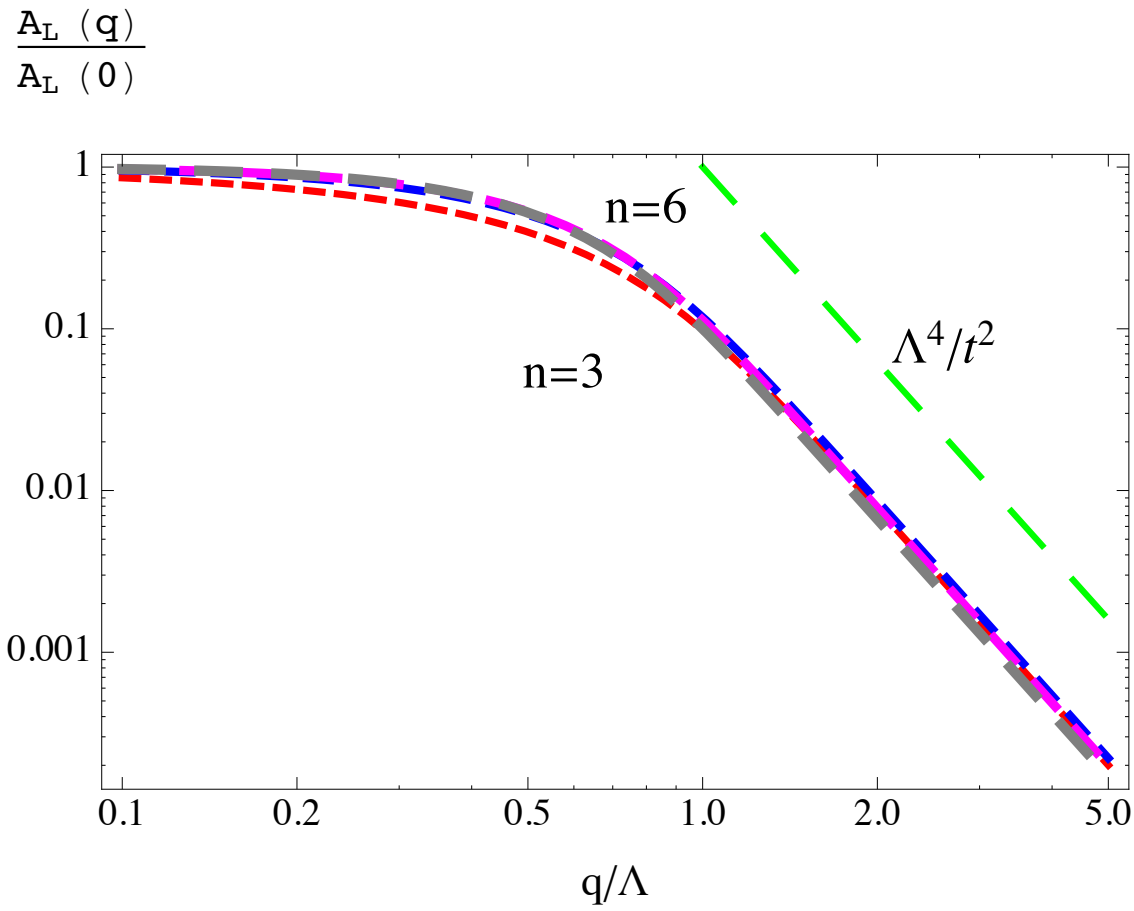

Figure 3.6: The linear approximation to the RG-improved Born amplitude for different numbers n of extra dimensions, normalised to the value of each amplitude at $t = 0$. Here we compare the amplitudes to their asymptotic limit $\sim 1/q^4$.

3.2.2 Eikonal phase

Quenched Approximation

For even n one can use the binomial expansion of $(1+t)^{n/2}$ in $\mathcal{A}_Q$ to express it in a way that can be integrated in Mathematica, and thus find the eikonal phase χ_Q expressed as

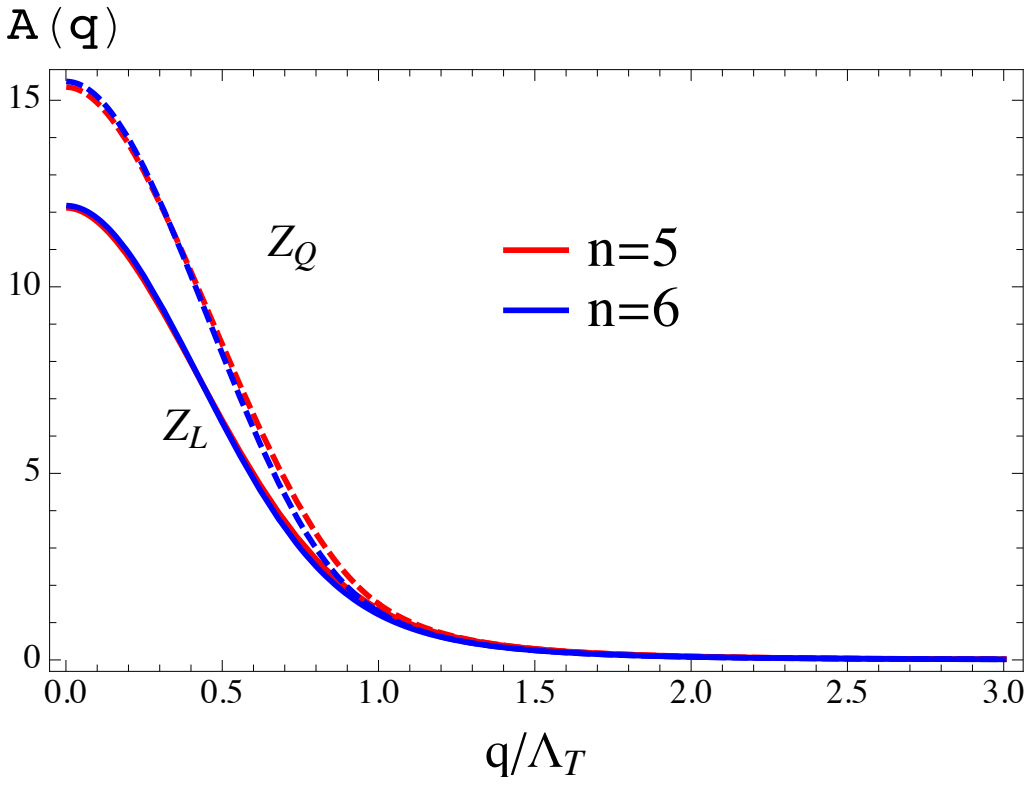

Figure 3.7: Here we compare different prescriptions for implementing asymptotic safety in the Born amplitude in $n = 5$ (red) and $n = 6$ (blue). The dashed curves show the quenched prescription (2.29) and the solid curves show the linear prescription (2.30).

a function of the dimensionless variable $b' = b\Lambda_T$:

$$\begin{aligned}
\chi_Q(b') &= \frac{C\Lambda_T^n}{4\pi s}\left(\frac{1}{2}(-1)^{n/2}\left[\sum_{j=1}^{\frac{n}{2}-1}\frac{(-1)^j\Gamma(j+1)\Gamma\left(\frac{n}{2}-j\right)\,{}_1\tilde{F}_2\left(\frac{n}{2}-j;1,\frac{n}{2}+1;-\frac{b'^2}{4}\right)}{2j}\right.\right.\\
&+ \frac{1}{n^2(n+2)^2}\left(b'^2\left((n+2)\,{}_1F_2\left(\frac{n}{2}+1;2,\frac{n}{2}+2;-\frac{b'^2}{4}\right)\right.\right.\\
&+ \left.\left.n\,{}_2F_3\left(\frac{n}{2}+1,\frac{n}{2}+1;2,\frac{n}{2}+2,\frac{n}{2}+2;-\frac{b'^2}{4}\right)\right)+2(n+2)^2J_0(b')\right)\Bigg]\\
&+ \frac{1}{n(n+2)}\left(\sum_{k=2}^{\frac{n}{2}}(-1)^k\binom{\frac{n}{2}}{k}\left(\frac{{}_1F_2\left(k-1;1,k;-\frac{b'^2}{4}\right)}{k-1}+\frac{n\,{}_1F_2\left(k;1,k+1;-\frac{b'^2}{4}\right)}{2k}\right)\right.\\
&- \left.\frac{n^2J_1(b')}{2b'}\right)-\frac{32\left((\gamma-1)b'^2+b'^2\log\left(\frac{b'}{2}\right)+2\right)-b'^4\,{}_2F_3\left(1,1;2,3,3;-\frac{b'^2}{4}\right)}{64n(n+2)}\Bigg)
\end{aligned}$$

For odd n we are forced to resort to to the construction of interpolating functions via direct numerical integration of (3.13). We plot these in fig. 3.8. We remark that for large impact parameters χ_Q oscillates wildly about the expected value $\sim b^{-n}$; this appears to be merely an artefact of the quenched prescription, due to the non-analyticity of the step function.

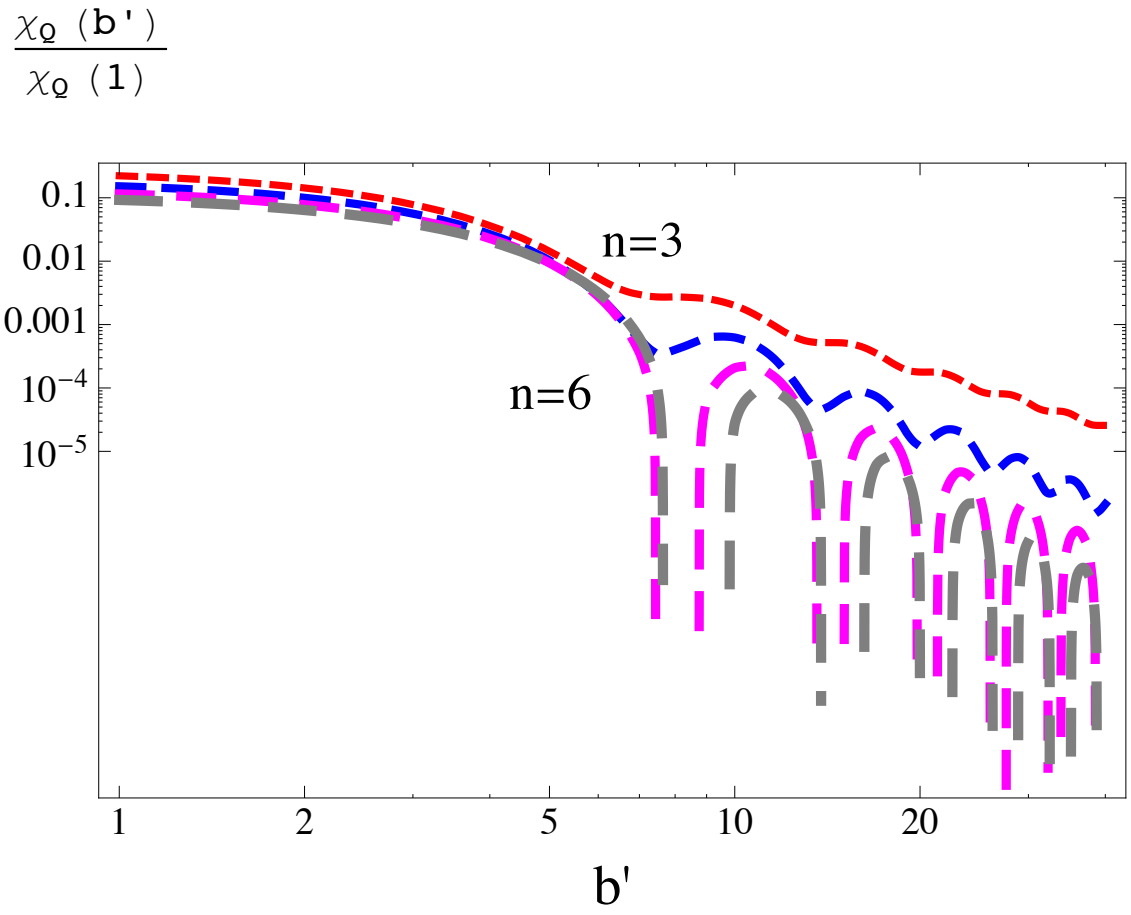

Figure 3.8: The quenched approximation to the RG-improved eikonal phase for different numbers n of extra dimensions. Here we see that in this approximation χ_Q oscillates wildly about the expected value $\sim b^{-n}$.

Linear Approximation

Deferring the calculational details to A.1, we find the general expression

$$\begin{aligned}\chi_L(b') &= -\frac{s\Lambda_T^n}{M_D^{n+2}}\frac{(2\pi)^{n/2+1-l}}{4\pi}\frac{b'^{-n/2}}{n+2} \\ &\times G^{k+l,l}_{l,2k+l}\left(\left(\frac{b'}{2k}\right)^{2k}\middle|\begin{matrix}\frac{1}{l}\left(1-\frac{n}{2n+4}\right),\ldots,\frac{1}{l}\left(l-\frac{n}{2n+4}\right)\\ \mathbf{w}\end{matrix}\right)\end{aligned} \tag{3.34}$$

where again $b' = b\Lambda_T$, k and l were defined in (3.33), and

$$\mathbf{w} = \frac{1}{l}\left(1-\frac{n}{2n+4}\right),\ldots,\frac{1}{l}\left(l-\frac{n}{2n+4}\right),\frac{1}{k}\frac{n}{4},\ldots,\frac{1}{k}\left(\frac{n}{4}+k-1\right),-\frac{1}{k}\frac{n}{4},\ldots,\frac{1}{k}(-\frac{n}{4}+k-1)$$

Using the formula (B.14) we find that for $b \gg \Lambda_T^{-1}$ we reproduce the now-familar result

$$\chi_L(b) \sim -\left(\frac{b_c}{b}\right)^n \tag{3.35}$$

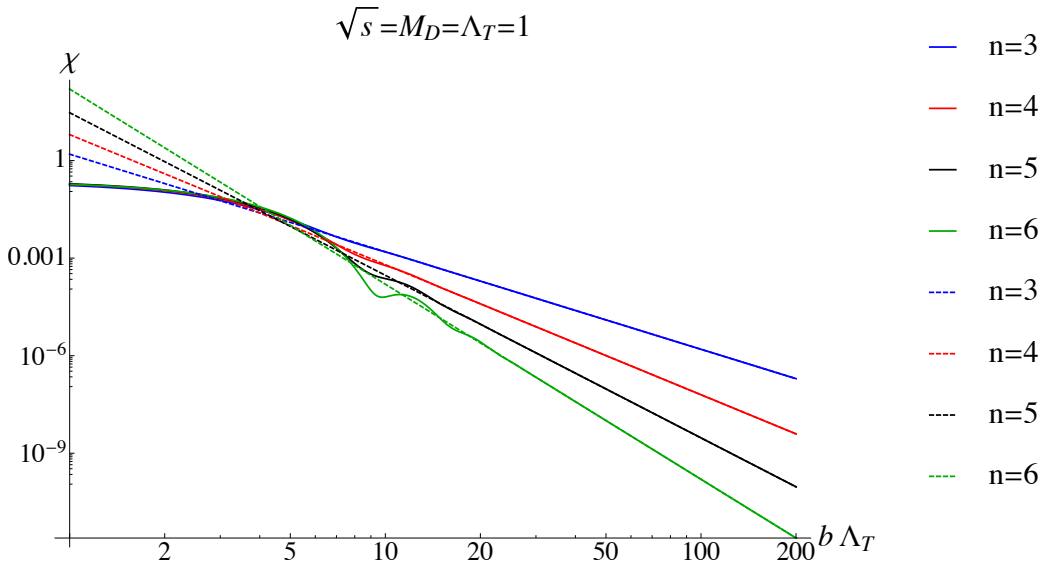

Figure 3.9: The linear approximation to the RG-improved eikonal phase (solid lines) for different numbers n of extra dimensions. In this approximation to the running of G_N, the asymptotic $\sim b^{-n}$ behaviour as expected from the semiclassical analysis (dashed lines) is clear.

We see that thanks to the continuous derivatives of the prescription (2.30) this exhibits none of the long-distance pathologies exhibited by χ_Q. For $b \to 0$ we find from (B.13) that

$$\chi_L(0) = -\frac{s\Lambda_T^n}{M_D^{n+2}} \frac{\pi^{n/2}}{2n(n+2)} \frac{\csc\left(\frac{n\pi}{n+2}\right)}{\Gamma\left(\frac{n}{2}\right)} \tag{3.36}$$

It is striking that in contrast to the effective field theory case (3.17) which diverged logarithmically at small arguments, χ_L tends to a finite value. This is because the EFT prescription only regulates the high energy modes of the KK tower, without fundamentally altering the behaviour of gravity at short distances. By contrast, the framework adopted here is intended to describe a fundamentally well-behaved theory of gravity. Indeed, we also find that the *derivative* of χ_L vanishes at zero impact parameter, and regard this as a signature of the underlying fixed point of the theory.

This argument can be generalised: using the matching (3.26), by the argument in A.1 we can write the eikonal phase corresponding to a generic field strength renormalisation $Z^{-1}(\mu)$ in the form

$$\chi(b) = X_n b^{-n/2} \int_0^\infty d\mu \mu^{n/2-1} Z^{-1}(\mu) J_{n/2}(b\mu) \tag{3.37}$$

with X_n an irrelevant n-dependent constant. At small arguments, by (B.2) $J_{n/2}(\mu b) \sim b^{n/2}$, so that this integral is finite as $b \to 0$, and converges due to the factor $Z^{-1}(\mu)$, so

that $\chi(0)$ is finite. Differentiating with respect to b, we have

$$\frac{d\chi}{db} = X_n \int_0^\infty d\mu \mu^{n/2-1} Z^{-1}(\mu) b^{-n/2} \left[\frac{-n}{2} \frac{1}{b} J_{n/2}(b\mu) + \frac{dJ_{n/2}(b\mu)}{db} \right] \tag{3.38}$$

Using (B.3), the term in square brackets becomes

$$\begin{aligned} &\tfrac{-n}{2}\tfrac{1}{b} J_{n/2}(b\mu) + \tfrac{\mu}{2}\left(J_{n/2-1}(\mu b) - J_{n/2+1}(\mu b)\right) \\ \xrightarrow{b\to 0} &\tfrac{-n}{2b}\left(\tfrac{b\mu}{2}\right)^{n/2} \tfrac{1}{\Gamma(n/2+1)} + \tfrac{\mu}{2}\left(\tfrac{b\mu}{2}\right)^{n/2-1} \tfrac{1}{\Gamma(n/2)} + \mathcal{O}(b^{n/2+1}) \\ &= 0 + \mathcal{O}(b^{n/2+1}) \end{aligned}$$

So we see that it is also a generic feature of our formulation that the first derivative of $\chi(b)$ vanishes at zero impact parameter. We find no such cancellation with the second derivative of χ, so that we might expect it to diverge in the small b limit due to the terms inversely proportional to powers of b. In fact, it seems that the integral softens this divergence slightly, so that we find for χ_L the expansion

$$\chi_L(b) \sim \chi_0 + b'^2(A_n + B_n \log(b')) \tag{3.39}$$

so we see that the second derivative of χ diverges *logarithmically*. It is interesting to reflect on this fact in light of the analogy between quantum field theory and the statistical mechanics of systems with infinitely many degrees of freedom; in applications of the renormalization group in the latter context, fixed points correspond to *second-order* phase transitions, in which the second derivatives of the thermodynamic free energy are discontinuous.

It is interesting to reconsider the connection between the eikonal phase and the classical potential in light of this result. We would have reproduced the qualitative features of χ_L if we had taken defined a gravitational constant that ran in *position space* as $G(b) \sim b^n$ at short distances, and remained approximately constant $\sim G_D$ at long distances. We might expect analogous remarks to apply to the Newtonian potential $\sim r^{-(1+n)}$, or equivalently to the metric components in a relativistic setting. Such methods have been applied to e.g. discussions of RG-improved black hole metrics in [28, 29, 30, 31]; this result seems to provide a further vindication of such approaches. In fact, using the identity (B.15), we can define a multiplicative renormalisation factor $H_n(b')$ for G_N that runs in position space, by

$$\chi_L(b') = -\left(\frac{b_c}{b}\right)^n H_n(b') \tag{3.40}$$

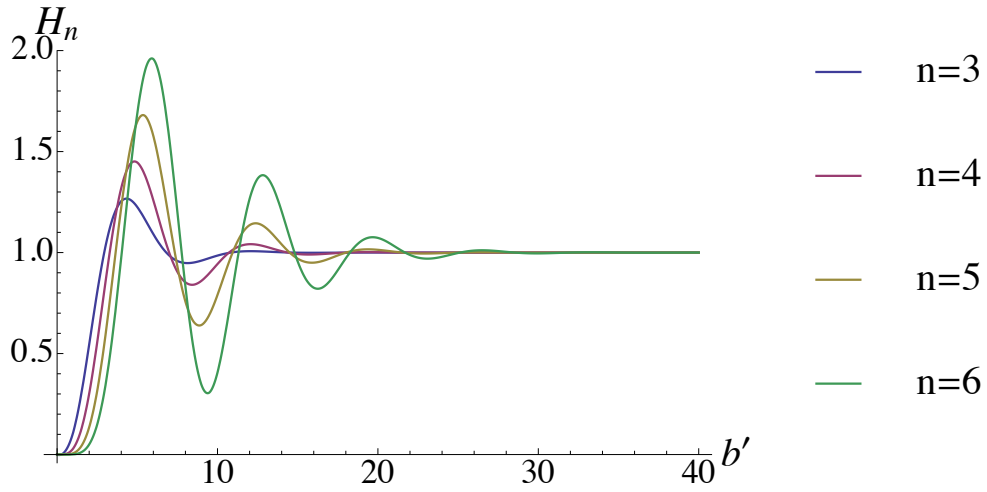

Figure 3.10: Here we plot the functions $H_n(b')$ for different numbers of extra dimensions. We see here that the functions grow as $\sim b^n$ at small arguments and settle to 1 at long distances, as required to reproduce the semiclassical result.

where

$$\begin{aligned} H_n(b') &= \frac{(2\pi)^{1-l}}{\Gamma(n/2)}\frac{2}{n+2}k^{n/2} \\ &\times G^{k+l,l}_{l,2k+l}\left(\left(\frac{b'}{2k}\right)^{2k}\middle|\begin{matrix}\frac{1}{l},\ldots,1\\ \frac{1}{l},\ldots,1,\frac{1}{k}\frac{n}{2},\ldots,\frac{1}{k}\left(\frac{n}{2}+k-1\right),0,\ldots,(k-1)/k\end{matrix}\right) \end{aligned} \tag{3.41}$$

The functions H_n are plotted in fig. 3.10.

We can use the finiteness of $\chi_L(0) \equiv \chi_0$ to define a length scale $b_T \sim 1/\Lambda_T$ characteristic of our RG improvement, by

$$\chi_0 = -\left(\frac{b_c}{b_T}\right)^n \tag{3.42}$$

b_T is thus the length scale at which the semi-classical eikonal phase (3.15) attains the maximal value of χ_L in our framework. It provides a strict *lower bound* on the length scale at which the effects of RG improvement must manifest themselves. Its explicit expression is

$$b_T = \Lambda_T^{-1}\left[\frac{2^{n-2}\,\Gamma^2\left(\frac{n}{2}\right)\,n\,(n+2)}{\pi\,\csc\left(\frac{n\,\pi}{n+2}\right)}\right]^{\frac{1}{n}} \tag{3.43}$$

There is one further important remark to be made in connection with the semi-classical limit χ_{DR}. We have seen that χ_L reproduces this limit at large arguments. This can be understood as saying that the RG-improvement only affects the short-distance physics of gravity. However, the dimensionless argument $b\Lambda_T$ of the complicated functions in

(3.35),(3.41) also becomes larger as we increase the scale Λ_T. There is then a sense in which gravity 'looks more classical' as we push the onset of fixed point scaling to ever higher energy scales. This point will become important in our discussion of the eikonal amplitudes.

3.2.3 Eikonal amplitude

We have numerically integrated the renormalisation-group-improved eikonal amplitudes $\mathcal{M}_{RG}(s,t)$ using χ_L. The most obvious question to address is how varying the new parameter Λ_T of our theory affects the absolute value of $\mathcal{M}_{RG}$, and hence on observable physics relevant for our discussion of phenomenological signals in chapter 4. We illustrate the effects of this variation in figure 3.11.

The first lesson to be gained from figure 3.11 is that for sufficiently large Λ_T our eikonal amplitudes coincide with those of dimensional regularisation. This was to be expected from our discussion of χ_L in the preceding section 3.2.2. As discussed there, in the large Λ_T limit $\chi_L \to \chi_{DR}$, as fewer momentum modes are affected by the weakening of gravity due to the fixed point. That this is realised at the level of the full eikonal amplitude amounts to an important consistency check.

The second immediately striking point about fig. 3.11 is that for values of $\Lambda_T < M_D$, the eikonal amplitude exhibits the same scaling behaviour $\sim q^{-4}$ as the Born amplitude. It is interesting to compare this to the situation in 4-dimensional gravity, where t'Hooft's amplitude (2.70) has the same absolute value as the Born amplitude (2.67). Here we see that the "semi-classical" amplitude in the ADD case does not share this feature, whilst our description in which the quantum field theoretic effects are most important appears to! This is, however, easily understood mathematically. In the case $\Lambda_T < M_D$, from (3.35) the absolute value of $\chi_L < 1$, and we can expand the exponential in (2.59)

$$e^{i\chi} - 1 \approx i\chi \tag{3.44}$$

The Fourier transform in (2.59) thus inverts that in (2.57), and we recover the Born amplitude. It is important to emphasise that this argument is only meaningful because the Born amplitude is well-defined within our framework; without a regularisation procedure in place, expanding the exponential $e^{i\chi}$ in (2.59) produces an infinite sum of divergent integrals.

The above arguments are quite general, and should hold in any number of extra dimensions. To facilitate further comparison with the amplitudes of dimensional regularisation,

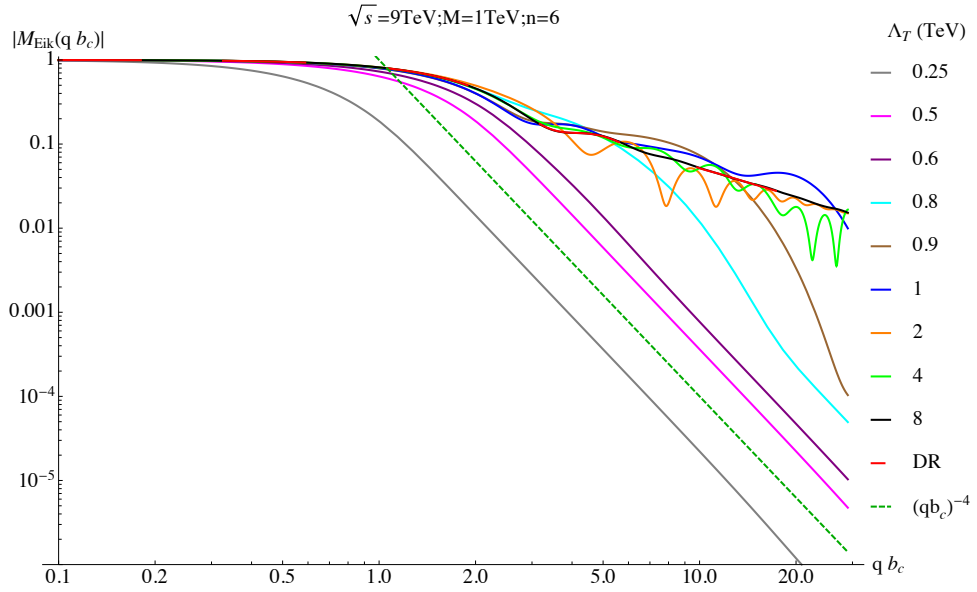

Figure 3.11: Variation of the eikonal amplitudes with Λ_T.

it is helpful to parametrise our results in a manner analogous to that in (3.21):

$$\mathcal{M}_{RG}(s,t) = -i4\pi s b_c^2 F(y,z) \tag{3.45}$$

where

$$y \equiv qb_c \tag{3.46}$$

$$z \equiv \frac{b_c}{b_T} = (-\chi_0)^{1/n} \tag{3.47}$$

where b_T was defined in (3.42). The functions $F_n(y)$ of dimensional regularisation depended only on the variable y; the variable z encodes the information about our RG improvement. It varies with the dimensionful parameters of our theory as

$$z \sim \left(\frac{s}{M_D^2}\right)^{1/n} \frac{\Lambda_T}{M_D} \tag{3.48}$$

Our condition for semi-classicality is thus that of large z. Fig. 3.12 shows the realisation of our physical picture in $n = 4$, expressed in terms of the variables y, z.

It is interesting to consider this variation of $F(y,z)$ for fixed y. In fig. 3.13 we plot this variation in $n = 3$. There we see clearly that for large values of z, $F_{RG}(y,z) \to F_{DR}(y)$ as desired. For small values of z, we see that $F(y,z)$ grows with z with a power law. This follows from the fact that in this limit we recover $\mathcal{A}_L$ from $\mathcal{M}_{RG}$, and the Born amplitude varies as $(\Lambda_T/M_D)^{n-2} \sim z^{n-2}$ from (3.48).

Fig.3.13 also reveals an interesting feature of this transition: that at a certain value of z that is largely insensitive to y, $|F(y,z)|$ reaches a supremum that is *larger* than

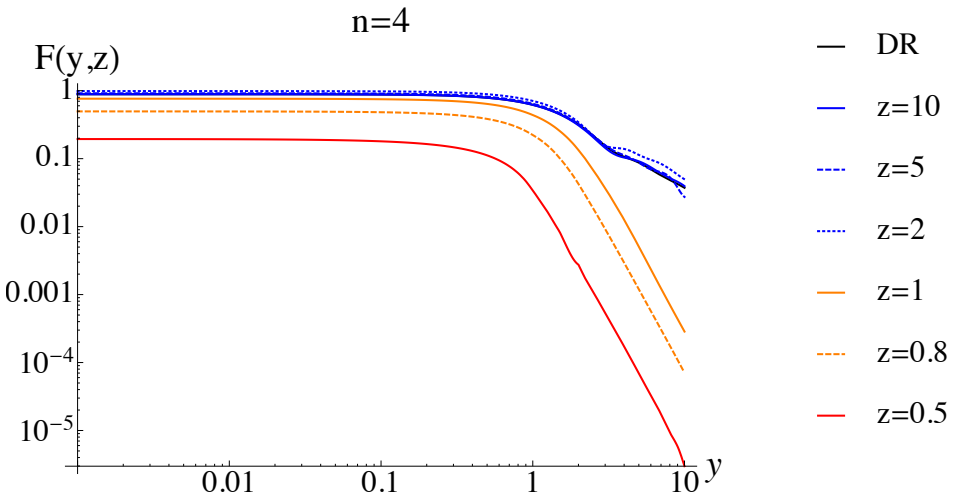

Figure 3.12: The absolute value of F_4 is plotted against y for different fixed z: The DR case (black), $z = 10$ (blue), $z = 5$ (blue,dashed), $z = 2$ (blue, dotted), $z = 1$ (orange), $z = 0.8$ (orange,dashed) and $z = 0.5$ (red).

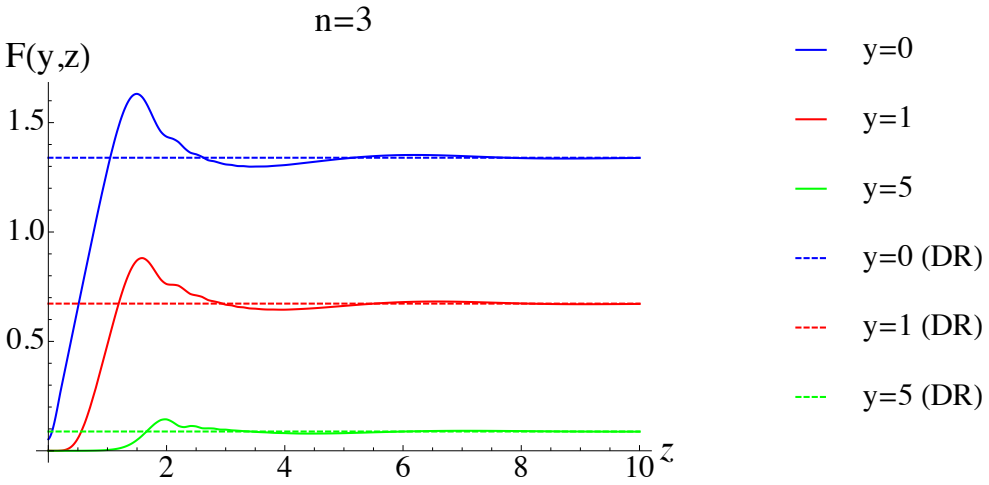

Figure 3.13: The absolute value of F_3 is plotted against z for different fixed y: $y = 0$ (blue), $y = 1$ (red) and $y = 5$ (green). The DR case is always given as a dashed line in the corresponding colour.

that attained in the semiclassical limit. This is a striking, almost paradoxical result: that by *suppressing* the contribution of some high-energy modes, we can *increase* the corresponding differential cross-section!

We can begin understand this if we reflect on how short-distance physics contributes to the semi-classical amplitude (3.20). At short distances $\chi_{DR} \sim b^{-n}$ becomes extremely large, and so the complex exponential $e^{i\chi_{DR}}$ oscillates extremely rapidly. In consequence, these rapid fluctuations serve to *cancel each other out*. This argument can be formalised using the methods of the *stationary phase approximation*, which we will discuss in detail in the next section. We see then that as we increase Λ_T, the absolute value of $\mathcal{M}_{RG}$ is subject to two competing effects: it is enhanced as the contribution of some modes is unsuppressed, but decreased due the increasingly rapid oscillations of $e^{i\chi_L}$.

3.3 The stationary phase approximation to the eikonal amplitude

We wish to make a stationary phase approximation of integrals of the form

$$\mathcal{M}_{eik} = -4\pi i s \int dbbJ_0(qb)(e^{i\chi} - 1) \tag{3.49}$$

For large arguments the Bessel function can be expanded as

$$J_0(x) \sim \sqrt{\frac{2}{\pi x}} \cos\left(x - \frac{\pi}{4}\right) \tag{3.50}$$

so upon expanding the cosine in terms of complex exponentials, in this limit we can express the integrand in (3.49) as a sum of terms with exponents $\chi \pm \left(qb - \frac{\pi}{4}\right)$. The stationary phase approximation defines a length scale b_s at which the derivative of this exponent with respect to b vanishes, so that

$$\frac{\partial \chi}{\partial b} \pm q = 0 \tag{3.51}$$

If the derivative $\frac{\partial \chi}{\partial b}$ has a constant sign, only one of the positive/negative frequency modes from expanding the Bessel function contributes to the approximation. The location of the stationary point b_s will clearly depend on q, as well as whatever parameters enter the definition of χ.

We remark that, formally speaking, q is playing the role of the large parameter which was denoted x above. However, we will see that the relative error in the stationary phase approximation is often much better than the $1/\sqrt{q}$ error estimate we would naively make based on the above logic. We will discuss this point in more detail below with reference to the semiclassical and RG-improved eikonal amplitudes.

3.3.1 Semiclassical analysis

Let us recall the integral representation of the functions $F_n(y)$ of Giudice et al. in terms of the variables $x = b/b_c$, $y = qb_c$,

$$F(y) = -i \int_0^\infty dx x J_0(xy) \left(e^{ix^{-n}} - 1 \right) \tag{3.52}$$

Expanding the Bessel function in terms of complex exponentials, the function $\sim \sqrt{x} e^{\pm i(xy - \pi/4)}$ has no stationary points, so we neglect the contribution of the "-1" term from the brackets. Then

$$F(y) \equiv \sum_{\pm} \int_0^\infty dx f(x) e^{iy\psi_\pm(x)} \tag{3.53}$$

where we have defined

$$\psi_\pm(x) = \pm(x - \frac{\pi}{4y}) - \frac{x^{-n}}{y} \tag{3.54}$$

and

$$f(x) = -i\sqrt{\frac{x}{2\pi y}} \tag{3.55}$$

To look for stationary points, we differentiate

$$\psi'_\pm(x) = \pm 1 + n\frac{x^{-(n+1)}}{y} \equiv 0 \tag{3.56}$$

so we see that only ψ_- will contribute to the expansion, and we identify

$$x_s(y) = \left(\frac{n}{y} \right)^{\frac{1}{n+1}} \tag{3.57}$$

To be explicit, this corresponds to a physical length scale

$$b_s(q) = b_c \left(\frac{n}{qb_c} \right)^{\frac{1}{n+1}} \tag{3.58}$$

We see that the second derivative

$$\psi''(x) = -n(n+1)\frac{x^{-(n+2)}}{y} \tag{3.59}$$

is always negative, so we choose a minus sign in the exponent of (C.7), which finally becomes

$$F(y) \sim -iy^{-\frac{n+2}{n+1}} \frac{n^{1/(n+1)}}{\sqrt{n+1}} \exp -i(n+1) \left(\frac{y}{n} \right)^{\frac{n}{n+1}} \tag{3.60}$$

The applicability of this approximation is frequently cited [1, 50] as an argument in favour of the semiclassical nature of the eikonal amplitude. It establishes a one-to-one correspondence between the momentum transfer (and hence the scattering angle) and the impact parameter of the collision, as would be found in classical physics. Furthermore, the characteristic length scale b_s defined in (3.58) grows with energy, so that at larger and larger centre-of-mass energies the short distance physics becomes less and less relevant.

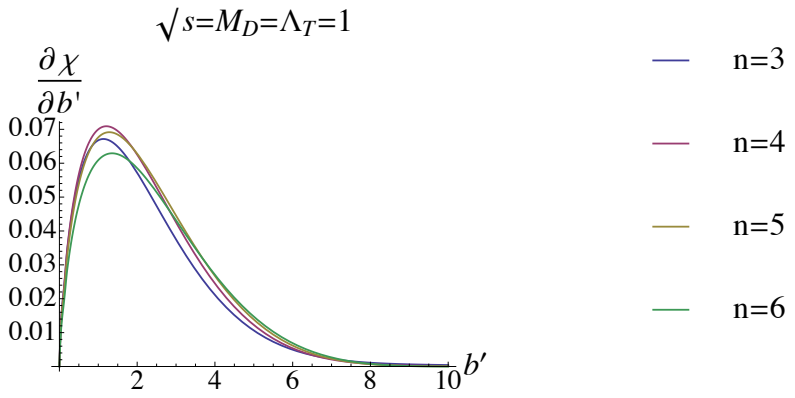

Figure 3.14: $\frac{\partial\chi}{\partial(b\Lambda_T)}$

Figure 3.15: The derivative of the eikonal phase with respect to its argument for varying n. The effect of the fixed point is to make the derivative of χ vanish at $b\Lambda_T = 0$, which together with the eventual onset of classical scaling behaviour, enforces the existence of a maximal value of the derivative.

3.3.2 RG improvement of the eikonal phase

Due to the complexity of our functions we must resort to determining b_s numerically. It is clear, however, from fig. 3.15 that the derivative is bounded, so that solutions to (3.51) do not exist for $q \gtrsim d_n \frac{s\Lambda_T^{n+1}}{M_D^{n+2}}$, where d_n is an n-dependent constant on the order of $d_n \sim 0.06$. This behaviour follows from the fact that $\chi'(b)$ vanishes at the origin as discussed in section 3.2, and at infinity as $\sim b_c^n b^{-(n+1)}$, and is well-behaved everywhere in between.

As the eikonal phase χ_L depends on the dimensionless variable $b\Lambda_T$, it is convenient in many cases to re-scale our integral in terms of Λ_T, so that

$$\mathcal{M}_{RG} = \frac{4\pi s}{\Lambda_T^2} f(n, c, q) \tag{3.61}$$

where

$$f(n, c, q) = -i \int_0^\infty db' b' J_0(q/\Lambda_T b')(e^{-ic\tilde{\chi}_L(b')} - 1) \tag{3.62}$$

From this equation we see that the condition for the large-argument expansion of the Bessel function is $q \gg \Lambda_T$. However, we also have the condition that $q \lesssim 0.06 \frac{s\Lambda_T^{n+1}}{M_D^{n+2}}$. From this it follows that, for there to be an extended stationary phase region, we require $b_T\Lambda_T \ll b_c$. This appears to be the same condition as that for the semi-classical approximation, but it does not automatically follow that the semiclassical stationary phase is a good approximation; this depends on the relative magnitude of q and Λ_T. The semiclassical approximation will work for $b_c^{-1} \ll q \ll \Lambda_T$, whilst the stationary phase approximation to

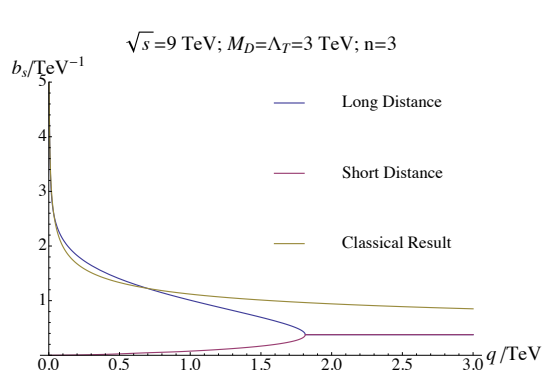

(a) q-dependence

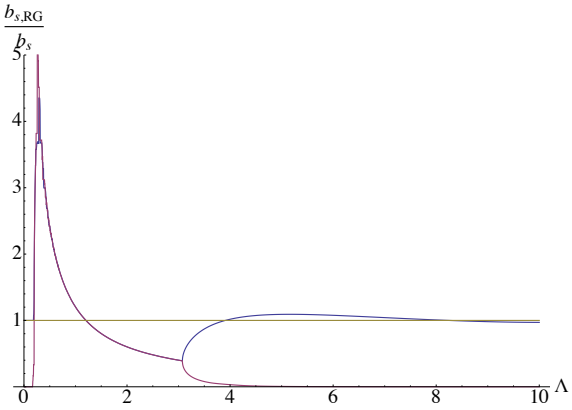

(b) Λ_T- dependence

Figure 3.16: These plots show the length scales defined by the stationary phase approximation in $n = 3$. The classical result is shown in gold. The blue and red lines are the numerical solutions of the stationary phase condition $\frac{\partial \chi}{\partial b} = q$, corresponding respectively to roots at long and short distances. Left: The blue and red curves merge when q is equal to the maximum value of $\frac{\partial \chi}{\partial b}$; for greater values of q the root finder returns this value for b_s as the best approximation to the stationary point, but no solutions exist. Right: We see that the ratio of the stationary phase length scale tends to the classical result as we take the semi-classical limit of large Λ_T.

the RG-improved eikonal may be useful when $1 \ll q/\Lambda_T \ll 0.06\frac{s\Lambda_T^n}{M_D^{n+2}}$. We check that we can differentiate between them in figure 3.17.

We compare the numerical evaluation of f with the corresponding stationary phase approximation in Fig 3.18 below, for two sets of choices of the parameters in the problem. We see that the stationary phase approximation works well within its expected domain of validity, but that for a realistic choice of values relevant for LHC physics this region does not exist.

We denote by b'_s and b'_l the short and long distance roots of the condition that $\frac{\partial \chi}{\partial b'} = q/\Lambda_T$. For $\chi''(b_s)$ not too small, we find that

$$f(n,c,q) \sim \sqrt{\frac{\Lambda_T}{q}} \left(\sqrt{\left| \frac{b'_s}{\chi''(b'_s)} \right|} \exp i(\chi(b'_s) - qb'_s/\Lambda_T + \pi/2) + \sqrt{\left| \frac{b'_l}{\chi''(b'_l)} \right|} \exp i(\chi(b'_l) - qb'_l/\Lambda_T) \right) \tag{3.63}$$

where $\chi''(b'_i)$ means $\frac{\partial^2 \chi}{\partial b'^2}\big|_{b'=b'_i}$

It is also interesting to compare the contributions coming from both the short and long distances. We see that the long distance effect dominates until q gets extremely close to its critical value. This can be understood from the fact that the modulus of each contribution

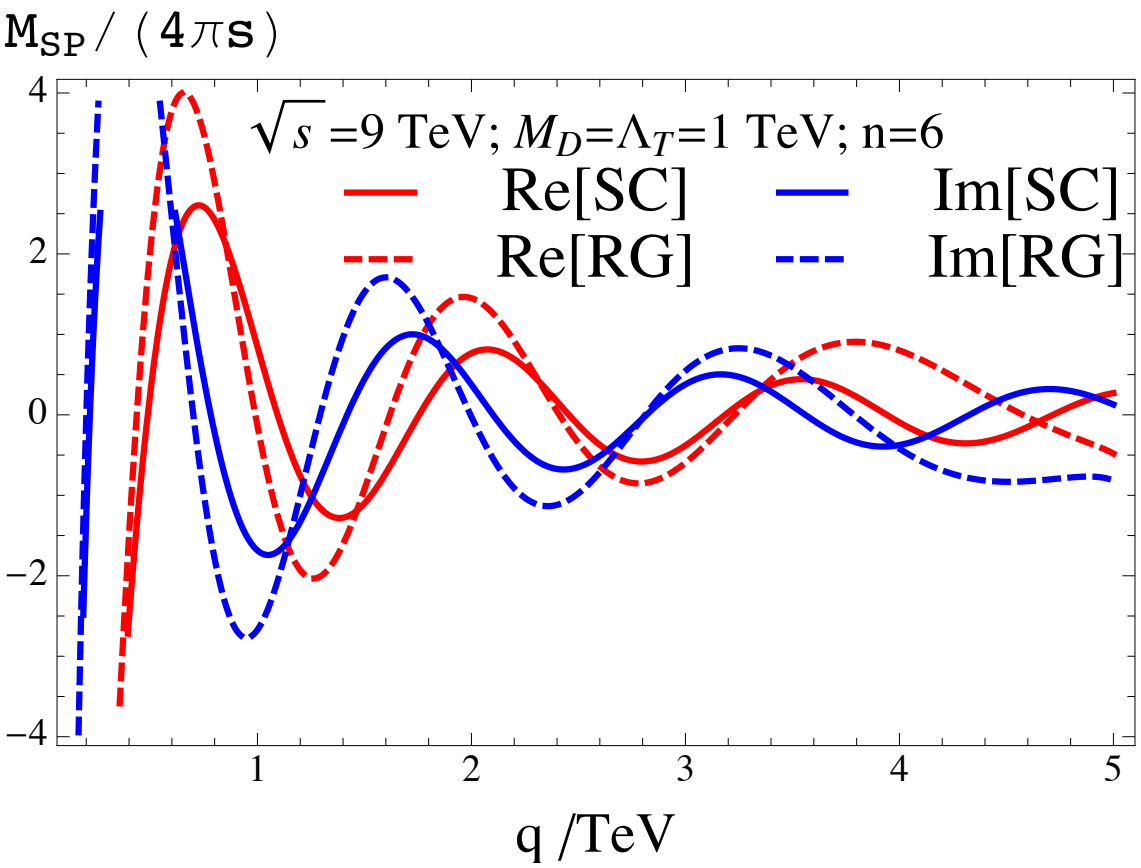

Figure 3.17: Here we check that we can indeed differentiate between the stationary phase approximations to the real (red) and imaginary (blue) parts of the semi-classical (SC, solid lines) and RG-improved amplitudes (dashed lines). In this plot for the purposes of comparison we have included dimensionful factors of b_c^2 and Λ_T^{-2}, so that each differs from the full eikonal amplitude by the same factor $4\pi s$.

varies as $\sqrt{\frac{\Lambda_T}{q}}\left(\sqrt{\left|\frac{b_i'}{\chi''(b_i')}\right|}\right)$. This effect is twofold: the length scale b_i enhances the relative contribution of the long to short distances, whilst the second derivative of χ gets large at short distances, diverging logarithmically at $b' = 0$.

Using this knowledge, we can return to the earlier discussion of the competing effects of varying Λ_T on the absolute value of the eikonal. Let us neglect the short-distance contribution in comparison to the long-distance one. Then the absolute value of $\mathcal{M}_{RG}$ depends on the ratio

$$\left|\frac{\mathcal{M}_{RG}}{\mathcal{M}_{DR}}\right| = \sqrt{\frac{b_l}{b_s}\frac{\chi''_{DR}(b)}{\chi''_L}} \tag{3.64}$$

We plot this ratio for $n = 3, y = 5$ in fig. 3.20. We see that the pattern of enhancement or suppression of this ratio with z exactly replicates that of 3.13 for large values of z, and that the peak in fig. 3.13 corresponds to the point at which the $\chi''_L(b)$ diverges. This is a

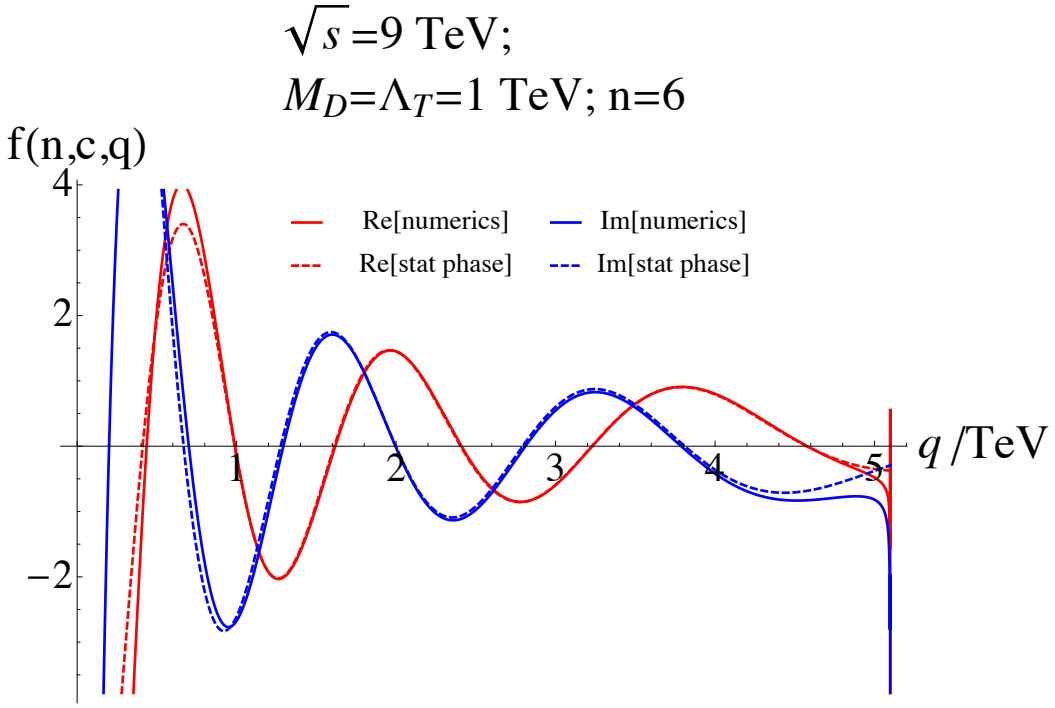

Figure 3.18: Here we show the stationary phase approximation to $f(n, c, q)$. With large enough $\sqrt{s}$, it is easy to satisfy the condition $1 \ll q/\Lambda_T \ll 0.06\frac{s\Lambda_T^n}{M_D^{n+2}}$ and we find that the stationary phase approximation works well unless q is very small (so that expanding the Bessel function is illegitimate) or close to the critical value where the two roots merge. At this value the expression (C.7) breaks down, because the second derivative of the eikonal phase vanishes.

precise sense in which the enhancement of $|\mathcal{M}_{RG}|$ relative to the semiclassical expectation corresponds to the integrand oscillating more slowly.

This expression becomes singular at the value $q = q_c$, when $\chi''(b_s) = 0$. At this point, it is obviously appropriate to instead make a third-order expansion of χ, i.e. use equation (C.7) with $p = 3$. However, this expression clearly also fails when $\chi''(b_s)$ is small but finite. When this is the case, the second-order approximation to $\chi(b)$ no longer suppresses the integration sufficiently rapidly. In this case we adopt the following strategy. We expand χ to third order about the stationary point, so that

$$\chi(b) - qb \approx \chi(b_s) + qb_s + \frac{1}{2}\chi''(b_s)(b - b_s)^2 + \frac{1}{3!}\chi'''(b_s)(b - b_s)^3 \quad (3.65)$$

$$\equiv -ax^3 + bx^2 + c \quad (3.66)$$

in which we have defined $x = (b - b_s)$ and introduced obvious constants a, b, c to simplify the presentation of what follows. Note, however, the minus sign inserted so that $a = -\frac{1}{3!}\chi'''(b_s)$

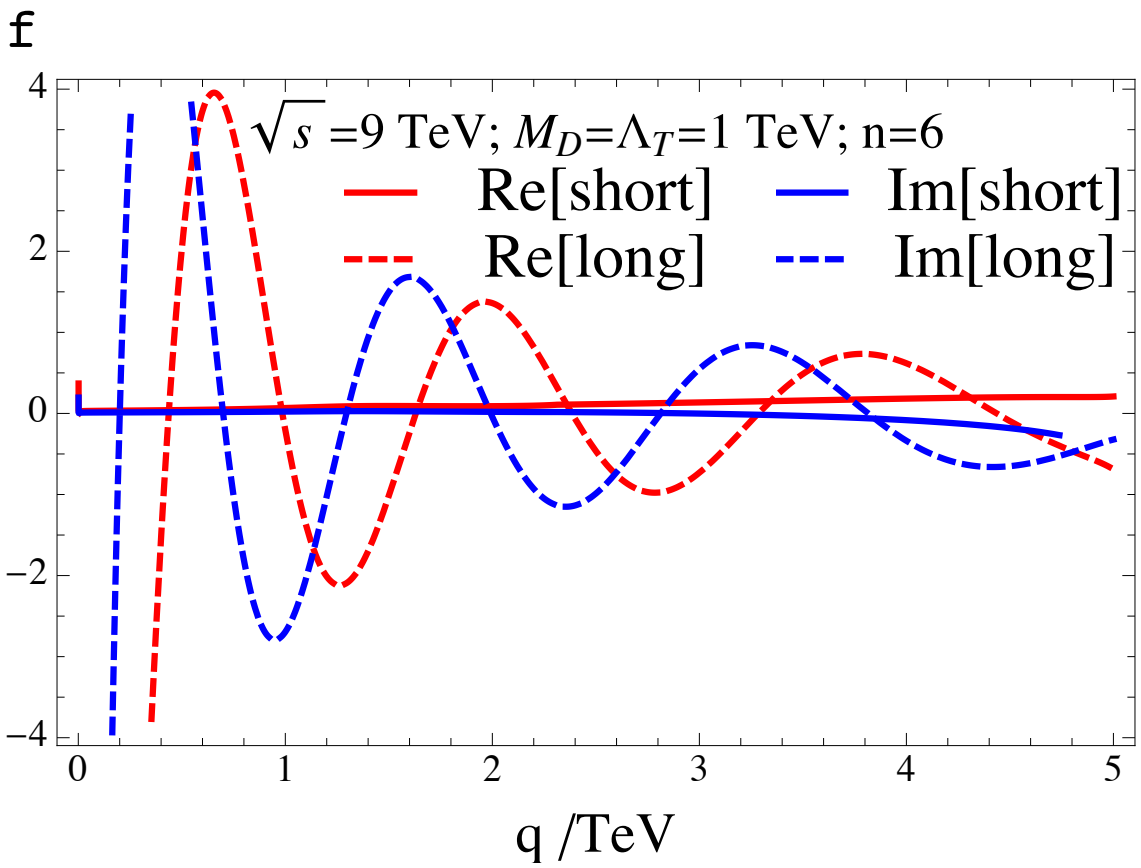

Figure 3.19: This plot shows the real (red) and imaginary (blue) parts of the short- (solid) and long- (dashed) distance stationary points to the stationary phase approximation. The dominance of the long distance physics is clear.

is positive. We can then write, near the critical point,

$$\int db\sqrt{\frac{b}{2\pi q}}e^{i(\chi-qb-\frac{\pi}{4})} \approx \sqrt{\frac{b_s}{2\pi q}}e^{i(c-qb_s-\frac{\pi}{4})}\int dx e^{-i(ax^3-bx^2)} \tag{3.67}$$

If we define y via the equation

$$x = y + \frac{b}{3a} \tag{3.68}$$

then this becomes

$$\int db\sqrt{\frac{b}{2\pi q}}e^{i(\chi-qb-\frac{\pi}{4})} \approx \sqrt{\frac{b_s}{2\pi q}}e^{i(c-qb_s-\frac{\pi}{4}-2b^3/27a^2)}\int dy e^{-i(ay^3-(b^2/3a)y)} \tag{3.69}$$

We now rescale the integration variable $y \to (3a)^{-1/3}y$, and extend the region of integration to the entire positive real y-axis. Using the integral representations of the Airy and Scorer functions,

$$\mathrm{Ai}(x) = \frac{1}{\pi}\int_0^\infty dt \cos\left(\frac{1}{3}t^3 - xt\right) \tag{3.70}$$

$$\mathrm{Gi}(x) = \frac{1}{\pi}\int_0^\infty dt \sin\left(\frac{1}{3}t^3 - xt\right) \tag{3.71}$$

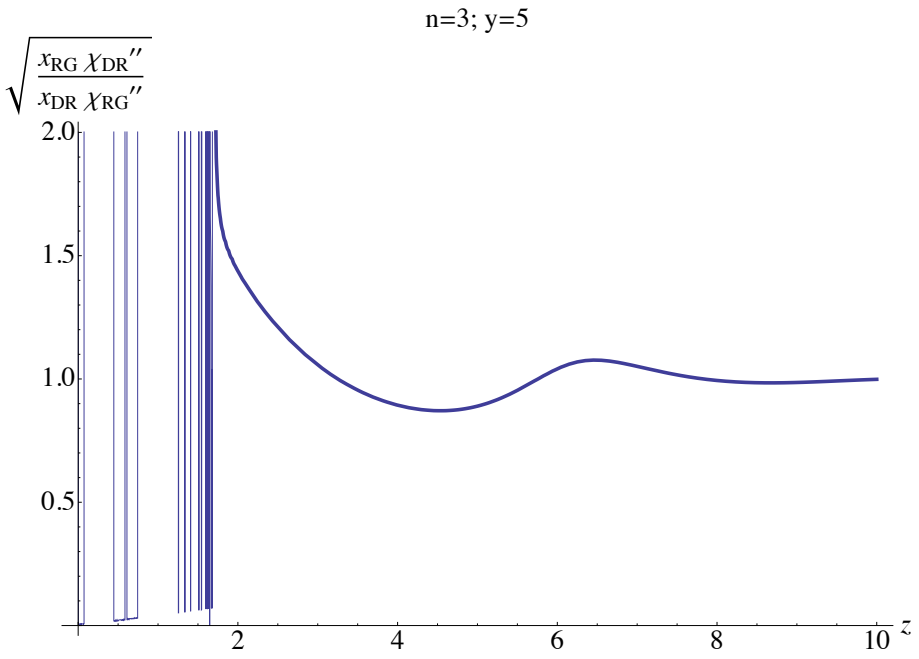

Figure 3.20: Here we show the ratio (3.64) with lengths expressed in units of b_c, plotted as a function of the variable z. The peak at $z \approx 2$ corresponds to the divergence of $\chi_L''(b)$; for values of z below this, the stationary phase approximation breaks down.

our result becomes, replacing the constants a, b, c by their expressions as the derivatives of χ at $b = b_s$,

$$\begin{aligned} f(n,c,q) &\approx \sqrt{\frac{b_s}{2\pi q}} e^{i(\chi(b_s) - q b_s - \frac{\pi}{4} - (1/3)(\chi'')^3/((\chi''')^2))} (\chi''')^{-(1/3)} \pi \\ &\times \left(\mathrm{Ai}\left(\frac{(\chi''/2)^2}{(\chi'''/2)^{4/3}} \right) - i\mathrm{Gi}\left(\frac{(\chi''/2)^2}{(\chi'''/2)^{4/3}} \right) \right) \end{aligned} \tag{3.72}$$

We compare this to the full numerical expression in fig. 3.21. We see that it works well in the vicinity of the critical point, but gets progressively worse as we move away from $q = q_c$. Naively, we might have expected that the inclusion of the third derivative in our approximation could only improve our approximation. However, we have to remember that the logic underlying the stationary phase approximation involves the extension of a *local* approximation to the exponent about the saddle point to an *infinite* integration region, and that the nature of this extension is qualitatively different for the case of cubic and quadratic approximations.

This raises the question of what happens for $q > q_c$. In fig. 3.22 we see that a transition occurs from the semiclassical scaling law $\sim q^{-\frac{n+2}{n+1}}$ to the Born law $\sim q^{-4}$.

We can understand this by the following heuristic argument. Let us consider the expansion of $e^{i\chi} - 1$ in powers of χ_L. As already discussed, the term of order χ_L merely

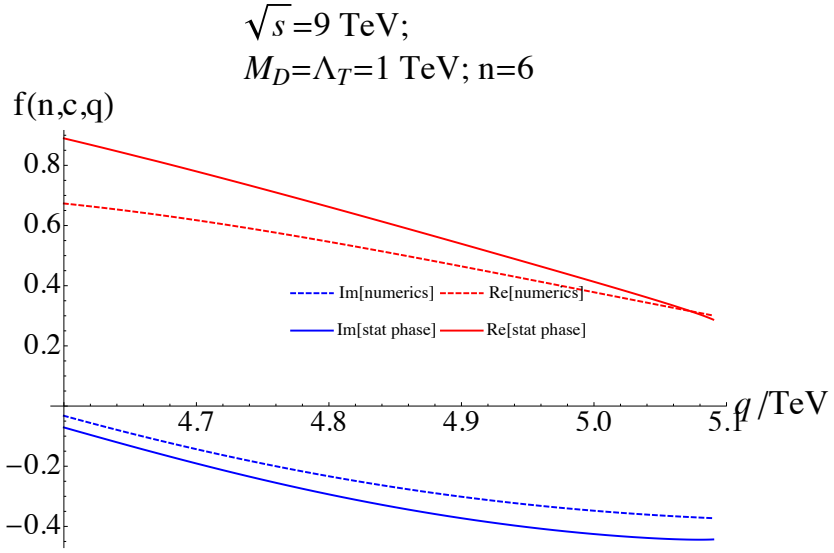

Figure 3.21: Comparison of (3.72) to the numerical evaluation of the eikonal.

reproduces the Born amplitude. At order χ^2 we have

$$\int d^2b e^{i\mathbf{q}\cdot\mathbf{b}}\chi_L^2 = \int d^2k \mathcal{A}_L(k)\mathcal{A}_L(q-k) \equiv \mathcal{M}^{(2)}(q) \tag{3.73}$$

by the convolution theorem. For q asymptotically large, we can neglect k in the argument of the second term over most of the integration region, and so the second term varies as $\sim q^{-4}$. The only region in which this is not true is that region in which k is itself on the order of q, in which event the first term $\mathcal{A}_L(k) \sim \mathcal{A}_L(q) \sim q^{-4}$. Having established that this term exhibits the Born scaling, we can proceed inductively and express the term of order χ^3 as a convolution of $\mathcal{A}_L$ with $\mathcal{M}^{(2)}(q)$; the same argument then suggests that $\mathcal{M}^{(3)}(q) \sim q^{-4}$.

Of course, it does not automatically follow that this transition between the scaling behaviours in q is experimentally observable, due to the kinematic limit $-t/s < 1$. Having investigated the theory of the RG-improved eikonal amplitudes in some detail, we now turn our attention to the corresponding experimental consequences.

3.4 Summary

We begun the chapter in section 3.1 by critically examining the claim that the eikonal amplitudes should be insensitive to the method used to regulate the sum over KK modes. We showed analytically how the dimensional regularisation procedure was related to adding a sharp cut off to the KK tower, both at the level of the Born amplitude and the eikonal

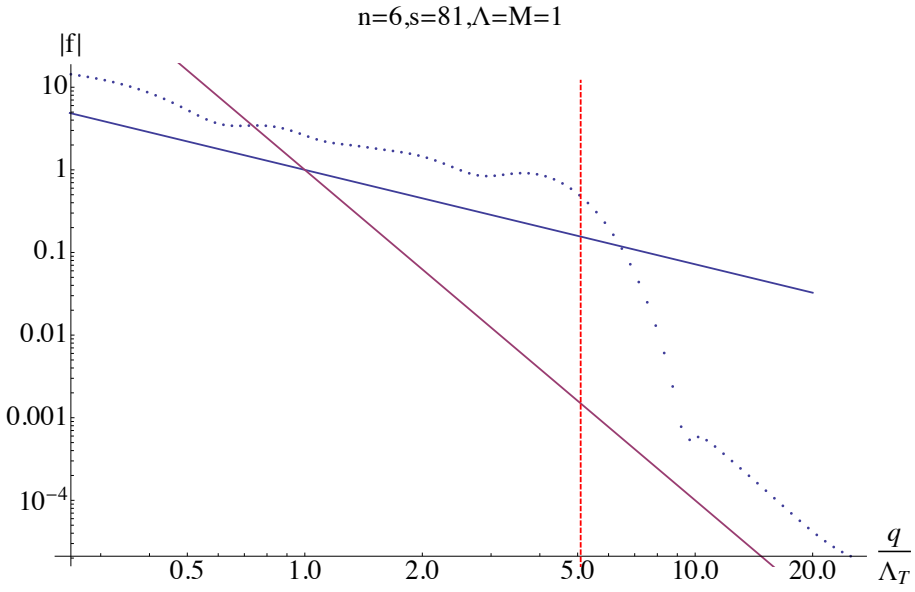

Figure 3.22: In this figure the blue dotted curve represents the absolute value of $|f|$ for the indicated parameters. The solid lines represent the scaling behaviours found in the semiclassical result (3.20) (blue) and in (3.33) (pink). The vertical red dashed line denotes the value of q/Λ_T at which the stationary phase approximation breaks down.

phase. We compared the resultant eikonal amplitudes, and found that in contrast to the theoretical consensus the two procedures gave different answers.

In section 3.2 we calculated the Born amplitude for the exchange of the KK tower of ADD gravitons on the assumption that gravity is asymptotically safe, to leading order in $-t/s$, in various approximations to the RG running of the gravitational coupling $G(\mu)$. These amplitudes depend upon a parameter Λ_T, which parametrises the energy scale at which the running of $G(\mu)$ changes from that associated with its classical dimension to that associated with the UV fixed point of the d-dimensional gravity theory. The corresponding eikonal phases were computed, and it was demonstrated that whilst the discontinuous derivative of Z_Q introduced long-distance pathologies into χ_Q, the eikonal phase χ_L given by (3.35) reproduced the expected $\sim b^{-n}$ behaviour at long distances whilst tending to a constant at short distances, reflecting the underlying fixed point of the theory. We commented upon the relation of this finding to other results such as spacetimes that depend on a gravitational coupling that runs in position space. Using this expression, we calculated an RG-improved eikonal amplitude for spacetimes of varying dimensionality. It was shown that at momentum transfers large compared to Λ_T the eikonal amplitude exhibited the same q^{-4} scaling behaviour as the Born amplitude, which had been argued to be another signature of fixed point scaling.

In section 3.3 we analysed the reasons for the failure of the arguments in favour of the semiclassical approximation, using the techniques of the stationary phase approximation. It was shown that whilst the unbounded growth of the semiclassical eikonal phases led to the existence of a stationary phase approximation at arbitrarily high momentum transfers, the vanishing derivative of χ_L at zero impact parameter led to a momentum transfer q_{crit} at which this approximation breaks down in our approach. It was shown numerically that this q_{crit} marks the onset of the q^{-4} scaling.

Chapter 4

Phenomenology of quantum gravity

In this chapter we discuss the phenomenology of the transplanckian elastic scattering amplitudes calculated in the previous chapter. Section 4.1 outlines the corresponding experimental signatures. In section 4.2 we reproduce some existing results based on the semiclassical approximation to these amplitudes, to compare our implementation to that of previous authors. Section 4.3 presents our main results, and discusses how they could play a role in constraining the theory parameters of our model.

4.1 Transplanckian scattering at hadron colliders

In order to deduce the experimental signatures through which quantum gravity might reveal itself at the Large Hadron Collider, we are forced to consider the well-known complications that arise due to the composite nature of the proton. The elastic scattering amplitudes calculated in the preceding chapter describe the collisions of the underlying *partons*, so we expect that the corresponding experimental signal will be dijet production. In order to investigate processes occurring at transplanckian energies $s \gg M_D^2$, we restrict our attention to dijet pairs with a very large invariant mass M_{JJ}; following [50, 2] we will demand that $M_{JJ} \geq M_{JJ,min} = 9$ TeV. To reduce the QCD background the cut $p_T > 100$ GeV is also imposed. The dijet signal that results from the Born amplitude calculated within effective field theory was calculated in [99], but their methods are clearly inapplicable at such high invariant masses.

The condition of small-angle scattering is slightly less straightforward to describe at a hadron collider, because the centre-of-mass of the colliding partons is *boosted* with respect

to the laboratory frame by an unknown amount that depends on the relative fractions x_i of the hadron momentum carried by the colliding partons, and hence transforming the scattering angle by an unknown amount. It is therefore useful to introduce the *pseudorapidity* separation of the jets, which in the limit of negligible particle mass is related to the Mandelstam variables and the centre-of-mass scattering angle $\hat{\theta}$ by [100]

$$\Delta\eta = \log\left(\frac{\hat{s}}{-\hat{t}} - 1\right) = \log\left(\frac{1+\cos\hat{\theta}}{1-\cos\hat{\theta}}\right) \tag{4.1}$$

This is a Lorentz invariant quantity, and we see that the limit of small $\hat{\theta}$ corresponds to large $\Delta\eta$. Our cuts on p_T together with the LHC restriction that $\sqrt{s} < 14$ TeV imply a maximum pseudorapidity separation of $\Delta\eta = 9.88$ [2]. Experimentally, we cannot differentiate between scattering through an angle θ and through $\pi - \theta$, which corresponds to swapping $\Delta\eta \leftrightarrow -\Delta\eta$. We therefore follow previous authors and plot $d\sigma/d|\Delta\eta|$ as our basic observable.

It was checked in [101] that the usual methods of factorization in QCD can be applied to the problem of transplanckian scattering in the ADD scenario, so that the observable differential cross-section is related to that for the underlying partonic event by

$$\frac{d\sigma}{d\Delta\eta} = \sum_{i,j}\int_0^1 dx_1 \int_0^1 dx_2 f_i(x_1,Q^2) f_j(x_2,Q^2) \frac{d\hat{\sigma}}{d\Delta\eta}(x_1,x_2)\theta(\hat{s}(x_1,x_2) - M_{J,min}^2) \tag{4.2}$$

where the partonic differential cross-section is related to the scattering amplitude $\mathcal{M}(s,t)$ via

$$\frac{d\hat{\sigma}}{d\Delta\eta}(x_1,x_2) = \frac{|\mathcal{M}(\hat{s}(x_{,1}\,,x_2), -\frac{\hat{s}(x_{,1},x_2)}{e^{\Delta\eta}+1})|^2}{16\pi\hat{s}(x_{,1}\,,x_2)} \frac{e^{\Delta\eta}}{(e^{\Delta\eta}+1)^2} \tag{4.3}$$

Here the partonic $\hat{s}(x_{,1}\,,x_2)$ is related to the hadronic Mandelstam variable S by

$$\hat{s}(x_{,1}\,,x_2) = x_1 x_2 S \tag{4.4}$$

The functions $f_i(x_1,Q^2)$ that appear in (4.2) are parton density functions (PDFs), describing the density of partons of species i carrying a fraction x_i of the hadron momentum. An illustrative plot is given in fig. 4.1.

We have implemented the eikonal scattering amplitudes discussed in the previous chapter in the PYTHIA 8.1 event generator [102, 103] as semi-internal processes, i.e. as derived C++ classes whose member functions return the partonic differential cross-section in a form appropriate for PYTHIA to use in the initial stage of generating LHC events. We use the MSTW08LO [104] PDF sets, but have checked against CTEQ5L [105] and find little difference.

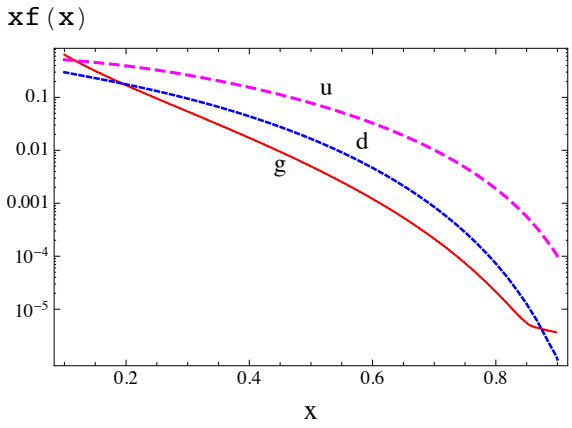

Figure 4.1: Illustrating the rapid decay of the PDFs at large x. Here we show the MST-WLO2008 pdfs at $Q = 1\text{TeV}$.

4.2 Dimensional regularisation

In order to make use of (4.2) it is necessary to choose a *factorization scale* Q at which to evaluate the parton density functions. For processes that are adequately characterised by the exchange of a single force-carrying boson, this would normally be taken to be proportional to the momentum of that boson. However, as we have discussed, transplanckian scattering through small angles intrinsically involves the exchange of many relatively *soft* gravitons, each carrying only a fraction of the total momentum transferred. As these gravitons will have a comparatively long wavelength λ, one might expect that their ability to resolve partons that appear as particle-antiparticle pairs that exist for time $\Delta t \ll 1/\lambda$ is limited. Ref. [106] therefore advocated a matching prescription based on the stationary phase approximation that $Q = \sqrt{-t} = q$ if $q < 1/b_c$, and $Q = 1/b_s < q$ if $q \geq 1/b_c$, where b_s was defined in (3.58).

PYTHIA does not have a provision for such custom factorisation scale matchings $Q = Q_c$, so in order to reproduce the results of [2] we evaluate our PDFs $f(x_i, Q^2)$ at a fixed scale Q_0, and when an event occurs we include a weight

$$w = \frac{f(x_1, Q_c^2)}{f(x_1, Q_0^2)} \frac{f(x_2, Q_c^2)}{f(x_2, Q_0^2)} \tag{4.5}$$

when assigning the event to the corresponding pseudorapidity bin in our histograms.

In fig. 4.2 we compare our results to those of [2]. Overall, we find good agreement, and in particular note that choice of smaller scales Q corresponds to a larger signal. There is a slight discrepancy in the matching $Q = q$ at around $|\Delta\eta| \approx 6$. We believe that this is accounted for by the different way in which we treat identical particles. When the colliding partons are identical, and carry identical color, the authors [2] symmetrise the

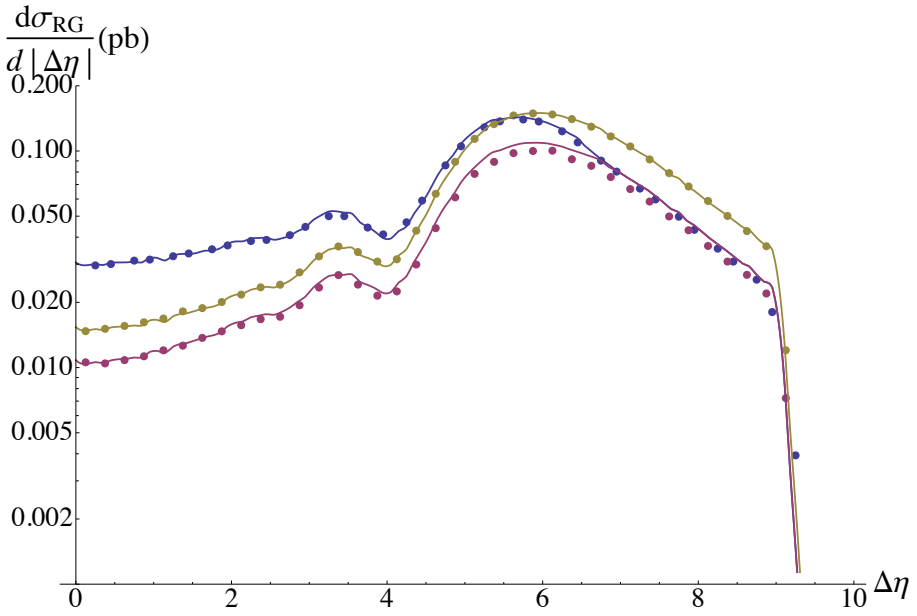

Figure 4.2: Comparison of our determination of the differential cross-section to that of the authors [2] for $Q = q$ (pink), $Q = P_T/2$ (yellow) and the stationary phase matching (blue). The solid curves are our results, and the data points are their results, kindly provided by E. Vryonidou.

amplitude in $t \leftrightarrow u$ to respect the quantum mechanics of indistinguishable particles [107]. In our view, however, this is not appropriate. Such symmetrisation occurs naturally in the sum over Feynman diagrams including t- and u- channel diagrams, but the latter is not included in the summation of diagrams which contribute to the eikonal amplitude, and is clearly subleading in $-t/s$ [8]. By symmetrising the amplitude in $t \leftrightarrow u$ after the summation one significantly- and in our view artificially- enhances the contribution of particles which scatter through extremely large angles. This effect can be seen in fig. 4.3.

The investigations [50, 2] both used leading-order codes in which the matrix elements were directly integrated against the PDFs using a VEGAS algorithm. By contrast, Pythia has the capability to produce a more realistic simulation, allowing for the production of extra jets by initial- and final- state radiation, or in the evolution of the parton shower. In this case the rapidity difference must be taken between the two hardest jets (ordered in terms of transverse momentum from the beam axis). We compare the inclusive and exclusive dijet cross-sections in fig. 4.4 and find little difference.

We reproduce the results of [2] varying M_D in fig. 4.5, as well as the comparison to the QCD background. We find that the QCD background, which dominates at the very largest rapidities, is reduced compared to their results. This appears to be a difference between PYTHIA and their VEGAS implementation, as the authors [50] used Pythia to simulate

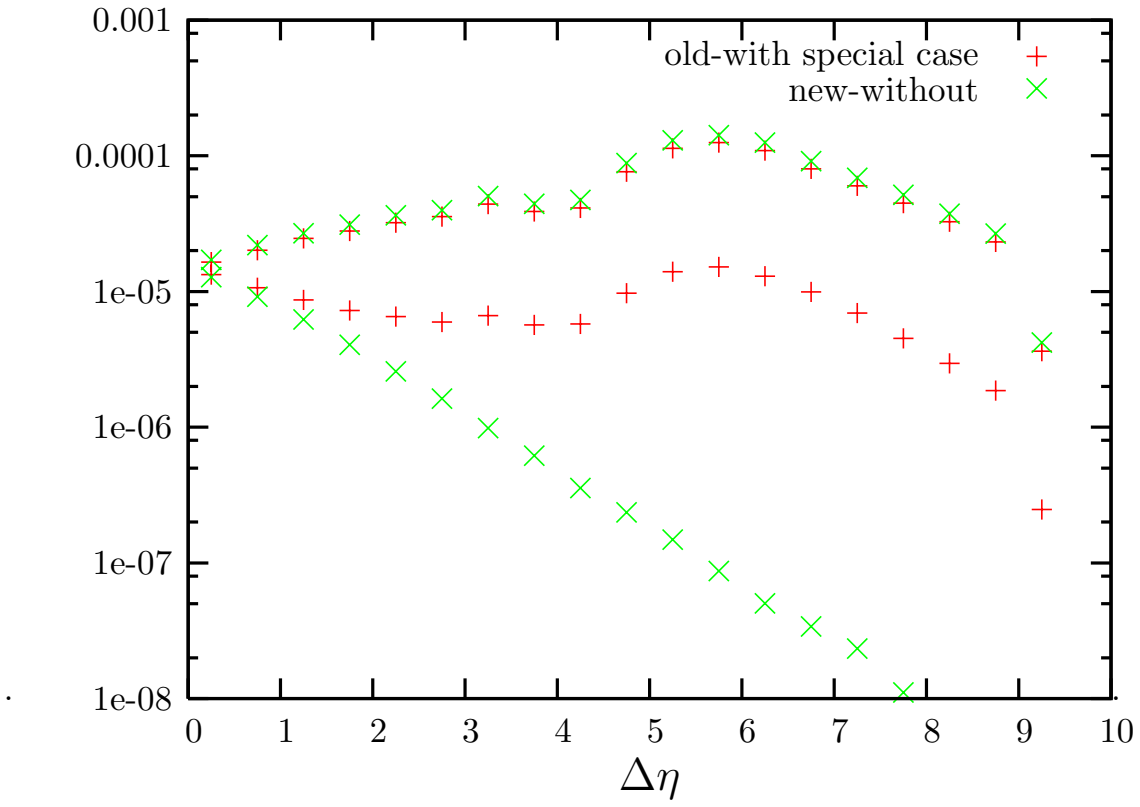

Figure 4.3: Comparison of positive and negative rapidity separations with and without imposing crossing symmetry on the amplitude, kindly provided by E.Vryonidou.

the QCD background, and our results agree with theirs. The important point that the transplanckian signal can clearly be distinguished from the QCD background at rapidities $|\Delta\eta| < 7.5$ is unaffected. In [50] the precise criteria imposed for forward scattering was that $\Delta\eta > 3$, so a clear range exists in which the eikonal approximation is kinematically reliable, and in which the signal can be distinguished from the background.

4.3 Phenomenology of quantum gravity

In this section we present the dijet signals corresponding to the RG-improved eikonal amplitude. The matrix elements were evaluated using the ALGLIB library to interpolate a 2-dimensional grid of data points tabulated using Mathematica 8.

We have seen in section 3.3 that there exists a critical momentum transfer q_c for which the stationary phase approximation breaks down. It follows that a matching of the factorisation or RG scales based on this approximation would likely introduce an unphysical discontinuity in observables at large momentum transfers, or equivalently at small rapidities. For this reason, we are forced to employ the simple prescription $\mu_{RG} = \mu_F = P_T/2$. As it was observed in the last section that harder scale choices tend to reduce

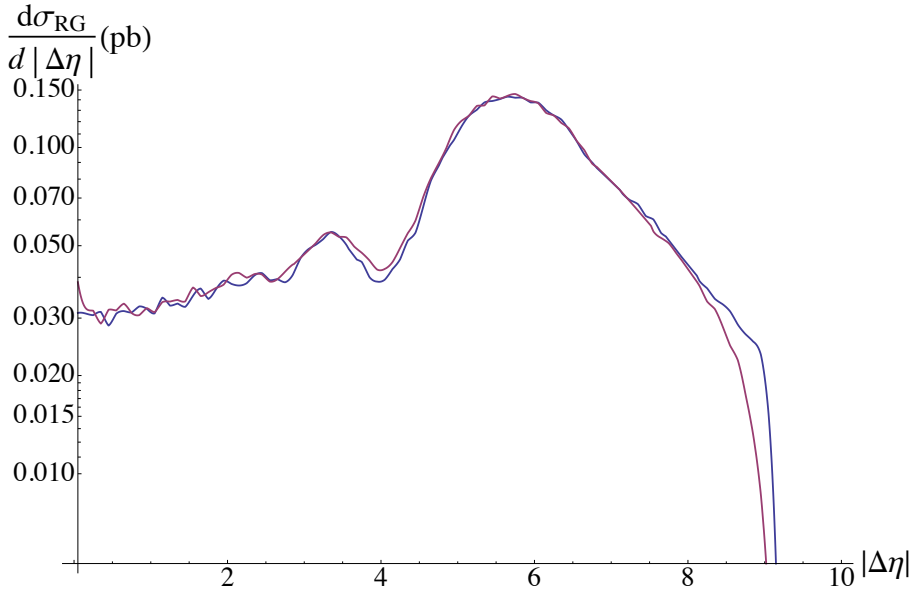

Figure 4.4: Comparison of the exclusive (blue) and inclusive (pink) dijet differential cross-sections.

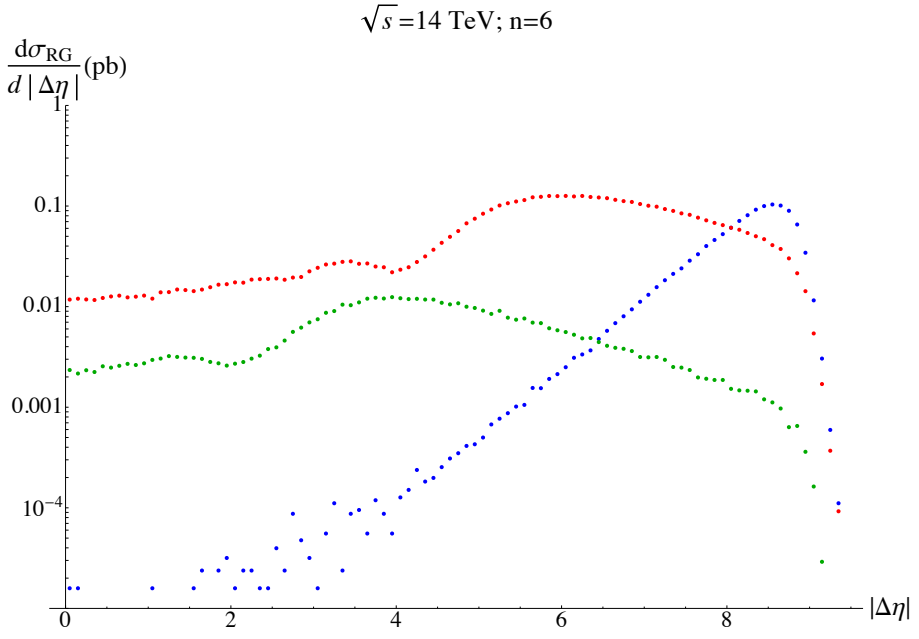

Figure 4.5: Illustration of the effect of varying M_D on the dijet signal, with M_D=1.5 TeV (red) and M_D=3 TeV (green). We also compare the signal to the QCD background (blue).

the signal, we expect that any softening of the factorisation scale due to multi-graviton exchange will only serve to increase the signal relative to our predictions. However, due to this theoretical uncertainty, we will try and indicate a key experimental signature for asymptotically safe gravity in the *shape* of the dijet distribution.

In principle, the relationship Λ_T/M_D is calculable, being related to the value g_* of the gravitational coupling at the ultraviolet fixed point via $g_* = (\Lambda_T/M_D)^{n+2}$. However, the study of higher-dimensional RG flows is not yet as developed as that in four dimensions, but has only been studied at the Einstein-Hilbert level. For this reason, it is prudent to treat Λ_T as a free parameter and investigate how the differential cross-section varies with it. Clearly, we expect that as Λ_T becomes large, our observables should reproduce those of dimensional regularisation. However, we have also seen before this limit is attained, we can see either an enhancement or a suppression of our signal depending on the variable z defined in (3.47). Furthermore, due to the integration over individual parton momenta in (4.2), for any fixed value of Λ_T we expect from (3.48) to sample a range of values of z.

However, it is known that the PDFs decrease extremely rapidly at high energies. This is illustrated in fig. 4.1. As our minimum invariant mass M_{JJ} is so high, partonic centre of mass energies significantly above the threshold make almost no contribution due to the smallness of the PDFs at large x. This allows us to identify a value of z that corresponds to a particular value of Λ_T,

$$z \sim \left(\frac{M_{JJ}^2}{M_D^2}\right)^{1/n} \frac{\Lambda_T}{M_D} \tag{4.6}$$

In fig. 4.6 we compare the eikonal differential cross-sections to those obtained from dimensional regularisation, and compare their relative sizes to the variation of the function $F(y,z)$ defined in (3.45) with z. The vertical dashed lines in the plots of $F(y,z)$ illustrate the values of z that correspond to the values of Λ_T for the cross-section curve of that colour. We see that the pattern of enhancements and suppressions in the cross-section exactly follows the variation of $F(y,z)$ about its semiclassical limit with z. In particular, the blue curves in figs. 4.6a,4.6c corresponding to values $M_{JJ} = 9$ TeV, $\Lambda_T = M_D = 1.5$TeV exhibit an *enhancement* of the differential cross-section relative to the semi-classical prediction; using (4.6) the corresponding values of z are indicated by the vertical dashed blue lines in figs. 4.6b, 4.6d, and in both cases we see that $|F_n(y,z)|$ is peaked above the limiting value of large z.

The most important message to be extracted from these plots is that one cannot straightforwardly use this signal to constrain M_D without simultaneous consideration of Λ_T. Indeed, whilst in the semiclassical theory we straightforwardly expect that increasing

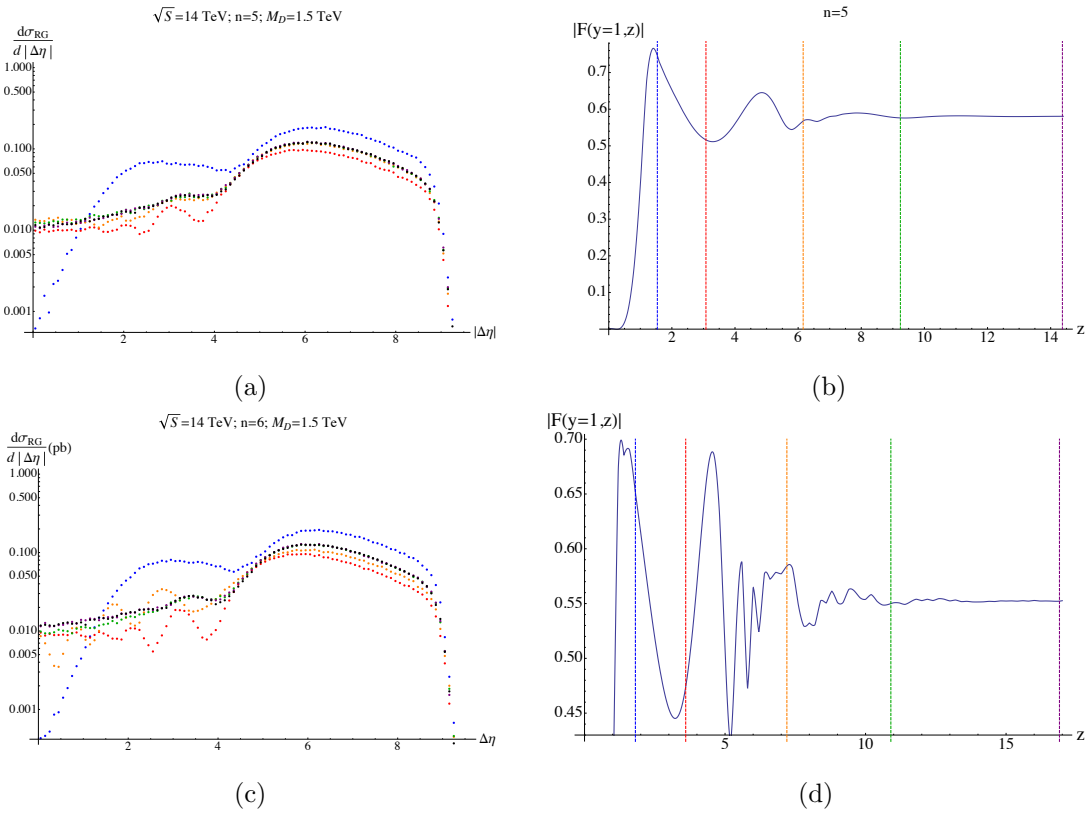

Figure 4.6: In these plots, we compare the variation of the differential cross section with Λ_T(left) to the variation of $F(y,z)$ with z in $n=5$ (above) and $n=6$ (below).

M_D serves to suppress the signal, we infer from this discussion that regions of parameter space exist in which increasing M_D reduces the value of the variable z such that the signal is actually *enhanced*.

The red curves in 4.6a,4.6c also merit comment. They correspond to a value of z in which the RG-improved amplitudes are lower than the semi-classical expectation. They are remarkable, however, for the complicated pattern of peaks at small rapidity separations. The peaks in the semi-classical differential cross-section were identified in [50] as a potential method by which the number n of extra dimensions might be identified. These oscillatory features serve as a warning of the possibility of more complicated distributions.

We also see that the blue curves in figs. 4.6a,4.6c are interesting not only because of the enhancement in the signal, but because of the different *shape* of the distribution, falling off much more rapidly with decreasing $|\Delta\eta|$. This can also be understood using (4.6), so that we can regard $|\Delta\eta|$ as a function only of the Mandelstam variable t with all other parameters fixed. We identify it as being due to the onset of fixed point scaling as

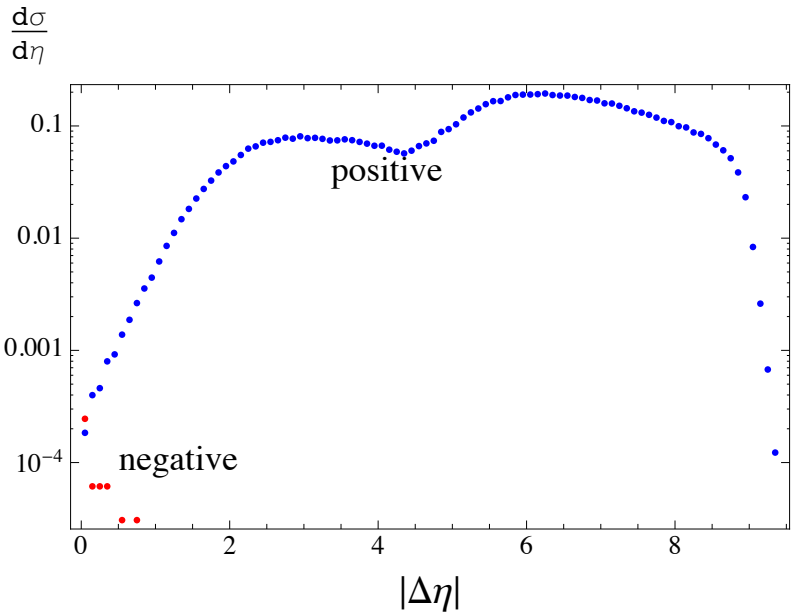

Figure 4.7: The RG-improved eikonal cross-section, with the contributions of positive (blue) and negative (red) rapidity separations of the jets separated. The increased dominance of positive over negative rapidities due to the more rapid decay of the RG-improved amplitude with t is clear.

seen in fig. 3.22; using eqs. (4.1), (4.3), if $|\mathcal{M}| \sim t^{-2}$, then it follows that for small $|\Delta\eta|$

$$\frac{d\hat{\sigma}}{d\Delta\eta} \sim e^{\Delta\eta}(e^{\Delta\eta}+1) \tag{4.7}$$

We also see in fig. 4.7 that this effect leads to a reduced contribution from negative $|\Delta\eta|$. We emphasise that this behaviour is *universal*, and will hold in any number of extra dimensions. The only requirement is that the $\sim t^{-2}$ scaling behaviour be kinematically accessible, i.e. $q_c < \sqrt{M_{JJ}}$.

What, then, if we find ourselves in the happy position of finding an excess of dijet events at high invariant masses over the standard model predictions when the LHC has completed its 14 TeV run? Our results suggest that the first thing to do is observe whether or not we see the exponential shape (4.7) in the distribution. If we do, then the rapidity separation at which it occurs could be used to infer the critical momentum transfer q_c at which we see the onset of fixed point scaling. Alternatively, we might find that the data are well-described by the semiclassical distribution. This would then mean that we were in a situation where the fixed point described extremely strong coupling in the ultraviolet, and the results of [2, 50] could be used to determine M_D and n.

To calculate the total cross-sections, the authors [2, 50] only integrate over rapidity separations $3 < |\Delta\eta| < 4$ in order to maximise their signal-to-background ratio. The above

discussion suggests that we can estimate estimate upper and lower bounds on a predicted cross-section in the eikonal regime by varying z so that $F(y,z)$ varies about its asymptotic limit; we carry this out by taking $M_D = 1.5$ TeV, and $\Lambda_T = 1.5, 3$ TeV (corresponding to the blue and red curves respectively in fig. 4.6c). We present these results in table4.1. We see that for these choices of parameter, the signal should be extremely clear. This is a consequence of both the fact that the gravitational coupling is large at transplanckian energies $\sqrt{s} > M_D$, and the fact that the QCD background for our cuts is small.

$3 < \lvert\Delta\eta\rvert < 4$; $p_T > 100$ GeV; $M_{JJ} > 9$TeV	$\Lambda_T = 1.5$ TeV	$\Lambda_T = 3$ TeV
σ (fb)	778	233
$S/\sqrt{B}$ L=30 fb^{-1}	4948	1480
$S/\sqrt{B}$ L=300 fb^{-1}	15600	4680

Table 4.1: Predicted cross-sections and $S/\sqrt{B}$ values for the specified choices of model parameters. The QCD background of dijets with very large invariant masses has been calculated in PYTHIA to be σ_{QCD} =0.7 fb.

Chapter 5

Conclusions

The scenario envisioned by the ADD authors in which large flat extra dimensions exist is tremendously exciting and theoretically challenging, with many observables not being strictly calculable due to the perturbative non-renormalisability of gravity. In this thesis we have examined graviton exchange at transplanckian energies in the ADD model, supplanted for the first time by calculations in a genuinely quantum framework for gravity, that of the asymptotic safety. We have argued that due to the high energies probed by the tower of exchanged Kaluza-Klein states of the graviton, a process that we would usually expect to be described well by semiclassical physics becomes exquisitely sensitive to the UV completion of gravity.

In chapter 2 we reviewed all the theoretical elements that underpin our work. We discussed the motivation and evidence for the asymptotic safety of gravity, including discussion of explicit RG equations and the beta function for the gravitational coupling in the simplest approximation. We reviewed the physics of the ADD model in detail, explaining how the divergent sums over KK modes of the graviton arise due to neglecting the bulk momentum of the brane on which we are trapped. We gave a complete and explicit derivation of the eikonal amplitude, and discussed its applicability to gravitational scattering at high energies, as well as its particularly pleasing features from the perspective of unitarity.

In chapter 3 we demonstrated explicitly that at LHC energies, the eikonal amplitude becomes sensitive to the methods used to define the naively divergent Born amplitude. We calculated the RG-improved Born amplitudes in various approximations. We determined the corresponding eikonal phases χ, and interpreted the short distance behaviour as being indicative of the underlying fixed point of the theory. From the physically acceptable 'linear' prescription Z_L for the running of $G(\mu)$ we calculated the corresponding eikonal scattering amplitudes, and showed that the semiclassical approximation was borne out

only in the limit of very strong coupling in the complete quantum gravity theory. We examined the stationary phase approximation to our amplitudes, demonstrating explicitly how the theoretical pillars that underlie the semiclassical nature of the eikonal amplitude fail in the ADD scenario: through the creation of a second saddle point at short distances; through a shortening of the length scale that characterises the process; and through the eventual breakdown of the approximation.

In chapter 4 we considered the phenomenology of transplanckian scattering in our framework, investigating the differential djiet cross section at large invariant masses and pseudorapidity separations. We reproduced known results, both using the semiclassical amplitudes and in the limit of large Λ_T in the RG-improved equations, as a check on the consistency of our framework. We explained how different regions of our parameter space could serve to either enhance or suppress the experimental signature relative to the semiclassical ansatz. We identified the power law (4.7) as a signature of fixed point scaling, and argued that in the event of an experimental signature at the LHC it would form a useful indicator as to whether the UV interacting fixed point of quantum gravity is strongly or weakly coupled.

Of course, this work could be extended in many directions. One fascinating extension would be to explore the transition from the elastic scattering regime to that of black hole formation, which due to Hawking radiation is usually expected to be strongly inelastic. In [108] it was argued that asymptotically safe black holes are *thermodynamically* stable, eventually forming Planck-sized remnants, but the question of whether or not they are stable *quantum mechanically* is an altogether different one- one that forces us to concede our ignorance of what is going on behind the event horizon of a black hole small enough for quantum mechanics to become important. This discussion would also be of interest in $d = 4$. Whilst the UV sensitivity of the eikonal in the ADD scenario can ultimately be traced back to the KK tower, the transition to black hole formation is associated with a loop diagram [1] which it would be interesting to investigate within asymptotic safety.

A more complete treatment of our phenomenology would also be desirable. The information we have been able to extract about our model parameters is at best partial; it would be interesting to adopt an integrated approach, using a combination of channels to determine each of the parameters Λ_T, M_D and n.

Bibliography

[1] Steven B. Giddings. The gravitational S-matrix: Erice lectures. *arXiv:1105.2036v1 [hep-th]*, 2011.

[2] W. J. Stirling, E. Vryonidou, and J. D. Wells. Eikonal regime of gravity-induced scattering at higher energy proton colliders. *Eur. Phys. J.*, C71:1642, 2011.

[3] R.P. Feynman. Quantum theory of gravitation. *Acta Phys.Polon.*, 24:697–722, 1963.

[4] S.W. Hawking. Information loss in black holes. *Phys.Rev.*, D72:084013, 2005.

[5] Steven Weinberg. *Gravitation and Cosmology: Principles and Applications of the General Theory of Relativity.* Wiley, New York, NY, 1972.

[6] G. t' Hooft. Graviton dominance in ultra-high-energy scattering. *Physics Letters B*, 198(1):61 – 63, 1987.

[7] Herman L. Verlinde and Erik P. Verlinde. Scattering at Planckian energies. *Nucl.Phys.*, B371:246–268, 1992.

[8] Daniel N. Kabat and Miguel Ortiz. Eikonal quantum gravity and Planckian scattering. *Nucl. Phys.*, B388:570–592, 1992.

[9] Kip Thorne. *Magic without magic: John Archibald Wheeler; a collection of essays in honor of his sixtieth birthday.* 1972.

[10] John F. Donoghue. Leading quantum correction to the Newtonian potential. *Phys.Rev.Lett.*, 72:2996–2999, 1994.

[11] John F. Donoghue. General relativity as an effective field theory: The leading quantum corrections. *Phys.Rev.*, D50:3874–3888, 1994.

[12] Marc H. Goroff and Augusto Sagnotti. QUANTUM GRAVITY AT TWO LOOPS. *Phys.Lett.*, B160:81, 1985.

[13] Marc H. Goroff and Augusto Sagnotti. The Ultraviolet Behavior of Einstein Gravity. *Nucl.Phys.*, B266:709, 1986.

[14] t'Hooft and Veltman. One-loop divergencies in the theory of gravitation. *Annales de l'Institut Henri Poincar : Section A, Physique thorique*, 20:69, 1974.

[15] Nima Arkani-Hamed, Savas Dimopoulos, and G. R. Dvali. The hierarchy problem and new dimensions at a millimeter. *Phys. Lett.*, B429:263–272, 1998.

[16] Ignatios Antoniadis, Nima Arkani-Hamed, Savas Dimopoulos, and G.R. Dvali. New dimensions at a millimeter to a Fermi and superstrings at a TeV. *Phys.Lett.*, B436:257–263, 1998.

[17] Steven Weinberg. *General Relativity: An Einstein Centenary Survey.* CUP, 1979.

[18] Peter Fischer and Daniel F. Litim. Fixed points of quantum gravity in higher dimensions. *AIP Conf.Proc.*, 861:336–343, 2006.

[19] Peter Fischer and Daniel F. Litim. Fixed points of quantum gravity in extra dimensions. *Phys.Lett.*, B638:497–502, 2006.

[20] Daniel F. Litim. Fixed points of quantum gravity. *Phys. Rev. Lett.*, 92:201301, 2004.

[21] Daniel F. Litim. On fixed points of quantum gravity. *AIP Conf. Proc.*, 841:322–329, 2006.

[22] Jan-Eric Daum, Ulrich Harst, and Martin Reuter. Running Gauge Coupling in Asymptotically Safe Quantum Gravity. *JHEP*, 1001:084, 2010.

[23] J.-E. Daum, U. Harst, and M. Reuter. Non-perturbative QEG Corrections to the Yang-Mills Beta Function. *Gen. Relativ. Gravit.*, 2010.

[24] Roberto Percacci and Daniele Perini. Constraints on matter from asymptotic safety. *Phys.Rev.*, D67:081503, 2003.

[25] Roberto Percacci and Daniele Perini. Asymptotic safety of gravity coupled to matter. *Phys.Rev.*, D68:044018, 2003.

[26] U. Harst and M. Reuter. QED coupled to QEG. *JHEP*, 1105:119, 2011.

[27] K. Falls, D.F. Litim, K. Nikolakopoulos, and C. Rahmede. A bootstrap towards asymptotic safety. 2013.

[28] Benjamin Koch and Frank Saueressig. Structural aspects of asymptotically safe black holes. *Class.Quant.Grav.*, 31:015006, 2014.

[29] Daniel F. Litim and Konstantinos Nikolakopoulos. Quantum gravity effects in Myers-Perry space-times. *JHEP*, 1404:021, 2014.

[30] Kevin Falls, Daniel F. Litim, and Aarti Raghuraman. Black Holes and Asymptotically Safe Gravity. *Int.J.Mod.Phys.*, A27:1250019, 2012.

[31] D. Becker and M. Reuter. Asymptotic Safety and Black Hole Thermodynamics. 2012.

[32] Kevin Falls. *Asymptotic safety and black holes*. PhD thesis, U. Sussex, 2013.

[33] Steven Weinberg. Asymptotically Safe Inflation. *Phys.Rev.*, D81:083535, 2010.

[34] Adriano Contillo. Inflation in asymptotically safe f(R) theory. *J.Phys.Conf.Ser.*, 283:012009, 2011.

[35] Edmund J. Copeland, Christoph Rahmede, and Ippocratis D. Saltas. Asymptotically Safe Starobinsky Inflation. 2013.

[36] Mark Hindmarsh, Daniel Litim, and Christoph Rahmede. Asymptotically Safe Cosmology. *JCAP*, 1107:019, 2011.

[37] J. P. Brinkmann, G. Hiller, Litim D. F., and J. Schröder. to appear.

[38] Jan Schröder. Unitarity Bounds for Higgs Scattering within a 4+n dimensional setup of Fixed Point Gravity. Diploma thesis, Lehrstuhl für Theoretische Physik III, Fakultät für Physik, Technische Universität Dortmund, 2011.

[39] JoAnne Hewett and Thomas Rizzo. Collider Signals of Gravitational Fixed Points. *JHEP*, 0712:009, 2007.

[40] Erik Gerwick, Daniel Litim, and Tilman Plehn. Asymptotic safety and Kaluza-Klein gravitons at the LHC. *Phys.Rev.*, D83:084048, 2011.

[41] Feynman, Morinigo, and Wagner. *Feynman Lectures on Gravitation*. Westview Press, 2003.

[42] S. Weinberg. Derivation of gauge invariance and the equivalence principle from lorentz invariance of the s-matrix. *Phys. Lett.*, 9:357, 1964.

[43] S. Weinberg. Photons and gravitons in perturbation theory: Derivation of maxwell's and einstein's equations. *Phys. Rev.*, 138:B988, 1965.

[44] Stanley Deser. Selfinteraction and gauge invariance. *Gen.Rel.Grav.*, 1:9–18, 1970.

[45] S. Weinberg. Infrared photons and gravitons. *Phys. Rev*, 140:B516–B524, 1965.

[46] Kenneth G. Wilson. Renormalization group and critical phenomena. 1. Renormalization group and the Kadanoff scaling picture. *Phys.Rev.*, B4:3174–3183, 1971.

[47] Kenneth G. Wilson. Renormalization group and critical phenomena. 2. Phase space cell analysis of critical behavior. *Phys.Rev.*, B4:3184–3205, 1971.

[48] Georges Aad et al. Observation of a new particle in the search for the Standard Model Higgs boson with the ATLAS detector at the LHC. *Phys.Lett.*, B716:1–29, 2012.

[49] Serguei Chatrchyan et al. Observation of a new boson at a mass of 125 GeV with the CMS experiment at the LHC. *Phys.Lett.*, B716:30–61, 2012.

[50] Gian F. Giudice, Riccardo Rattazzi, and James D. Wells. Transplanckian collisions at the LHC and beyond. *Nucl. Phys.*, B630:293–325, 2002.

[51] Daniel F. Litim. Renormalisation group and the Planck scale. *Phil. Trans. R. Soc.*, A 369:2759–2778, 2011.

[52] Roberto Percacci and Daniele Perini. On the ultraviolet behaviour of Newton's constant. *Class.Quant.Grav.*, 21:5035–5041, 2004.

[53] Christof Wetterich. Exact evolution equation for the effective potential. *Phys.Lett.*, B301:90–94, 1993.

[54] Holger Gies. Introduction to the functional RG and applications to gauge theories. *Lect.Notes Phys.*, 852:287–348, 2012.

[55] Michael E. Peskin and Dan V. Schroeder. *An Introduction To Quantum Field Theory (Frontiers in Physics)*. Westview Press, 1995.

[56] Daniel F. Litim. Optimization of the exact renormalization group. *Phys.Lett.*, B486:92–99, 2000.

[57] Daniel F. Litim. Optimized renormalization group flows. *Phys.Rev.*, D64:105007, 2001.

[58] M. Niedermaier. The asymptotic safety scenario in quantum gravity: An introduction. *Class. Quant. Grav.*, 24:R171–230, 2007.

[59] Martin Reuter and Frank Saueressig. Quantum Einstein Gravity. *New J.Phys.*, 14:055022, 2012.

[60] Daniel F. Litim and Tilman Plehn. Signatures of gravitational fixed points at the LHC. *Phys.Rev.Lett.*, 100:131301, 2008.

[61] Robert C. Myers and M.J. Perry. Black Holes in Higher Dimensional Space-Times. *Annals Phys.*, 172:304, 1986.

[62] Gian F. Giudice, Riccardo Rattazzi, and James D. Wells. Quantum gravity and extra dimensions at high-energy colliders. *Nucl. Phys.*, B544:3–38, 1999.

[63] Raman Sundrum. Effective field theory for a three-brane universe. *Phys.Rev.*, D59:085009, 1999.

[64] Schuyler Cullen and Maxim Perelstein. SN1987A constraints on large compact dimensions. *Phys. Rev. Lett.*, 83:268–271, 1999.

[65] Vernon D. Barger, Tao Han, C. Kao, and Ren-Jie Zhang. Astrophysical constraints on large extra dimensions. *Phys. Lett.*, B461:34–42, 1999.

[66] Csaba Csaki. TASI lectures on extra dimensions and branes. 2004.

[67] Tao Han, Joseph D. Lykken, and Ren-Jie Zhang. On Kaluza-Klein states from large extra dimensions. *Phys. Rev.*, D59:105006, 1999.

[68] Leif Lonnblad and Malin Sjodahl. Classical and non-classical ADD-phenomenology with high-E (perpendicular) jet observables at collider experiments. *JHEP*, 10:088, 2006.

[69] Greg Landsberg. Searches for Extra Spatial Dimensions with the CMS Detector at the LHC. *Mod. Phys. Lett.*, A30(15):1540017, 2015.

[70] Michael Kruskal. Searches for dark matter and extra dimensions with the ATLAS detector. *EPJ Web Conf.*, 95:04034, 2015.

[71] Clifford M. Will. The Confrontation between General Relativity and Experiment. *Living Rev. Rel.*, 17:4, 2014.

[72] Tom Banks and Willy Fischler. A Model for high-energy scattering in quantum gravity. 1999.

[73] Savas Dimopoulos and Greg L. Landsberg. Black holes at the LHC. *Phys.Rev.Lett.*, 87:161602, 2001.

[74] Steven B. Giddings and Scott D. Thomas. High-energy colliders as black hole factories: The End of short distance physics. *Phys.Rev.*, D65:056010, 2002.

[75] S.W. Hawking. Particle Creation by Black Holes. *Commun.Math.Phys.*, 43:199–220, 1975.

[76] Philip C. Argyres, Savas Dimopoulos, and John March-Russell. Black holes and submillimeter dimensions. *Phys.Lett.*, B441:96–104, 1998.

[77] Patrick Meade and Lisa Randall. Black Holes and Quantum Gravity at the LHC. *JHEP*, 0805:003, 2008.

[78] Ted Jacobson. Introduction to quantum fields in curved space-time and the Hawking effect. In *Lectures on quantum gravity. Proceedings, School of Quantum Gravity, Valdivia, Chile, January 4-14, 2002*, pages 39–89, 2003.

[79] Steven Weinberg. *The Quantum theory of fields. Vol. 1: Foundations.* 1995.

[80] Maurice Levy and Joseph Sucher. Eikonal approximation in quantum field theory. *Phys.Rev.*, 186:1656–1670, 1969.

[81] Henry D.I. Abarbanel and Claude Itzykson. Relativistic eikonal expansion. *Phys.Rev.Lett.*, 23:53, 1969.

[82] G. Tiktopoulos and S.B. Treiman. Relativistic eikonal approximation. *Phys.Rev.*, D3:1037–1040, 1971.

[83] Hung Cheng and Tai Tsun Wu. Impact factor and exponentiation in high-energy scattering processes. *Phys.Rev.*, 186:1611–1618, 1969.

[84] Hung Cheng and T.T. Wu. *EXPANDING PROTONS: SCATTERING AT HIGH-ENERGIES.* MIT Press, 1987.

[85] Jun John Sakurai. *Modern Quantum Mechanics.* Addison-Wesley, 1994.

[86] Steven B. Giddings and Mark Srednicki. High-energy gravitational scattering and black hole resonances. *Phys.Rev.*, D77:085025, 2008.

[87] Steven B. Giddings, Maximilian Schmidt-Sommerfeld, and Jeppe R. Andersen. High energy scattering in gravity and supergravity. *Phys.Rev.*, D82:104022, 2010.

[88] D. Amati, M. Ciafaloni, and G. Veneziano. Planckian scattering beyond the semi-classical approximation. *Phys.Lett.*, B289:87–91, 1992.

[89] D. Amati, M. Ciafaloni, and G. Veneziano. Superstring Collisions at Planckian Energies. *Phys.Lett.*, B197:81, 1987.

[90] D. Amati, M. Ciafaloni, and G. Veneziano. Classical and Quantum Gravity Effects from Planckian Energy Superstring Collisions. *Int.J.Mod.Phys.*, A3:1615–1661, 1988.

[91] D. Amati, M. Ciafaloni, and G. Veneziano. Can Space-Time Be Probed Below the String Size? *Phys.Lett.*, B216:41, 1989.

[92] D. Amati, M. Ciafaloni, and G. Veneziano. Higher Order Gravitational Deflection and Soft Bremsstrahlung in Planckian Energy Superstring Collisions. *Nucl.Phys.*, B347:550–580, 1990.

[93] P.C. Aichelburg and R.U. Sexl. On the Gravitational field of a massless particle. *Gen.Rel.Grav.*, 2:303–312, 1971.

[94] Malin Sjodahl and Gosta Gustafson. Gravitational scattering in the ADD-model at high and low energies. *Eur. Phys. J.*, C53:109–119, 2008.

[95] Leif Lonnblad and Malin Sjodahl. Classical and non-classical ADD-phenomenology with high-E (perpendicular) jet observables at collider experiments. *JHEP*, 0610:088, 2006.

[96] Dmitry V. Gal'tsov, Georgios Kofinas, Pavel Spirin, and Theodore N. Tomaras. Classical ultra-relativistic scattering in ADD. *JHEP*, 0905:074, 2009.

[97] J.I. Illana, M. Masip, and D. Meloni. TeV gravity at neutrino telescopes. *Phys.Rev.*, D72:024003, 2005.

[98] E.M. Sessolo and D.W. McKay. Eikonal contributions to ultra high energy neutrino-nucleon cross sections in low scale gravity models. *Phys.Lett.*, B668:396–403, 2008.

[99] David Atwood, Shaouly Bar-Shalom, and Amarjit Soni. Dijet production at hadron colliders in theories with large extra dimensions. *Phys.Rev.*, D62:056008, 2000.

[100] Tao Han. Collider phenomenology: Basic knowledge and techniques. pages 407–454, 2005.

[101] Paolo Lodone and Vyacheslav S. Rychkov. Radiation Problem in Transplanckian Scattering. *JHEP*, 0912:036, 2009.

[102] Torbjorn Sjostrand, Stephen Mrenna, and Peter Z. Skands. PYTHIA 6.4 Physics and Manual. *JHEP*, 0605:026, 2006.

[103] Torbjorn Sjostrand, Stephen Mrenna, and Peter Z. Skands. A Brief Introduction to PYTHIA 8.1. *Comput.Phys.Commun.*, 178:852–867, 2008.

[104] A.D. Martin, W.J. Stirling, R.S. Thorne, and G. Watt. Parton distributions for the LHC. *Eur.Phys.J.*, C63:189–285, 2009.

[105] H.L. Lai, J. Botts, J. Huston, J.G. Morfin, J.F. Owens, et al. Global QCD analysis and the CTEQ parton distributions. *Phys.Rev.*, D51:4763–4782, 1995.

[106] Roberto Emparan, Manuel Masip, and Riccardo Rattazzi. Cosmic rays as probes of large extra dimensions and TeV gravity. *Phys.Rev.*, D65:064023, 2002.

[107] E.Vryonidou. Private communication.

[108] Kevin Falls and Daniel F. Litim. Black hole thermodynamics under the microscope. *Phys.Rev.*, D89:084002, 2014.

[109] I. S. Gradshteyn and I. M. Ryzhik. *Table of integrals, series, and products*. Elsevier/Academic Press, Amsterdam, seventh edition, 2007. Translated from the Russian, Translation edited and with a preface by Alan Jeffrey and Daniel Zwillinger, With one CD-ROM (Windows, Macintosh and UNIX).

[110] Yudell L. Luke. *Special functions and their approximations*, volume 1. Academic Press, 1969.

[111] Wolfram Research. Wolfram functions.

Appendix A

Calculations with linear RG running

A.1 Calculation of $\mathcal{A}_L$ & χ_L

Using the prescription (2.30) in (3.13), we have

$$\chi_L = -\frac{C\Lambda_T^{n+2}}{4\pi s}\int_0^\infty dq \int_0^\infty dm\; qJ_0(b'q)\frac{m^{n-1}}{q^2+m^2}\frac{1}{1+(q^2+m^2)^{n/2+1}} \tag{A.1}$$

Here m and q are the dimensionless 4-momentum and KK mass, expressed in terms of the transition scale Λ_T, whilst again $b' = b\Lambda_T$. We evaluate this integral by switching to polar co-ordinates in (dimensionless) momentum space via the prescription $q \to \mu\sin\theta, m \to \mu\cos\theta$, so that μ is now our dimensionless RG scale. It then becomes

$$\begin{aligned}
\chi_L &= -\frac{C\Lambda_T^{n+2}}{4\pi s}\int_0^\infty d\mu \int_0^{\pi/2} d\theta \frac{\mu^{n-1}}{1+\mu^{n+2}} J_0(b'\mu\sin\theta)\cos^{n-1}\theta\sin\theta \\
&= -\frac{C\Lambda_T^{n+2}}{4\pi s}\frac{1}{n}\int_0^\infty d\mu \frac{\mu^{n-1}}{1+\mu^{n+2}}\;{}_0F_1\left(1+\frac{n}{2}, -\frac{1}{4}b'^2\mu^2\right) \\
&= -\frac{C\Lambda_T^{n+2}}{4\pi s}\frac{\Gamma\left(1+\frac{n}{2}\right)2^{n/2}}{nb^{n/2}}\int_0^\infty d\mu \frac{\mu^{n/2-1}}{1+\mu^{n+2}} J_{n/2}(b'\mu) \\
&= -\frac{C\Lambda_T^{n+2}}{4\pi s}\frac{\Gamma\left(\frac{n}{2}\right)2^{n/2-1}}{b'^{n/2}}\int_0^\infty d\mu \frac{\mu^{n/2-1}}{1+\mu^{n+2}} G_{0,2}^{1,0}\left(\frac{b'^2\mu^2}{4}\middle|_{\frac{n}{4},-\frac{n}{4}}\right) \\
&= -\frac{C\Lambda_T^{n+2}}{4\pi s}\frac{\Gamma\left(\frac{n}{2}\right)2^{n/2-1}}{b'^{n/2}}\frac{1}{n+2}\int_0^\infty dz \frac{z^{-\frac{(n/2+2)}{n+2}}}{1+z} G_{0,2}^{1,0}\left(\frac{b'^2 z^{\frac{2}{n+2}}}{4}\middle|_{\frac{n}{4},-\frac{n}{4}}\right)
\end{aligned}$$

This is now in the form in which we can apply (B.12). The only proviso is that the fractional exponent of the argument of the G-function must be fully simplified, which motivates the definitions of l and k given in the main text. The corresponding Born

amplitude (3.33) is then determined from χ_L by inverting the Fourier transform, using (2.62), re-writing the Bessel function as a Meijer-G function, and using (B.16).

A.2 Contour integral

We wish to evaluate the eikonal phase, starting with the integral representation

$$\begin{aligned}\chi(b) &= -\frac{s\Lambda_T^n}{M_D^{n+2}} S_n \frac{\Gamma\left(\frac{n}{2}\right) 2^{n/2-1}}{b^{n/2}} \int_0^\infty d\mu \frac{\mu^{n/2-1}}{1+\mu^{n+2}} J_{n/2}(b\mu) && \text{(A.2)}\\ &\equiv -\frac{s\Lambda_T^n}{M_D^{n+2}} \tilde{\chi} && \text{(A.3)}\end{aligned}$$

where $S_n = \frac{2\pi^{n/2}}{\Gamma(n/2)}$ is the area of the unit-n sphere and b is the impact parameter in units of inverse Λ_T.

We work throughout in even n.

The integral (A.2) is ill-suited to evaluation via contour methods, because the Bessel function grows exponentially with the modulus of the imaginary part of its argument. We instead use the Hankel function

$$H_\nu^{(1)}(z) = J_\nu(z) + iY_\nu(z) \tag{A.4}$$

For $x > 0 \in \mathbb{R}$ the Bessel function of the second kind $Y_\nu(x)$ is real, so (A.2) becomes

$$\begin{aligned}\tilde{\chi}(b) &= S_n \frac{\Gamma\left(\frac{n}{2}\right) 2^{n/2-1}}{b^{n/2}} \mathrm{Re}\left[\int_0^\infty d\mu \frac{\mu^{n/2-1}}{1+\mu^{n+2}} H_{n/2}^{(1)}(b\mu)\right] && \text{(A.5)}\\ &\equiv S_n \frac{\Gamma\left(\frac{n}{2}\right) 2^{n/2-1}}{b^{n/2}} \mathrm{Re}\left[\int_0^\infty d\mu R(\mu) H_{n/2}^{(1)}(b\mu)\right] && \text{(A.6)}\end{aligned}$$

The advantage of this replacement is that $H_\nu(z)$ has the asymptotic behaviour

$$H_\nu(z) \sim \sqrt{\frac{2}{\pi z}} e^{i(z-\nu\pi/2-\pi/4)} \tag{A.7}$$

so that it decays exponentially in the upper complex plane. (c.f. Evaluating integrals of $\cos(x)$ with a rational function by identifying $\cos(x) = \mathrm{Re}\left[e^{ix}\right]$, rather than expanding the cosine in terms of complex exponentials.)

We can extend this to an integral over the entire real axis. Using the identity

$$Y_\nu(ze^{m\pi i}) = e^{m\nu\pi i} Y_\nu(z) + 2i \sin(m\nu\pi) \cot(\nu\pi) J_\nu(z) \tag{A.8}$$

for integer m, with $m = 1$, we see that for real positive x

$$\begin{aligned}H_{n/2}^{(1)}(-x) &= J_{n/2}(-x) + i(e^{i\pi n/2} Y_{n/2}(x) + 2i\cos(n\pi/2) J_{n/2}(x))\\ &= -(-1)^{n/2} J_{n/2}(x) + i(-1)^{n/2} Y_{n/2}(x) && \text{(A.9)}\end{aligned}$$

where we have used that Bessel functions of odd order ν are odd. (We remark that Y_ν in general has a branch point and a pole at the origin, with a branch cut along the real negative axis; this is identity is consistent with the continuity of $Y_\nu(x+i\epsilon)$ for decreasing positive ϵ). We also have that in even n

$$R(-\mu) = (-1)^{n/2-1} R(\mu) \tag{A.10}$$

so that the real part of the integrand in (A.2) is an even function. We can therefore multiply by $1/2$ and extend the integral to the whole real axis:

$$\tilde{\chi}(b) = S_n \frac{\Gamma\left(\frac{n}{2}\right) 2^{n/2-1}}{b^{n/2}} \mathrm{Re}\left[\int_{-\infty}^{\infty} d\mu \frac{\mu^{n/2-1}}{1+\mu^{n+2}} H^{(1)}_{n/2}(b\mu)\right] \tag{A.11}$$

It follows from (A.9) that the imaginary part is an odd function if $n/2$ is an odd integer, so that in e.g. $n = 6$ "Re" is actually superfluous in this equation, but it is required in general.

We evaluate this integral via the residue theorem, with a contour illustrated in Fig. A.1. The rational function $R(\mu)$ has poles when $\mu^{n+2} = (-1)$; in the upper complex plane, this corresponds to the numbers $\mu = \{e^{i\pi m/(n+2)} : \mathrm{m} = 1, \ldots, (\mathrm{n}+2)/2\}$, the residues at which are straightforwardly evaluated using standard methods. To identify the residue at $\mu = 0$ we expand $Y_{n/2}(b\mu)$ in the series for integer m

$$Y_m(z) = \frac{1}{\pi}\left(2J_m(z)\ln\frac{z}{2} - \sum_{k=0}^{m-1}\frac{(m-k-1)!}{k!}\left(\frac{z}{2}\right)^{2k-m} + \text{finite}\right) \tag{A.12}$$

As this appears in the integrand multiplied by $\mu^{n/2-1}$, the residue is given by the $k = 0$ term:

$$\mathrm{Res}(R(\mu)H^{(1)}_{n/2}(b\mu)) = i\frac{(n/2-1)!}{\pi}\left(\frac{2}{b}\right)^{n/2} \tag{A.13}$$

(Note that the contribution from this residue is weighted by $1/2$ relative to those poles that lie inside the contour of integration.) We then find that

$$\begin{aligned}\tilde{\chi}(b) = S_n \frac{\Gamma\left(\frac{n}{2}\right) 2^{n/2-1}}{b^{n/2}} \quad \mathrm{Re} \quad \Bigg[(2\pi i)\Bigg(& \sum_{m=1}^{(n+2)/2} \frac{(e^{i\pi m/(n+2)})^{n/2-1} H_{n/2}((e^{i\pi m/(n+2)})b)}{(n+2)(e^{i\pi m/(n+2)})^{n+1}} \\ + \quad & i\frac{(n/2-1)!}{2\pi}\left(\frac{2}{b}\right)^{n/2}\Bigg)\Bigg]\end{aligned}$$

Note that as the Hankel function decays exponentially at large arguments, this expression makes the $\sim b^{-n}$ behaviour of χ manifest; it originates from the contribution from the pole at $\mu = 0$.

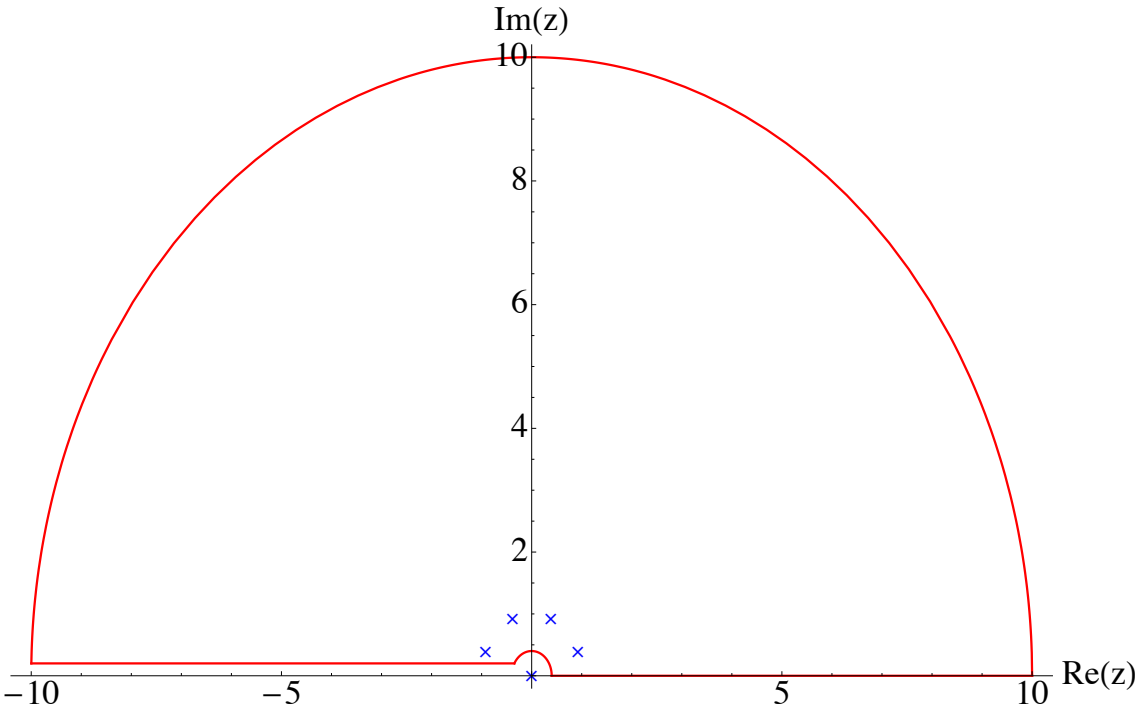

Figure A.1: The contour used to evaluate the eikonal phase, with poles corresponding to $n = 6$. The contribution from a semicircular contour of radius R (here shown with $R = 10$) decays exponentially. The poles of the integrand are denoted by the blue crosses (for $b = 1$). We make a semicircular indentation around the pole at $z = 0$, and approach the branch cut along the negative axis from above. Obviously we take the limit in which these indentations tend to zero.

Appendix B

Special Functions

Here we present the definitions of and some relations involving the special functions used in the text. These relations can be found in [109, 110, 111]

B.1 Bessel Function

$$\int_0^\infty z^a J_b(z) = 2^b \Gamma\left(\frac{1+a+b}{2}\right) / \Gamma\left(\frac{1+a-b}{2}\right) \tag{B.1}$$

$$J_\nu(z) = \sum_{k=0}^{\infty} \frac{(-1)^k (z/2)^{2k+\nu}}{k!\Gamma(k+\nu+1)} \tag{B.2}$$

$$\frac{dJ_\nu}{dz} = \frac{1}{2}\left(J_{\nu-1} - J_{\nu+1}\right) \tag{B.3}$$

$$K_\nu(z) = \sum_{k=0}^{\nu-1} (-1)^k \frac{(\nu-k-1)!}{k!(z/2)^{\nu-2k}} + (-1)^{\nu+1} \sum_{k=0}^{\infty} \frac{(z/2)^{\nu+2k}}{k!(\nu+k)!} \left[\ln(z/2) - \frac{1}{2}\psi(k+1) - \frac{1}{2}\psi(\nu+k+1)\right] \tag{B.4}$$

$$K_\nu(z) \approx \sqrt{\frac{\pi}{2z}} e^{-z} \left[1 + \mathcal{O}\left(1/z\right)\right] \tag{B.5}$$

which holds for any ν at this leading order.

B.2 Hypergeometric functions

The Hypergeometric function${}_2F_1 \equiv F$ is defined for $|z| < 1$ by the series

$$F(\alpha, \beta; \gamma; z) = \sum_0^\infty \frac{(\alpha)_n (\beta)_n}{(\gamma)_n} \frac{z^n}{n!} \tag{B.6}$$

where

$$(\alpha)_n = \frac{\Gamma(\alpha+n)}{\Gamma(\alpha)} = \alpha(\alpha+1)\dots(\alpha+n-1) \tag{B.7}$$

is the Pochammer symbol. ${}_pF_q$ is defined analogously. It admits the integral representation

$$F(\alpha,\beta;\gamma;z) = \frac{\Gamma(\gamma)}{\Gamma(\beta)\Gamma(\gamma-\beta)}\int_0^1 dt t^{\beta-1}(1-t)^{\gamma-\beta-1}(1-tz)^{-\alpha} \tag{B.8}$$

For $\alpha-\beta$ not an integer, the hypergeometric function F satisfies

$$\begin{aligned} F(\alpha,\beta;\gamma;z) &= \frac{\Gamma(\gamma)\Gamma(\beta-\alpha)}{\Gamma(\beta)\Gamma(\gamma-\alpha)}(-z)^{-\alpha}F(\alpha,\alpha+1-\gamma;\alpha+1-\beta;\frac{1}{z}) \\ &+ \frac{\Gamma(\gamma)\Gamma(\alpha-\beta)}{\Gamma(\gamma)\Gamma(\gamma-\beta)}(-z)^{-\beta}F(\beta,\beta+1-\gamma;\beta+1-\alpha;\frac{1}{z}) \end{aligned} \tag{B.9}$$

$${}_1F_2(a;b_1,b_2;z) \sim \frac{\Gamma(b_1)\Gamma(b_2)}{\Gamma(a)}\frac{1}{(4\pi)^{1/2}}e^{2\sqrt{z}}z^{\sigma}\left[1+\mathcal{O}\left(1/z\right)\right] \tag{B.10}$$

where

$$\sigma = \frac{1}{2}\left(\frac{1}{2}+a+b_1-b_2\right) \tag{B.11}$$

B.3 Meijer-G functions

$$\int_0^\infty d\tau \frac{\tau^{\alpha-1}}{(z+\tau)^\lambda} G_{pq}^{mn}\left(\omega\tau^{\frac{l}{k}}\middle|\begin{matrix}\mathbf{a}\\ \mathbf{b}\end{matrix}\right) = \frac{k^\mu l^{\lambda-1}z^{\alpha-\lambda}}{(2\pi)^{(k-1)c*+l-1}\Gamma(\lambda)} G_{kp+l,kq+l}^{km+l,kn+l}\left(\frac{\omega^k z^l}{k^{q-p}}\middle|\begin{matrix}\mathbf{c}\\ \mathbf{d}\end{matrix}\right) \tag{B.12}$$

$$\begin{aligned} \mathbf{c} &= \frac{1-\alpha}{l},\dots,\frac{l-\alpha}{l},\frac{a_1}{k},\dots,\frac{a_1+k-1}{k}\frac{a_n}{k},\dots, \\ &\frac{a_n+k-1}{k},\frac{a_{n+1}}{k},\dots,\frac{a_{n+1}+k-1}{k},\dots,\frac{a_p}{k},\dots,\frac{a_p+k-1}{k} \\ \mathbf{d} &= \frac{\lambda-\alpha}{l},\dots,\frac{\lambda-\alpha+l-1}{l},\frac{b_1}{k},\dots,\frac{b_1+k-1}{k},\dots,\frac{b_m}{k},\dots,\frac{b_m+k-1}{k}, \\ &\frac{b_{m+1}}{k},\dots,\frac{b_{m+1}+k-1}{k},\dots\frac{b_q}{k},\dots\frac{b_q+k-1}{k} \end{aligned}$$

This formula assumes that the greatest common denominator of (l,k) is one.

The following formulae relate the Meijer-G functions to the generalised hypergeometric function, ${}_pF_{q-1}$. Their utility for making asymptotic expansions of the Meijer-G function follow from the observation that ${}_pF_q(\mathbf{a};\mathbf{b};0)\equiv 1$ for any p parameters a_n and q parameters b_q. Here the asterisks denote the omission of the parameter b_h from the corresponding lists.

$$\begin{aligned} G_{pq}^{mn}\left(x\middle|\begin{matrix}\mathbf{a}\\ \mathbf{b}\end{matrix}\right) =& \sum_{h=1}^{m}\frac{\prod_{j=1}^m *\Gamma(b_j-b_h)\prod_{j=1}^m\Gamma(1+b_j-a_h)}{\prod_{j=m+1}^q\Gamma(1+b_h-b_j)\prod_{j=1}^p\Gamma(a_j-b_h)}x^{b_h} \\ &\times\ {}_pF_{q-1}(1+b_h-a_1,\dots,1+b_h-a_p;1+b_h-b_1,\dots,*,\dots,1+b_h-b_q; \\ &(-1)^{p-m-n}x) \end{aligned} \tag{B.13}$$

$$G_{pq}^{mn}\left(x\left|\begin{matrix}\mathbf{a}\\ \mathbf{b}\end{matrix}\right.\right)=\sum_{h=1}^{m}\frac{\prod_{j=1}^{m}{}*\Gamma(a_h-a_j)\prod_{j=1}^{m}\Gamma(1+b_h-a_j)}{\prod_{j=1}^{p}\Gamma(a_j-a_h+1)\prod_{j=m+1}^{q}\Gamma(a_h-b_j)}x^{a_h-1} \tag{B.14}$$

$$\times\ {}_pF_{q-1}(1+b_1-a_h,\ldots,1+b_q-a_h;1+a_1-a_h,\ldots,*,\ldots,1+a_p-a_h;$$

$$(-1)^{q-m-n}x^{-1})$$

$$x^kG_{pq}^{mn}\left(x\left|\begin{matrix}\mathbf{a}\\ \mathbf{b}\end{matrix}\right.\right)=G_{pq}^{mn}\left(x\left|\begin{matrix}\mathbf{a}+k\\ \mathbf{b}+k\end{matrix}\right.\right) \tag{B.15}$$

$$\int_0^\infty \tau^{\alpha-1}G_{p,q}^{m,n}\left(\tau z\left|\begin{matrix}a_1,\ldots,a_n,a_{n+1},\ldots,a_p\\ b_1,\ldots,b_m,b_{m+1},\ldots,b_q\end{matrix}\right.\right)G_{u,v}^{s,t}\left(\tau w\left|\begin{matrix}c_1,\ldots,c_t,c_{t+1},\ldots,c_u\\ d_1,\ldots,d_s,d_{s+1},\ldots,d_v\end{matrix}\right.\right)d\tau$$

$$=\frac{G_{v+p,m+q}^{m+t,n+s}\left(\frac{z}{w}\left|\begin{matrix}\mathbf{x}\\ \mathbf{y}\end{matrix}\right.\right)}{w^\alpha} \tag{B.16}$$

where

$$\mathbf{x} = a_1,\ldots,a_n,-\alpha-d_1+1,\ldots,-\alpha-d_s+1,-\alpha-d_{s+1}+1,\ldots,-\alpha-d_v+1,a_{n+1},\ldots,a_p$$

$$\mathbf{y} = b_1,\ldots,b_m,-\alpha-c_1+1,\ldots,-\alpha-c_t+1,-\alpha-c_{t+1}+1,\ldots,-\alpha-c_u+1,b_{m+1},\ldots,b_q$$

Appendix C

The Stationary Phase Approximation

C.1 Asymptotic expansion of integrals

The purpose of the stationary phase approximation is to estimate the behaviour of integrals of the form

$$I(x) = \int_a^b dt f(t) \exp(x\phi(t)) \tag{C.1}$$

for asymptotically large x. Changing variables to $s = -\phi(t)$ gives

$$I(x) = \int ds \frac{f(t(s))}{-\phi'(t(s))} e^{-xs} \tag{C.2}$$

Repeated integration by parts yields a power series in $1/x$. This procedure, however, fails when $\phi'(t) = 0$ on the interior of the integration region. If such a *stationary point* t^* exists, then we argue that, for asymptotically large x, such integrals are dominated by those stationary points which correspond to a maximum value of $\phi(t)$. Near such a point we can expand

$$\phi(t) \approx \phi(t^*) + \frac{1}{p!}\phi^{(p)}(t^*)t^p \tag{C.3}$$

where p is the order of the first nonvanishing derivative of ϕ at t^*, and $\phi^{(p)}(t^*) < 0$ as t^* is a maximum of ϕ. The contribution of such a point to $I(x)$ is given by

$$I(x, \epsilon) \approx \int_{t^*-\epsilon}^{t^*+\epsilon} dt f(t^*) \exp(\phi(t^*) + \frac{1}{p!}\phi^{(p)}(t^*)t^p) \tag{C.4}$$

We can evaluate such an integral by now letting $\epsilon \to \infty$; the additional integration region contains no stationary points of our *approximated* integrand, so by our earlier argument about integrating by parts, the error thus introduced is of order $1/x$, and is therefore

subleading to the contributions that we isolate here. One then finds that

$$I(x) = \kappa \frac{2\Gamma(1/p)(p!)^{1/p}}{p(-x\phi^{(p)}(t^*))^{1/p}} f(t^*) \tag{C.5}$$

where

$$\kappa = \begin{cases} \frac{1}{2} & \text{if } \mathrm{t}^* = \mathrm{a} \text{ or } \mathrm{b} \\ 1 & \text{if } \mathrm{t}^* \in (\mathrm{a},\mathrm{b}) \end{cases}$$

An exectly analagous argument applies to integrals of the form

$$I(x) = \int dt f(t) \exp(ix\phi(t)) \tag{C.6}$$

for x, ϕ real; instead of the exponential decay suppressing the integrand, the stationary points dominate because for large x the period of the oscillations becomes extremely short, so that neighbouring regions in the integral cancel each other out. Here one finds that

$$I(x) = \kappa 2 f(t^*) e^{i(x\phi(t^*) \pm \pi/2p)} \left(\frac{p!}{x|\phi(t^*)|} \right)^{1/p} \frac{\Gamma(1/p)}{p} \tag{C.7}$$

The sign of $\pm i\pi/2$ is that of the second derivative $\phi''(t*)$. In this context with an imaginary exponent in the integrand, this approximation is known as the method of *stationary phase*; for a purely real exponent, it is usually referred to as *Laplace's method*.

It is important to understand the logic underlying this approximation: in the $x \to \infty$ limit, only very small changes δt are needed to shift the value of the phase by $\delta\phi = 2\pi$, so that $f(t)$ changes very little over a period of the exponential. It is for this reason that the integral is dominated by the contribution from regions in the immediate neighbourhood of points at which $\phi'(t) = 0$. It is the smallness of such regions that allows us to Taylor expand our exponent about the critical points, and the large suppression of contributions from regions away from the stationary point that allows us to then *extend* the region of integration of the polynomial approximation of ϕ from the immediate neighbourhood of the stationary point to e.g. the *entire real axis* (or any other convenient extended contour) for ease of evaluating the integral.